

2007

Stereochemical and Regiochemical Trends in the Selective Spectrophotometric Detection of Biological Molecules

Shan Jiang

Louisiana State University and Agricultural and Mechanical College, sjiang1@lsu.edu

Follow this and additional works at: https://digitalcommons.lsu.edu/gradschool_dissertations

 Part of the [Chemistry Commons](#)

Recommended Citation

Jiang, Shan, "Stereochemical and Regiochemical Trends in the Selective Spectrophotometric Detection of Biological Molecules" (2007). *LSU Doctoral Dissertations*. 2088.

https://digitalcommons.lsu.edu/gradschool_dissertations/2088

This Dissertation is brought to you for free and open access by the Graduate School at LSU Digital Commons. It has been accepted for inclusion in LSU Doctoral Dissertations by an authorized graduate school editor of LSU Digital Commons. For more information, please contact gradetd@lsu.edu.

**STEREOCHEMICAL AND REGIOCHEMICAL TRENDS IN THE SELECTIVE
SPECTROPHOTOMETRIC DETECTION OF BIOLOGICAL MOLECULES**

A Dissertation

Submitted to the Graduate Faculty of the
Louisiana State University and
Agricultural and Mechanical College
in partial fulfillment of the
requirements for the degree of
Doctor of Philosophy

In

The Department of Chemistry

By

Shan Jiang

B.E., Beijing Institute of Clothing Technology, 1997

M.S., New Mexico Highlands University, 2002

May, 2007

DEDICATION

I dedicate this dissertation to my family. First of all, to my father Wenjing Jiang and mother Shulan Lu. Thank you for all your love, support and guidance that you have afforded ever since I was born. I hope that I have made you proud. Next, to my loving wife Liqin Zhang, thank you for your love and support. I am lucky to have you as my life partner. Third, to my brother Hai Jiang. Thank you for all your support and help in my graduate study in the United States. Finally, to the rest of my family, thank you all for your love and support. I love you all.

ACKNOWLEDGMENTS

First of all, I would like to give my deepest and sincerest thanks to my research advisor, Dr. Robert Strongin, for affording me the opportunity to work in his group and guiding me in my research. Thank you for always being there to help me and support my research. I would like to give my special thanks to Dr. Jorge O. Escobedo for his great help in my research and thesis writing as well as being a good friend. My thanks also go to my colleague and friend Dr. Oleksandr Rusin. Thank you for all your unselfish and timely help. To my former colleagues Dr. Kyu Kwang Kim, Dr. Weihua Wang, Dr. Rolanda J. Johnson and Dr. Nadia St. Luce, I thank you all for the help you offered to me in my research. My thanks also go to my current colleagues, Onur Alpturk, Xiangyang Xu, Youjun Yang, and George Samoei, for their help in my research work. Thanks to Dr. W. Dale Treleaven, Guangyu Li and Jianan Dong for countless and timely help in the NMR study of my research. Finally, I would like to thank Dr. David Spivak, Dr. William Crowe, Dr. Bin Chen and Dr. Richard Tulley for their help to my research and for being my research committee members.

TABLE OF CONTENTS

DEDICATION.....	ii
ACKNOWLEDGMENTS.....	iii
LIST OF TABLES.....	vi
LIST OF FIGURES.....	vii
LIST OF SCHEMES.....	xii
LIST OF ABBREVIATIONS.....	xiii
ABSTRACT.....	xvii
CHAPTER 1. INTRODUCTION.....	1
1.1 History of Resorcinarenes.....	1
1.2 Complexation of Polar Organic Molecules by Resorcinarenes.....	5
1.3 Complexation of Boronic Acids to Saccharides.....	7
1.4 Significance In Saccharides Detection.....	10
1.5 References.....	11
CHAPTER 2. MECHANISTIC STUDIES AND THE SELECTIVE SPECTROPHOTOMETRIC DETECTION OF SACCHARIDES WITH RESORCINATENE BORONIC ACID	14
2.1 Background of Resorcinarene Color Formation.....	14
2.2 Results and Discussion.....	21
2.3 Conclusion.....	41
2.4 Experimental Section.....	41
2.5 References.....	43
CHAPTER 3. STEREOCHEMICAL AND REGIOCHEMICAL TRENDS IN THE SELECTIVE SPECTROPHOTOMETRIC DETECTION OF SACCHARIDES APPLYING RHODAMINE BORONIC ACID.....	46
3.1 Introduction	46
3.2 Discussion.....	52
3.3 Conclusion.....	61
3.4 Experimental Section	62
3.5 References.....	63
CHAPTER 4. SELECTIVE DETECTION OF CYSTEINE AND HOMOCYSTEINE USING A FLUORESCEIN DERIVATIVE	65
4.1 Induction.....	65
4.2 Formation of Cysteine and Homocysteine	65
4.3 Homocysteine in Plasma.....	68

4.4	Relevance of Homocysteine to Public Health	68
4.5	Synthesis of Fluorescein Dialdehyde Derivative.....	69
4.6	Results and Discussion.....	70
4.7	Conclusion.....	75
4.8	Experimental Section	76
4.9	References.....	76
APPENDIX A.	STRUCTURES OF TWELVE HEXOSES AND FOUR PENTOSES...	79
APPENDIX B.	STRUCTURES OF FIFTEEN SELECTED DISACCHARIDES.....	83
APPENDIX C.	STRUCTURES OF TWELVE SELECTED TRISACCHARIDES.....	87
APPENDIX D.	STRUCTURES OF THREE SELECTED OLIGOSACCHARIDES....	90
APPENDIX E.	COLORIMERIC DETECTION OF BIOLOGICAL MOLECULES....	91
APPENDIX F.	LETTERS OF PERMISSION.....	95
VITA.....		97

LIST OF TABLES

2.1	MALDI MS of acyclic oxidized and unoxidized products from the thermolysis of 2.2b	19
2.2	Selectivity of arylboronic acid chemosensors to various monosaccharides	23
2.3	Proportions (%)[*] of fructose p-tolyboronic acid complexes and free fructose isomers in (CD ₃) ₂ SO. Equilibrium mixtures at different boronic acid:fructose ratios	26
2.4	Representative color tests based on non-enzymatic assays. Note the harsh conditions required. The assays often suffer from significant interference from competing analytes	39
3.1	Apparent binding constants (K_{eq}) of the complexes of various monosaccharides and compound 3.1 ($7.2 \times 3.10^{-5} M$ in 9:1 DMSO:phosphate buffer 60 mM, pH 7.4). Values are the average of three runs rounded to two significant figures.....	53

LIST OF FIGURES

1.1	Structures of the crystalline compound obtained from Baeyer’s synthesis proposed by Michael (1.1), Nierdel and Vogel (1.2), R = aliphatic.....	1
1.2	Mechanism of the acid-catalyzed synthesis of resorcinarenes.....	3
1.3	Relative configuration of the substituents at methylene bridges	4
1.4	Structures of three selected monosaccharides and the complex between Resorcinarene and D-ribose	6
1.5	Boronate ester formation with phenylboronic acid in alkaline aqueous solution (top) and aprotic media (bottom). Exaples of sp ³ and sp ² complexes between phenyl boronic acid and fructose are included (right).....	8
1.6	Complex structures between <i>p</i> -tolylboronic acid and fructose.....	8
1.7	Complex structures between <i>p</i> -tolylboronic acid and fructose.....	9
2.1	Chair (2.1) and crown (2.2a) stereoisomers of tetraarlboronnac acid resorcinarenes.....	14
2.2	Resorcinarene substructures of methine-bridged condensation products (2.3) and some xanthene dyes (2.4).....	16
2.3	Dehydration and oxidation of methine-bridged resorcinol oligomers leading to xanthenes.....	16
2.4	2.2a (1.0 mg) and 2.3a (1.0 mg) each in 0.9 mL DMSO were heated to gentle reflux over two minutes and cooled to room temperature before 0.1 mL H ₂ O was added to each solution. The final concentrations of 2.2a and 2.3a in 9:1 DMSO:H ₂ O are 1.03 × 10 ⁻³ M and 1.96 × 10 ⁻³ M respectively. A solution of 2.4b (5.0 × 10 ⁻⁶ M) was prepared at rt in 9:1 DMSO:H ₂ O.....	17
2.5	Compound 2.7 and Oak Ridge Thermal Ellipsoid Plot (ORTEP).....	18
2.6	A selective solution color change is observed for D-fructose when added to colored solutions of 2.8 and 2.9 : (a) D-fructose, (b) D-glucose, (c) D-psicose, (d) D-allose, (e) D-ribose, (f) D-xylose, (g) D-trehalose, (h) melezitose, (i) D-turanose, (j) D-maltose, (k) sucrose, (l) D-raffinose. Sugars in vials labeled a, b and g-l are found in honey.....	22
2.7	Plots of relative absorbance changes vs. concentration of various sugars in solutions comprised of phosphate buffer (0.1 mL, 60 mM, pH = 7.4) added to 2.8 in DMSO (3.4 mM, 0.9 mL) at 355 (A) nm and (B) 535 nm.....	24

2.8	Pyranose forms of sugars used in the study shown in Figure 2.7. Only those compounds containing pairs of vicinal <i>cis</i> -diols on opposite faces of the pyranose ring (i.e., ribose, altrose, galactose and fructose) afford colorimetric responses...	25
2.9	Left: Representation of the complete structure of complex 2.11 . Right: Expansion showing the fructopyranose region of the AM-1 simulated structure of one isomeric <i>bis</i> -boronate complex 2.11 , showing fructose in a twist conformation.....	28
2.10	Di-and trisaccharides studied.....	30
2.11	(A) Concentration vs. absorbance spectral responses at 355 nm of four of the disaccharides shown in Figure 2.10. (B) Concentration vs. absorbance spectral responses at 355 nm of eight of the disaccharides shown in Figure 2.10. The largest spectral responses of all of the sugars in Figure 2.10 are observed for lactulose and maltulose solutions. The UV-Vis spectra of the remaining di- and trisaccharides shown in Figure 2.10 exhibit no significant spectral responses at 355 nm or 535 nm (see also Figure E1 of Appendix E).....	31
2.12	UV-Vis spectra responses of a solution of 2.9 ($1 \times 10^{-3} M$) and 2.8 with added di- and trisaccharides ($5 \times 10^{-3} M$), all in 9:1 DMSO:phosphate buffer (0.06 M, pH 7.4) of the disaccharides shown in Figure 2.10.....	32
2.13	Fluorescence emission spectra of a solution of 2.8 ($1 \times 10^{-3} M$) and 2.8 with added di- and trisaccharides ($1.85 \times 10^{-3} M$), all in 9:1 DMSO:phosphate buffer (0.05 M, pH 7.4) excited at 535 nm. This result shows the selectivity for lactulose and maltulose. The other di- and tri saccharides tested afford no detectable signal. Only lactulose and maltulose can adapt the proper terminal residue configurational preference (Figure 13). The selectivity is confirmed by UV-Vis spectroscopy (supporting information).....	32
2.14	Anionic fructofuranose-boronate ester structures.....	33
2.15	Plots of relative absorbance changes at 355 nm vs. the concentration of various sugars in solutions comprised of carbonate buffer (0.1 mL, 40 mM, pH = 10.0) added to 2.8 in DMSO (3.4 mM, 0.9 mL) at 355 nm. Analogous trends in absorbance changes vs. concentration are also observed at 535 nm.....	34
2.16	Furanose forms of sugars. Only aldoses with hydroxyls on carbons 1,2 and 5, and ketoses with hydroxyls on carbons 2,3 and 6 residing on the same side of the furanose ring exhibit signal transduction (Figure 2.17).	36
2.17	Plots of absorbance vs. the concentration of various monosaccharides in phosphate buffer (0.1 mL, 60 mM, pH = 7.4) added to 2.8 in DMSO (3.4 mM, 0.9 mL) at 355 nm.....	36
2.18	(A) UV-Vis spectra of solutions of 2.8 with fructose, glucose or their mixture in 9:1 DMSO:phosphate buffer (60 mM pH 7.4). (B) UV-Vis spectra of solutions of	

	2.8 with different concentrations of fructose ([Fruc]) in 9:1 DMSO:phosphate buffer (60 mM pH 7.4).....	37
2.19	The calibration curve validated by the addition of fructose standards to a solution of honey (0.32 mg/mL) and 2.8 (3.4 mM) in a 1:9 mixture of phosphate buffer (0.1 mL, 60 mM, pH = 7.4) and DMSO at 355 nm.....	40
3.1	(a) Relative absorbance changes vs. concentration of various monosaccharides in phosphate buffer (0.1 mL, 60 mM, pH 7.4) added to 3.1 ($7.2 \times 10^{-5} M$) in DMSO (0.9 mL) and monitored at 560 nm. (b) The UV-Vis spectra of a solution of 3.1 ($7.2 \times 10^{-5} M$) alone and 3.1 with added ribose ($4 \times 10^{-4} M$). (c) Relative fluorescence emission spectra at 597 nm of 3.1 ($4 \times 10^{-9} M$) and saccharides and saccharide-containing molecules ($1.85 \times 10^{-3} M$) in 9:1 DMSO:phosphate buffer (0.05 M, pH 7.4) excited at 565 nm. (d) Fluorescence emission spectra of a solution of 3.1 ($4 \times 10^{-9} M$) and 3.1 with added ribose ($1.85 \times 10^{-3} M$) in 9:1 DMSO:phosphate buffer (0.05 M, pH 7.4) excited at 565 nm.....	47
3.2	UV-Vis spectra of solutions containing 3.1 ($7.2 \times 10^{-5} M$) in 9:1 DMSO:phosphate buffer (0.06 M, pH 7.4) and 3.1 in the presence of $4 \times 10^{-4} M$ solutions of ATP, adenosine and AICAr.....	50
3.3	Structures of the resorcinarene boronic acid 3.2 and its chromophoric products (3.3) formed <i>in situ</i>	51
3.4	Relative absorbance changes vs. concentration of ribose, fructose, galactose and glucose in solutions comprised of phosphate buffer (0.1 mL, 60 mM, pH = 7.4) added to 3.1 (0.07 mM) in DMSO (0.9 mL) and 3.2 (1.9 mM) monitored at 560 nm. A comparison to Figure 3.1a shows that the use of 3.1 combined with 3.2 removes significant fructose interference under these conditions.....	52
3.5	Xanthene Expansion of the 1H NMR spectra of solutions of (a) D-ribose and (b) a mixture of 3.1 and D-ribose (0.15 M NaOD/D ₂ O). The resonances shown correspond the anomeric protons of each of the four cyclic forms. The assignments are: δ (ppm): 5.30 (α -ribofuranose), 5.18 (β -ribofuranose), 4.85 (β -ribopyranose) and 4.79 (α -ribopyranose). Upon the addition of 3.1 only the resonances corresponding to the ribofuranoses exhibit a downfield shift. This is expected as a result of cyclic boronate formation with ribofuranose (reference 3.3c).....	54
3.6	Structures of 11 monosaccharides in their furanose forms. Compound 3.1 is selective for sugars with hydroxyls shown in blue. Compound 3.3 is selective for sugars with hydroxyls shown in red).....	55
3.7	Plots of relative absorbance changes vs. concentration of 11 monosaccharides in solutions comprised of phosphate buffer (0.1 mL, 60 mM, pH = 7.4) added to 3.1 (0.07 mM) in DMSO (0.9 mL) and 3.2 (1.9 mM) monitored at 560 nm.....	56

3.8	The effect of solvation on the B-N bond in <i>o</i> -(<i>N,N</i> -dialkylaminomethyl)phenylboronic esters (adapted from reference 3.18).....	57
3.9	Energy-minimized structures of boronates derived from 3.1 and ribofuranose (“endo” isomer, structure A), fructofuranose (3 rotamers, structures B) and glucofuranose (“exo” isomer, structure C, the complementary conformers of the ribo- and glucofuranose boronates are included in Figure E4). A subunit of the the rhodamine chromophore moiety is shown for clarity and used in the simulations in order to simplify the calculations. The above calculated structures show that the ribofuranose complex exhibits the relatively best geometry for promoting direct contacts between the bound sugar moiety and the chromophore moiety of 3.1 . Studies aimed at evaluating the specific interactions between ribose, adenosine, ribosides and ribotides with 3.1 that might involve π - π stacking, σ - π interactions and/or charged hydrogen bonding between the sugar and the rhodamine carboxylate functionality, are ongoing.....	58
3.10	Relative fluorescence emission spectra at 574 nm of 3.2 ($5.75 \times 10^{-5} M$) and monosaccharides ($1.85 \times 10^{-3} M$) in 9:1 DMSO:phosphate buffer (0.05 <i>M</i> , pH 7.4) excited at 550 nm.....	59
3.11	Relative absorbance changes vs. the concentration of various monosaccharides in phosphate buffer (0.1 mL, 60 mM, pH = 7.4) added to 3.2 in DMSO (3.4 mM, 0.9 mL) at 535 nm.....	60
3.12	Anionic fructofuranose-boronate ester structures.....	60
4.1	Compound 4.6	69
4.2	Top: color changes of solutions of 4.6 and various analytes. A = no analyte, B = cysteine, C = homocysteine, D = bovine serum albumin, E = glycine and F = <i>n</i> -propylamine. Bottom: co-spots of 4.6 ($1.0 \times 10^{-3} M$) with and without various analytes ($1.0 \times 10^{-3} M$) under visible and UV light.....	72
4.3	Left: Absorption spectra of dialdehyde ($2.5 \times 10^{-6} M$) and cysteine ($4 \times 10^{-6} M - 8 \times 10^{-5} M$) in H ₂ O, pH 9.5, rt, 5 min. Right: Interaction of the 4.6 ($4 \times 10^{-6} M$) and cysteine (4.9×10^{-5} to $7.4 \times 10^{-4} M$) in deproteinized human blood plasma containing 5.0 mM glutathione at room temperature. Detection limit is $4 \times 10^{-5} M$	72
4.4	Absorbance vs. concentration plots for cysteine (▲) and homocysteine (O) in aqueous solutions of dialdehyde ($2.5 \times 10^{-6} M$) at pH 9.5.....	73
4.5	Successive addition of serine (to final concentrations of $4 \times 10^{-5} M$ to $8 \times 10^{-4} M$) to an aqueous solution of dialdehyde ($2.5 \times 10^{-6} M$) at pH 9.5 results only in an absorbance change at 480 nm. Addition of cysteine (to final concentrations of $4 \times 10^{-6} M - 8 \times 10^{-5} M$) to the serine-dialdehyde solution produces an absorbance change at 505 nm.....	74

4.6 Fluorescence emission spectra of **4.6** (5.2×10^{-7} M) and homocysteine (2.9×10^{-6} - 2.5×10^{-3} M) in deproteinized human plasma excited at 460 nm (pH 9.5). (Inset) Fluorescence emission plotted vs [homocysteine].....75

LIST OF SCHEMES

2.1	The <i>in situ</i> ring opening of resorcinarene boronic acid macrocycle 2.8 affords acyclic oligomers (2.9) containing xanthene chromophores. The ratio of 2.8 to 2.9 under our conditions is ca. 1000:1.....	20
3.1	Structure of compound 3.1	46
3.2	Structures of ribose and selected ribosides and ribotides.....	48
3.3	Formation of ribose acetonide via selective reaction of the 2,3-hydroxyls in 90 % yield (reference 3.11).....	56
4.1	Metabolism of Homocysteine.....	71
4.2	Synthesis of compound 4.6	74
4.3	Reaction of cysteine with aldehydes to form thiazolidines.....	74
4.4	Reaction of 4.6 with cysteine 4.1 . Reaction conditions: 0.25 M Na ₂ CO ₃ buffer pH 9.5, followed by precipitation with MeOH.....	75
4.5	Reaction of 4.6 with homocysteine 4.2 . Reaction conditions: 0.25 M Na ₂ CO ₃ buffer pH 9.5, followed by precipitation with MeOH.....	75

LIST OF ABBREVIATIONS

amu	Atomic Mass Units
ATP	Adenosine triphosphate
ASFB	4-Aminosulfonyl-7-fluoro-2,1,3-benzoxadiazole
A.U.	Absorbance Unit
BMF	Bromomethylfluorescein
BSA	Bovine serum albumin
Ca²⁺	Calcium ion
calcd	Calculated
CE	Capillary electrophoresis
CMPI	2-Chloro-1-methylpyridinium iodide
Cys	Cysteine
DCM	Dimethylmethane
DMF	Dimethylformamide
DMSO	Dimethyl sulfoxide
DNA	Deoxyribonucleic acid
<i>e.g.</i>	<i>exempli gratia</i> (for example)
Eq.	Equation
EIA	Enzyme immunoassay
<i>et al.</i>	<i>et alii</i> (and others)
EtOAc	Ethyl acetate
FB	Fluorone black
FeCl₃	Ferric chloride

FT-IR	Fourier transform infrared
GC	Gas chromatography
GC-MS	Gas chromatography-mass spectrometry
GSH	Glutathione
HCl	Hydrochloric acid
Hcy	Homocysteine
HEPES	N-2-hydroxyethylpiperazine-N'-2-ethanesulfonic acid
HNO₃	Nitric acid
H₂O	Water
H₂O₂	Hydrogen peroxide
HPLC	High performance liquid chromatography
H₂S	Hydrogen sulfide
IR	Infrared
K₂CO₃	Potassium carbonate
KOH	Potassium hydroxide
LC	Liquid chromatography
LC-MS	Liquid chromatography – mass spectrometry
M	Molar
MALDI	Matrix-Assisted Laser Desorption/Ionization
MeOH	Methanol
MHz	Megahertz
min	Minute
mM	Millimolar
Mn²⁺	Manganese ion

MS	Mass spectrometry
m/z	Mass-to-charge ratio in mass spectrometry
NAD⁺	Nicotinamide adenine dinucleotide
NaHCO₃	Sodium bicarbonate (sodium hydrogen carbonate)
Na₂SO₄	Sodium sulphate
NH₃	Ammonia
nm	Nanometer
NMDA	N-methyl-D-aspartate
NMR	Nuclear Magnetic Resonance
NO	Nitric oxide
OPA	<i>O</i> -phthalaldehyde
pH	Measure of the acidity of a solution
pKa	Measure of the strength of an acid
PPh₃	Triphenylphosphine
ppm	Parts per million
psi	Pounds per square inch
RSD	Relative standard deviation
SAH	S-adenosylhomocysteine
SAM	S-adenosylmethionine
UV/Vis	Ultraviolet/visible
vs.	Versus
BHT	Butylated hydroxytoluene, 2,6-Di- <i>tert</i> -butyl-4-methylphenol
DCC	1,3-Dicyclohexylcarbodiimide
DCM	Dichloromethane

DMAP	4-Dimethylaminopyridine
DMF	<i>N,N</i> -Dimethylformamide
DMSO	Dimethyl sulfoxide
HOBT	1 <i>H</i> -Benzotriazole
Ms	Mesylate, Methanesulfonate
THF	Tetrahydrofuran
THP	3,4-Dihydro-2 <i>H</i> -pyran
Ts	Tosylate, <i>p</i> -Toluenesulfonate

ABSTRACT

Useful mechanistic studies to date concerning sugar detection by arylboronic acid chemosensors have mainly involved the elucidation of equilibrium constants and the role of boron-nitrogen interactions in signal transduction. However, several discreet sugar-boronate complexes exist in solution. This is due to the complex equilibria between isomeric species of even the simplest monosaccharides. Relatively few reports have been devoted to a systematic study of the structures of each of the corresponding individual sugar-boronate complexes. We have investigated some of the precise regio- and stereochemical features of the various equilibrating sugar isomers that induce selective signal transduction. As a result of this study, one may be better able to predict selective spectrophotometric responses of a monosaccharide in a natural matrix. Additionally, our findings are potentially applicable to selective analyses of more complex compounds via their terminal sugar residue structures. Additionally, during the course of this work, a unique example of a chemosensor (**3.1**) that is selective for ribose, adenosine, nucleotides, nucleosides and congeners was discovered. The combined use of chemosensors exhibiting complementary reactivities was shown to obtain enhanced selectivity for ribose and rare saccharides. A structurally-related xanthene chemosensor (**4.6**) that is selective for the sulfur-containing amino acids cysteine and homocysteine is also described herein.

CHAPTER 1

INTRODUCTION

1.1 History of Resorcinarenes

Calix[4]resorcinarenes or resorcinol-derived calix[4]arenes were first synthesized by Adolf von Baeyer^{1,1} (Figure 1.1) in 1872. He was attempting to synthesize new dyes to build on his discovery of fluorescein. The cyclic tetrameric product is colorless; however, our group recently discovered that xantheno dyes are also present in resorcinarene-containing solutions.

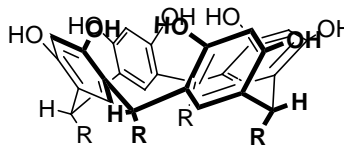
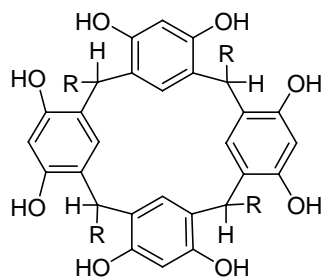
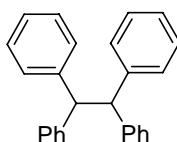


Figure 1.1. Structures of the crystalline compound obtained from Baeyer's synthesis proposed by Michael (1.1), Nierdel and Vogel (1.2), R = aliphatic.

Most resorcinarenes can be derived from condensation reactions between resorcinol and an aliphatic or aromatic aldehyde. Lewis acids are normally used as

catalysts in this reaction.^{1.2, 1.3, 1.4} Usually, cyclotetramer isomers precipitate from the reaction mixtures. The addition of water, in some cases, is required to isolate the condensation product.^{1.5, 1.6} An unsubstituted resorcinol (1,3 dihydroxybenzene) is normally used in the synthesis of resorcinarenes, however, the use of pyrogallol (1,2,3-trihydroxybenzene) or some 2-substituted resorcinols, such as 2-methylresorcinol are also reported to yield isolable amounts of tetrameric products.^{1.7, 1.8} Products typically are not formed if the hydroxyl groups are partially alkylated^{1.9} or when the resorcinol derivatives bear electron-withdrawing substituents such as NO₂ or Br^{1.5} at the 2-position. Exceptions also include aliphatic aldehydes possessing functionality proximal to the reaction center, such as ClCH₂CHO or glucose,^{1.5} or very sterically crowded aldehydes, such as 2,4,6-trimethylbenzaldehyde.^{1.9}

The mechanism of the condensation reaction for the formation of resorcinarenes via acid-catalization is shown in Figure 1.2.^{1.9} Under acidic conditions, resorcinol serves as the initial nucleophile which attacks the protonated aldehyde. Subsequent protonation of alcoholic hydroxyl of the resulted adduct generates a mole of water. A carbocation intermediate, formed by removal of water, undergoes a second nucleophilic addition with another resorcinol molecule to afford a dimer. Further analogous addition reactions with resorcinol units result in trimer, tetramer and higher oligomers containing more than four monomers. Most of the larger oligomers present disappear towards the end of the reaction since the condensation reaction is reversible under acidic conditions except for the last step in which the linear tetramers cyclize rapidly to form resorcinarenes once they are formed. The linear tetramers are not isolable due to the fast cyclization reaction. Little conformational strain as well as charged hydrogen bonds between the phenolic

hydroxyl groups of adjacent resorcinol favor a cyclized *ccc* product (Figure 1.3) in many cases.

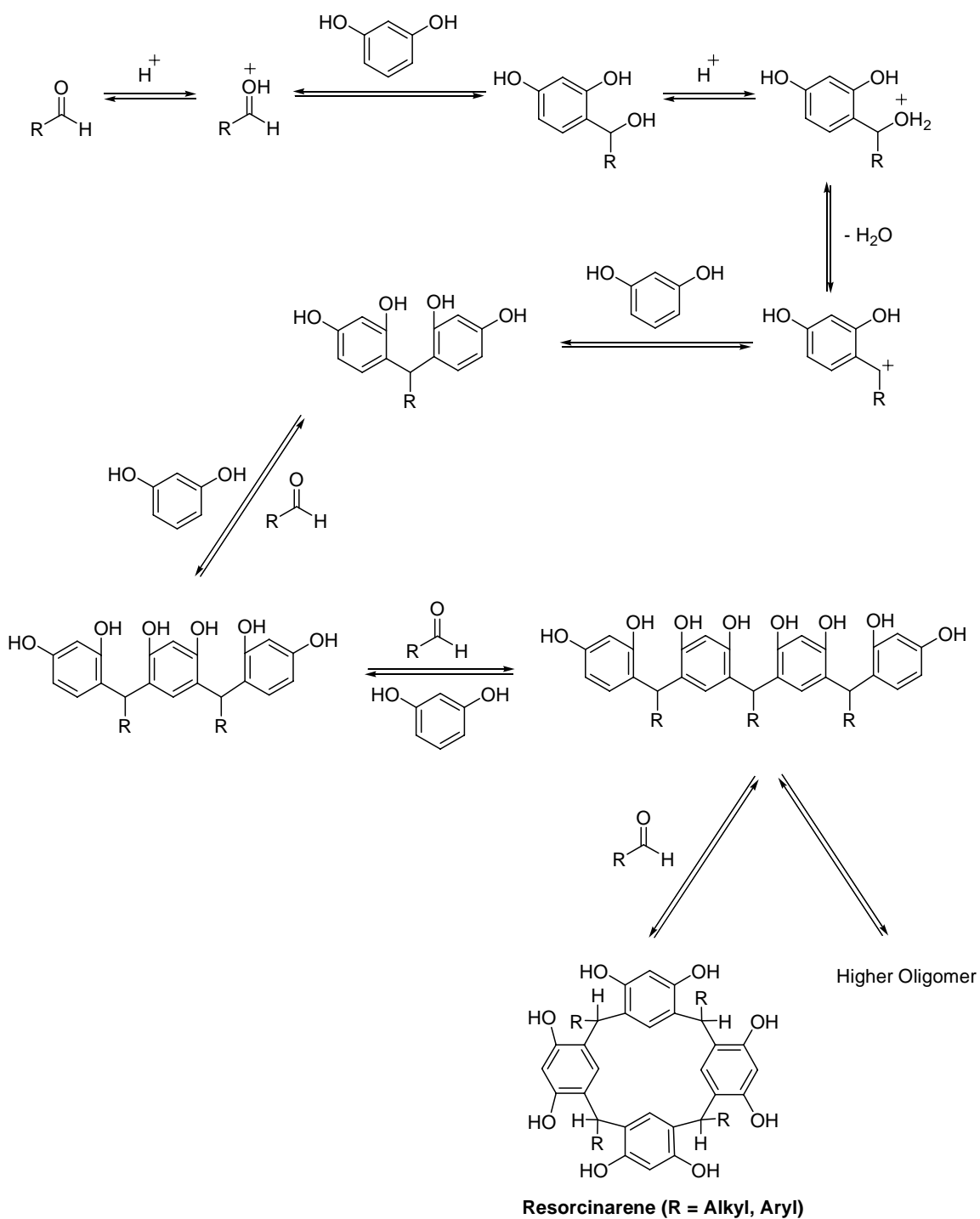


Figure 1.2. Mechanism of the acid-catalyzed synthesis of resorcinarenes.

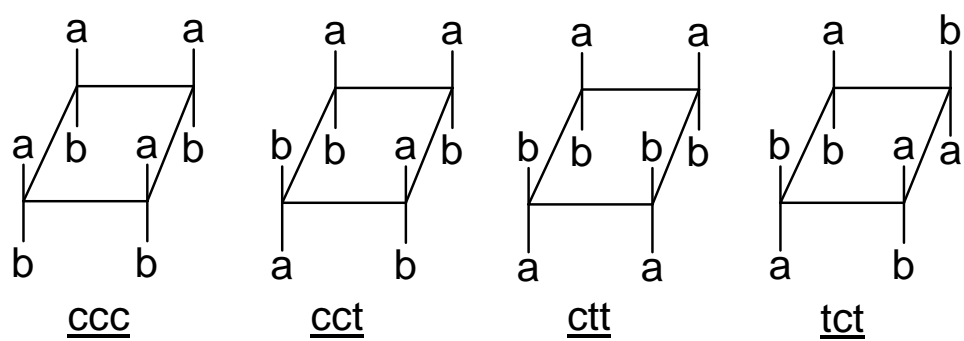


Figure 1.3. Relative configuration of the substituents at methylene bridges.

The stereochemistry of resorcinarenes is generally defined according to the relative configuration of the substituents at the methylene bridges. Four resorcinarene stereoisomers, i.e. all-*cis* (ccc), *cis-cis-trans* (cct), *cis-trans-trans* (ctt) and *trans-cis-trans* (tct), are given in Figure 1.3.^{1,5}

1.2 Complexation of Polar Organic Molecules by Resorcinarenes

Over a decade ago, Aoyama et al. found that resorcinarenes can complex organic molecules containing polar substituents. Their tetrameric phenolic moieties groups at the upper rim resulted in a variety of binding modes which he extensively studied.^{1,10, 1.11} The complexation behavior of resorcinarenes for a variety of guest molecules such as triethylamine, sugars, steroids,^{1.12, 1.13, 1.14} amino acids^{1.15} and [2,2,2] cryptand^{1.16} has been investigated.

Having studied the complexation of several cyclohexanediols with resorcinarenes, Aoyama recognized that, among all possible isomers, *cis*-1,4-cyclohexanediol was the most tightly bound. It binds eight times stronger than that of the corresponding *trans* isomer.^{1.17} This *cis/trans* selectivity favors the geometry in which the related *cis*-isomer contains one equatorial hydroxyl and one axial hydroxyl moiety. The rule of 1,4-*cis* selectivity was also extended to carbohydrate complexation.^{1.12} D-ribose was found to be readily extracted into concentrated resorcinarenes solution in CCl₄ although it is essentially insoluble in pure CCl₄. NMR studies indicated that resorcinarenes complex D-ribose only in its α -pyranose form,^{1.12b} which has *cis* oriented -OH groups at C-1 through C-4 (Figure 1.4). 2-Deoxyribose and fucose were more readily extractable than ribose, while xylose could not be extracted at all, although its configuration only differs at the C-3 position. This suggests that, to form stable complexes, the OH at C-2 should

be absent to avoid disfavored exposure to the apolar solvent or else exist in a *cis* relationship with the C-1 and C-4 OHs. Since *trans* 3-OH gave unfavorable steric interactions with one of the aryl rings involved in the binding, it was concluded that it is very important for the 3-OH to be *cis* to the C-1 and C-4 hydroxys also. Hydrophobic substituents on C-5 are preferred because they can interact favorably with the apolar solvent.

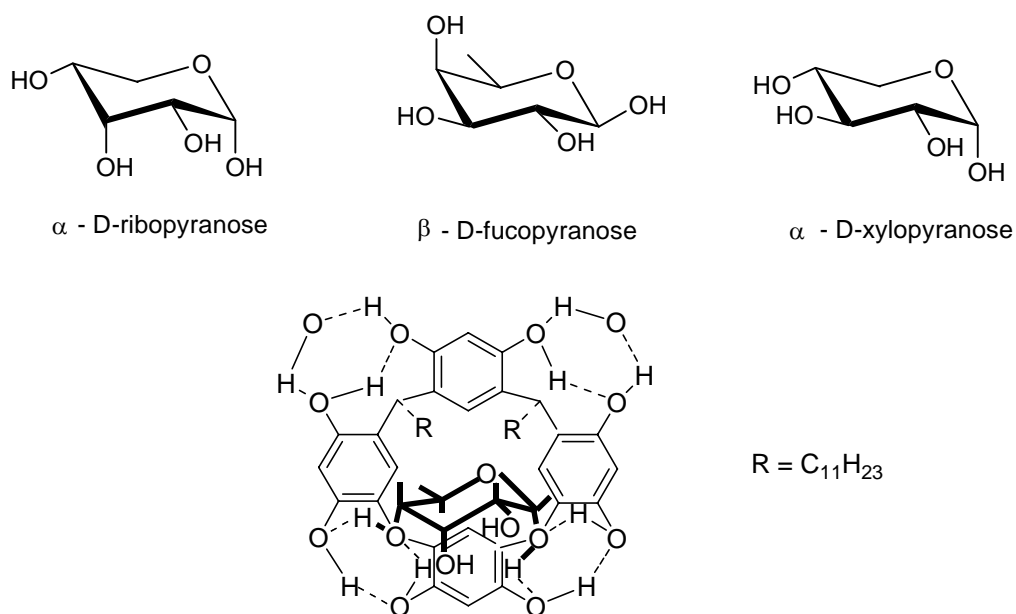


Figure 1.4. Structures of three selected monosaccharides and the complex between a resorcinarene and D-ribose.

Hydrogen bonding has been reported by Aoyama and his co-workers to be the major force for binding to the four pair of hydroxyl groups of the resorcinarenes in apolar organic solvents. Moreover, the interaction between the electron-rich aromatic rings in the host and an aliphatic moiety at the guest (CH- π interactions) also contributes to the binding.^{1.13, 1.18}

In aqueous systems,^{1.15, 1.19} H₂O prevents hydrogen bonding from serving as a driving force for guest complexation. The affinity of resorcinarenes for polar guests is mainly determined by hydrophobic interactions. If the guest molecules are hydrophobic, CH- π interactions play an enhanced role in the binding.^{1.18}

1.3 Complexation of Boronic Acids to Saccharides

Boronic acids have been known since 1880, when Michaelis and Becker first synthesized phenylboronic acid.^{1.20} Although borates have been important for over a century in organic synthesis and were known for polyhydroxyl binding,^{1.21} it wasn't until 1954 that first extensive quantitative binding studies of diols with boronic acids were published.^{1.22}

It is well accepted now that, under neutral nonaqueous or alkaline aqueous conditions, boronic acids form covalent bonds with 1,2- or 1,3-diols to give five- or six-membered ring cyclic esters (Figure 1.5). Compared to acyclic diols such as ethylene glycol, saccharides have been reported to form more stable cyclic esters due to their rigid, cyclic *cis* diol structures, in solution.

Detailed conformational studies of the complexes formed between boronic acids and saccharides were performed by Norrild and later by Nicholls, using ¹H and ¹³C NMR spectroscopy.^{1.23} One can better evaluate the saccharide selectivity of a boronic acid-based sensor with a careful study of the complexes involved, due to the complicated equilibria between saccharides and arylboronic acids. Complexes of *p*-tolylboronic acid and glucose or fructose, as assigned by Norrild are shown in Figure 1.6 and Figure 1.7, respectively.^{1.23(a,b)}

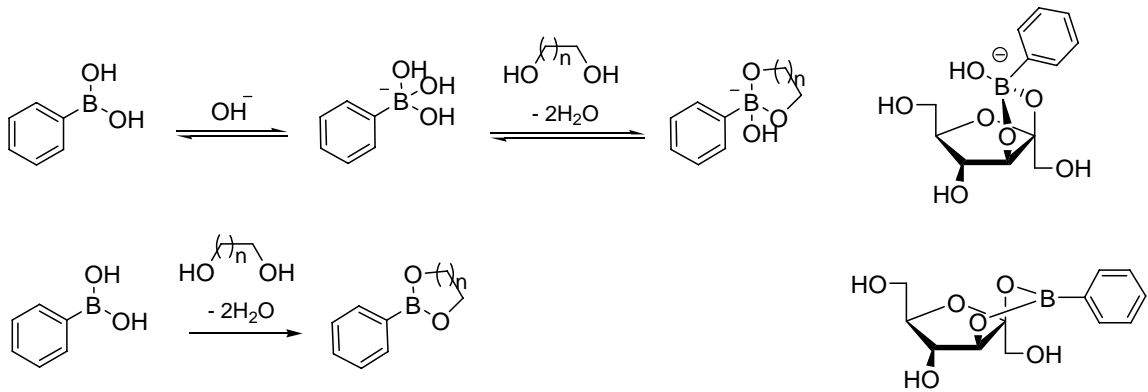


Figure 1.5. Boronate ester formation with phenylboronic acid in alkaline aqueous solution (top) and aprotic media (bottom). Examples of sp^3 and sp^2 complexes between phenyl boronic acid and fructose are included (right).

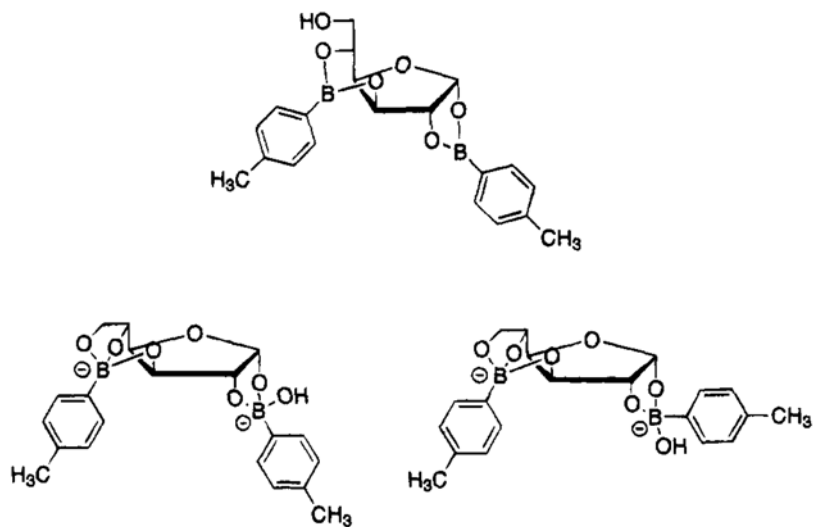


Figure 1.6. Structures of selected complexes between *p*-tolylboronic acid and glucose.

1.4 Significance in Saccharides Detection

Sugar monitoring is vital in diagnosing, understanding and treating disease. A better understanding of glycosylation products and protein-carbohydrate interactions are current goals of biomedical research.^{1,24} Carbohydrates are, however, relatively difficult to analyze. They exhibit a great variety of similar, naturally-occurring structures. They are transparent in the visible spectral region. Several isomeric forms of a specific monosaccharide may be present in equilibrium in solution. Challenges are compounded when studying oligo- and polysaccharides. Glycolipids, glycoproteins and related biomolecules can contain a variety of sugar residues and linkage patterns.

The detection of sugars via arylboronic acid-appended chromophores and fluorophores has shown great promise for monitoring saccharides.^{1,25} A major goal is the determination of specific sugars in natural media. Glucose detection, for example, has been a main focus to date. However, boronic acids are well-known to exhibit relatively high affinity for fructose.^{1,25} In fact, boronic acids sensing agents can, both in principle and practice, bind and signal the presence of most vicinal *cis*-diol-containing sugars; i.e., those which readily form 5-membered ring cyclic boronate ester complexes.^{1,25} Novel methods have been devised to achieve the selective binding and signaling of the presence of specific sugars.^{1,26} Among the most well-known are compounds that contain appropriately spaced chelating *bis*-boronic acids, typically assisted via an interaction with a neighboring amino moiety.^{1,27-1,33} The majority of the synthetic *bis*-boronic acids that are glucose-selective bind the α -furanose conformer.^{1,28} This chelation mechanism is notable, since the α -furanose anomer is present in H₂O only at levels of 0.14 %.^{1,23(b), 1,34}

A *bis*-boronic acid fluorescent receptor has also been designed for the selective detection of the glucose α -pyranose isomer.^{1,36}

There is a complicated equilibrium between even the simplest monosaccharides and aryl boronic acids.^{1,23(b)} Most of the recent mechanistic studies on boronate-based chemosensing have focused on elucidating equilibrium constants and the putative role of boron-nitrogen interactions in signal transduction.^{1,25,1.27-1.33}

The investigation of the relationship between the various equilibrating isomers of sugars and their corresponding boronate complexes is needed in order to fully understand selective signal transduction (*vide supra*). A comparison of the detailed structures of the specific bound complexes has been addressed in relatively few studies.^{1,23} An investigation of the specific regio- and stereochemical patterns of discrete saccharide isomers that result in selective signal transduction in boronic acid chromophores and fluorophores is needed. It would be useful towards predicting and understanding chemoselective signal transduction. The next chapter describes my use of arylboronic acid-appended resorcinarene-derived materials in addressing these issues.

1.5 References

- 1.1 Baeyer, A. *Ber. Dtsch. Chem. Ges.* **1872**, 5, 25. (b) Baeyer, A. *Ber. Dtsch. Chem. Ges.* **1872**, 5, 280.
- 1.2 Botta, B.; Iacomacci, P.; Di Giovanni, C.; Delle Monache, G.; Gacs-Baitz, E.; Botta, M.; Tafi, A.; Corelli, F.; Misiti, D. *J. Org. Chem.* **1992**, 57, 3259; (b) Botta, B.; Di Giovanni, C.; Delle Monache, G.; De Rosa, M. C.; Gacs-Baitz, E.; Botta, M.; Corelli, F.; Tafi, A.; Santini, A.; Benedetti, E.; Pedone, C.; Misiti, D. *Org. Chem.* **1994**, 59, 1532. (c) Benedetti, E.; Pedone, C.; Iacovino, R.; Botta, B.; Delle Monache, G.; De Rosa, M. C.; Botta, M.; Corelli, F.; Tafi, A.; Santini, A. *J. Chem. Research (S)* **1994**, 476.
- 1.3 Pieroni, O. I.; Rodriguez, N. M.; Vuano, B. M.; Cabaleiro, M. C. *J. Chem. Research (S)* **1994**, 188.

- 1.4 Falana, O. M.; Al-Farhan, E.; Keehn, P. M.; Stevenson, R. *Tetrahedron Lett.* **1994**, *35*, 65.
- 1.5 Tunstad, L. M.; Tucker, J. A.; Dalcanale, E.; Weiser, J.; Bryant, J.A.; Sherman, J. C.; Helgeson, R. C.; Knobler, C.B.; Cram, D. J. *J. Org. Chem.* **1989**, *54*, 1305.
- 1.6 Högberg, A. G. S. *J. Org. Chem.* **1980**, *45*, 4498.
- 1.7 Cometti, G.; Dalcanale, E; Du Vosel, A.; Levelut, A.-M. *Liquid Crystals* **1992**, *11*, 93.
- 1.8 Konishi, H.; Iwasaki, Y.; Morikawa, O.; Okano, T.; Kiji, J. *Chem. Express* **1990**, *5*, 869.
- 1.9 Weinelt, F.; Schneider, H.-J. *J. Org. Chem.* **1991**, *56*, 5527.
- 1.10 As a result of this extensive study, resorcinarenes were awarded "reagent of the year in 1993" by Fluka: *J. Org. Chem.* **1993**, *58*, 2A.
- 1.11 a) Aoyama, Y. *Advances in Supramolecular Chemistry* Gokel, G.W., Ed.; JAI Press Inc.: Greenwich, **1992**, *2*, 65. (b) Aoyama, Y. *Trends in Anal. Chem.* **1993**, *12*, 23.
- 1.12 (a) Aoyama, Y.; Tanaka, Y.; Toi, H.; Ogoshi, H. *J. Am. Chem. Soc.* **1988**, *110*, 634. (b) Aoyama, Y.; Tanaka, Y.; Sugahara, S. *J. Am. Chem. Soc.* **1989**, *111*, 5397.
- 1.13 Kobayashi, K.; Asakawa, Y.; Kikuchi, Y.; Toi, H.; Aoyama, Y. *J. Am. Chem. Soc.* **1993**, *115*, 2648 and references cited there.
- 1.14 (a) Kikuchi, Y.; Lobayashi, K.; Aoyama, Y. *J. Am. Chem. Soc.* **1992**, *114*, 1351; (b) Aoyama, Y. *Hydrogen Bonding in Supramolecular Functions, in Supramolecular Chemistry*; Balzani, V., De Cola, L., Eds.; Kluwer Academic Publishers; Dordrecht, **1992**, p 17.
- 1.15 Kobayashi, K.; Tominaga, M.; Asakawa, Y.; Aoyama, Y. *Tetrahedron Lett.* **1993**, *34*, 5121.
- 1.16 Danil de Namor, A. F.; Blackett, P. M.; Garrido Pardo, M. T.; Pacheco Tanaka, A.; Suros Velarde, F. J. *Pure Appl. Chem.* **1993**, *65*, 415.
- 1.17 Kikuchi, Y.; Kato, Y.; Tanaka, Y.; Toi, H.; Aoyama, Y. *J. Am. Chem. Soc.* **1991**, *113*, 1349.
- 1.18 Nishio, M.; Hirota, M. *Tetrahedron* **1989**, *45*, 7201.
- 1.19 Kobayashi, L.; Asakawa, Y.; Kato, Y.; Aoyama, Y. *J. Am. Chem. Soc.* **1992**, *114*, 10307 and references cited therein.

- 1.20 Michaelis, A. Becker, P. *Ber. Dtsch. Chem. Ges.* **1880**, *13*, 58.
- 1.21 (a) J. Böesken, V. Rossem, *Recl. Trav. Chim. Pays-Bas Belg.* **1912**, *30*, 392; (b) J. Böesken, *Ber. Dtsch. Chem. Ges.* **1913**, *46*, 2612.
- 1.22 H. G. Kuivila, A. H. Keough, E. J. Soboczanski, *J. Org. Chem.* **1954**, *19*, 780.
- 1.23 (a) Norrild, J. C.; Eggert, H. *J. Am. Chem. Soc.* **1995**, *117*, 1470. (b) Norrild, J. C.; Eggert, H. *J. Chem. Soc., Perkin Trans 2* **1996**, 2583. (c) Nicholls, M. P.; Paul, P. K. C. *Org. Biomol. Chem.* **2004**, *2*, 1434.
- 1.24 Recent Review: Pohl, N. L. *Current Opinion in Chemical Biology* **2005**, *9*, 76.
- 1.25 Reviews: (a) James, T. D.; Shinkai, S. *Top. Curr. Chem.* 2002, *218*, 159. (b) Wang, W.; Gao, X.; Wang, B. *Curr. Org. Chem.* **2002**, *6*, 1285.
- 1.26 *J. Fluoresc.* **2004**, *14*, entire issue.
- 1.27 James, T. D.; Sandanayake, K. R. A. S.; Iguchi, R.; Shinkai, S. *J. Am. Chem. Soc.* **1995**, *117*, 8982.
- 1.28 James, T. D.; Linnane, P.; Shinkai, S. *Chem. Commun.* **1996**, 281.
- 1.29 Eggert, H.; Frederiksen, J.; Morin, C.; Norrild, J. C. *J. Org. Chem.* **1999**, *64*, 3846.
- 1.30 Karnati, V. V.; Gao, X.; Yang, W.; Ni, W.; Sankar, S.; Wang, B. *Biomed. Chem. Lett.* **2002**, *5*, 4615.
- 1.31 Norrild, J. C.; Sotofte, I. *J. Chem. Soc., Perkin Trans 2* **2002**, 303.
- 1.32 Gao, X.; Zhang, Y.; Wang, B. *Org. Lett.* **2003**, *5*, 4615.
- 1.33 Yang, W.; Yan, J.; Springsteen, G.; Deeter, S.; Wang, B. *Biomed. Chem. Lett.* **2003**, *13*, 1019.
- 1.34 Norrild, J. C.; Eggert, H. *J. Am. Chem. Soc.* **1995**, *117*, 1470.
- 1.35 Maple, S. R.; Allerhand, A. *J. Am. Chem. Soc.* **1987**, *109*, 3186.
- 1.36 Norrild, J. C.; Eggert, H. *J. Chem. Soc., Perkin Trans 2* **1996**, 2583.

CHAPTER 2

MECHANISTIC STUDIES AND THE SELECTIVE SPECTROPHOTOMETRIC DETECTION OF SACCHARIDES WITH A RESORCINARENE BORONIC ACID*

2.1 Background of Resorcinarene Color Formation

The spectrophotometric properties of resorcinarenes in the visible region have been rarely investigated since its initial synthesis by Baeyer. Condensation of commercially available 4-formylphenyl boronic acid and resorcinol gives rise to the resorcinarene boronic acid stereoisomers **2.1** and **2.2a** (Figure 2.1) in one step in a combined 90% yield.^{2,1}

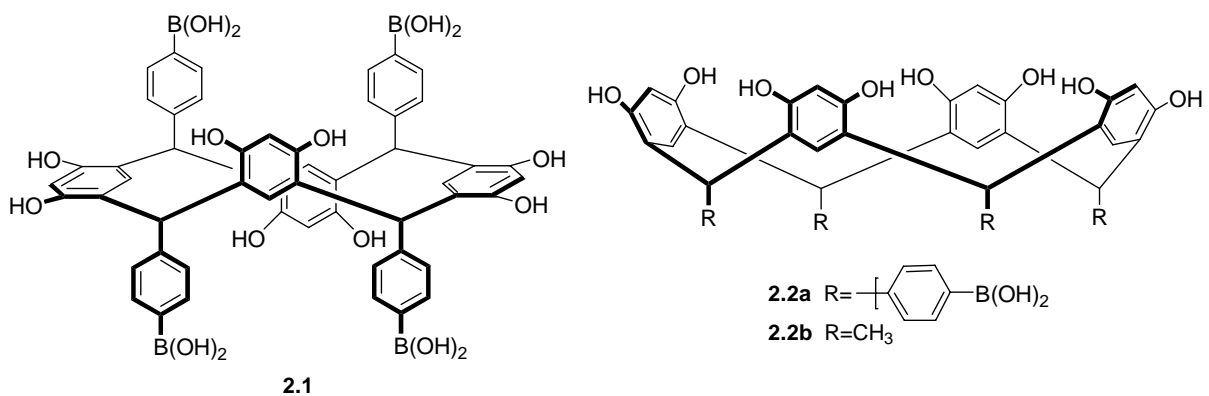


Figure 2.1. Chair (**2.1**) and crown (**2.2a**) stereoisomers of tetraarylboronic acid resorcinarenes.

*Reprinted in part with permission from *Journal of the American Chemical Society*, 2006, Volume 128, pages 12221-12228; Shan Jiang, Jorge O. Escobedo, Kyu Kwang Kim, Onur Alpturk, George K. Samoei, Sayo O. Fakayode, Isiah M. Warner, Oleksandr Rusin, and Robert M. Strongin; Stereochemical and Regiochemical Trends in the Selective Detection of Saccharides. Copyright 2006 American Chemical Society.

It was reported by our research group that solutions containing resorcinarene macrocycles develop color upon heating or standing. Pinkish-purple color is developed upon heating the colorless DMSO solutions of freshly crystallized **2.1** or **2.2a** at 90 °C for 1 min, (5.2 mM), or standing for several hours.^{2,2} The solution color formation was monitored via UV-vis spectroscopy. Strong evidence has been amassed to prove that the color formation is primarily due to xanthene formation via macrocycle ring opening and oxidation.

Extensive experiments were conducted by Dr. Strongin's group in order to understand the origin of the solution color.^{2,2} Upon heating solutions of **2.1** in the dark or in O₂ degassed conditions, relatively diminished solution color was observed, as evidence by both visual inspection and UV-vis spectroscopy.^{2,3} On the other hand, when a solution of acylated **2.1** (at the phenolic hydroxyls) was heated to reflux, the solution remained colorless.^{2,2} Solutions of phenylboronic acid or resorcinol were also tested by heating as an equimolar mixture or separately using the above mentioned conditions and concentrations, with and without added monosaccharides. Only very faint colors in solution were visually observed in these cases,^{2,3} showing that a methine-bridged resorcinol/aldehyde architectural framework may be needed for effective chromophore formation. Methine-bridged condensation products of resorcinarene and aldehyde substructures, such as compounds **2.3a-c** listed in Figure 2.2, were noted as reaction intermediates in standard xanthene dye syntheses (e.g., the transformation of **2.5** to **2.6**, n=m=0, Figure 2.3) in older work.^{2,4} It was concluded from all of these initial studies that the chromophore arises via oxidation of a resorcinol moiety to a quinone^{2,3,2,5} (Figure 2.3).

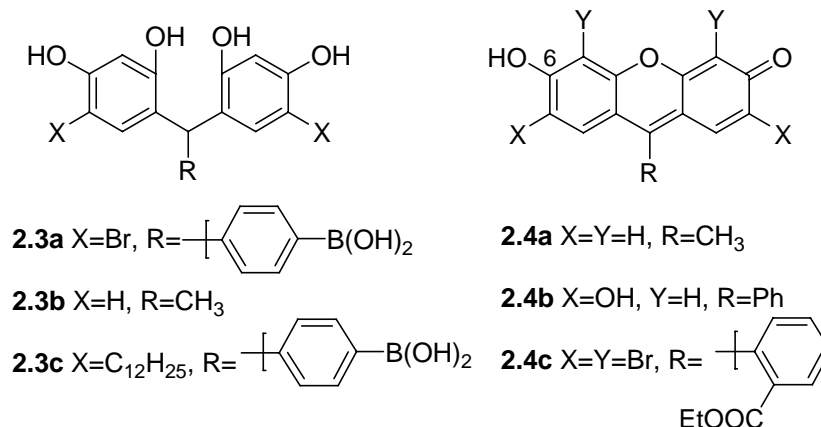


Figure 2.2. Resorcinarene substructures of methine-bridged condensation products (**2.3**) and some xanthene dyes (**2.4**).

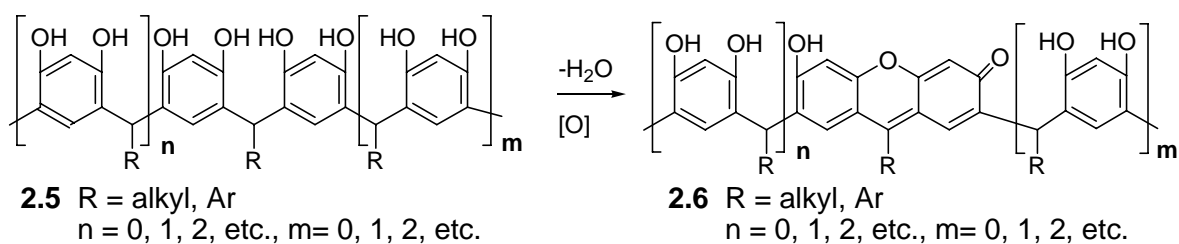


Figure 2.3. Dehydration and oxidation of methine-bridged resorcinol oligomers leading to xanthenes.

Xanthenes, such as **2.4a**, **2.4b** and **2.4c** (Figure 2.2) are some of the oldest known synthetic dyes. The colorimetric properties of xanthenes are derived from the ionization state of the C-6 OH moiety.^{2.6} They typically exhibit two absorbance maxima in the visible region, i.e. λ_{\max} at 530 nm and a less intense λ_{\max} at 500 nm in 9:1 DMSO:H₂O.^{2.6} The absorption spectrum of **2.4b** (5.0×10^{-6} M) in 9:1 DMSO:H₂O is shown in Figure 2.4. The spectral features and λ_{\max} absorbance values are similar to those observed for DMSO solutions of **2.1** as previously reported.^{2.5}

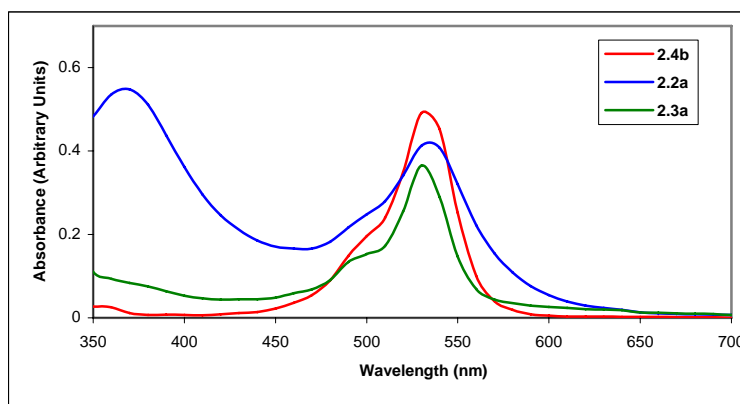


Figure 2.4. **2.2a** (1.0 mg) and **2.3a** (1.0 mg) each in 0.9 mL DMSO were heated to gentle reflux over two minutes and cooled to room temperature before 0.1 mL H₂O was added to each solution. The final concentrations of **2.2a** and **2.3a** in 9:1 DMSO:H₂O are 1.03×10^{-3} M and 1.96×10^{-3} M respectively. A solution of **2.4b** (5.0×10^{-6} M) was prepared at rt in 9:1 DMSO:H₂O.

Incorporation of a planar xanthene moiety within a cyclic resorcinarene via the transformation shown in Figure 2.3 would result in a dramatic strain energy increase. Simulations (Sybil 6.6) showed that to form a xanthene substructure within **2.2b** will lead to a 34.2 kcal/mol strain energy increase. This result is in accordance with the prior reported studies of the structure related calixarenes (macrocycles formally derived from phenol/formaldehyde condensations).^{2,7}

Ring opening to acyclic oligomers would therefore be a prerequisite for formation of xanthene from resorcinarenes. It has been proven that the condensation between resorcinol and aldehyde to produce resorcinarene is reversible under acidic conditions due to the detailed mechanism studies of macrocycle genesis by Weinelt and Schneider.^{2,8, 2,9} They found that **2.2b** and its stereoisomers interconverted through the ring opening and re-closing processes in MeOH in the presence of anhydrous HCl. Evidence from NMR, HPLC and especially X-ray crystallography, indicates the

formation of $(\text{CH}_3)_3\text{S}^+\text{CH}_3\text{SO}_3^-$ under the conditions used to develop resorcinarene chromophores.^{2,10} This compound was produced from a thermolysis reaction of **2.2b** in DMSO. It is known that $(\text{CH}_3)_3\text{S}^+\text{CH}_3\text{SO}_3^-$ forms along with acids $\text{CH}_3\text{SO}_3\text{H}$, $\text{CH}_3\text{SO}_2\text{H}$, CH_3SOH and several other products via the decomposition of DMSO.^{2,11} Apparently these acids catalyze the ring opening process which leads to the eventual chromophore formation.

The thermolysis of a **2.2b** DMSO solution produces stereoisomer **2.7** (Figure 2.5) which requires breaking and re-forming of two covalent bonds starting from **2.2b**.^{2,2} This is evidence for the formation of **2.5**.

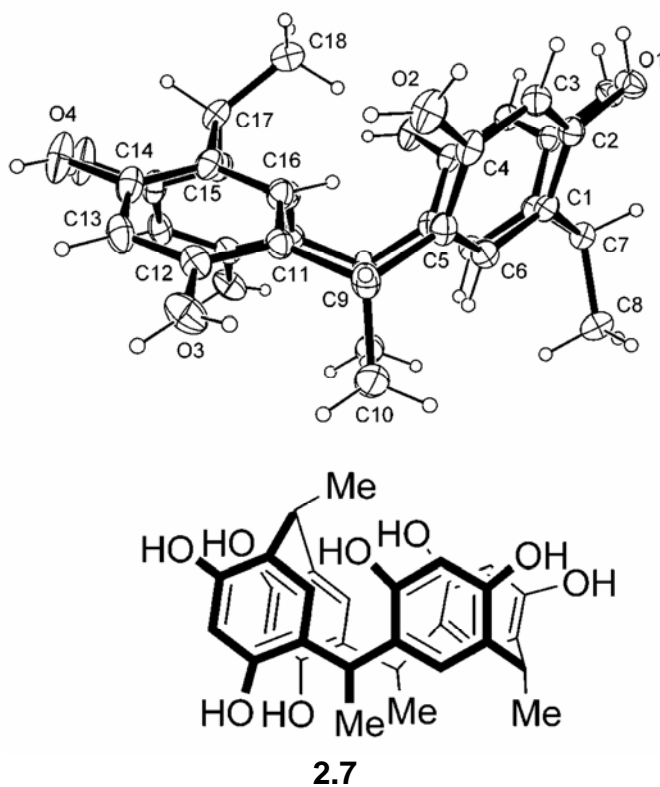


Figure 2.5. Compound **2.7** and Oak Ridge Thermal Ellipsoid Plot (ORTEP).

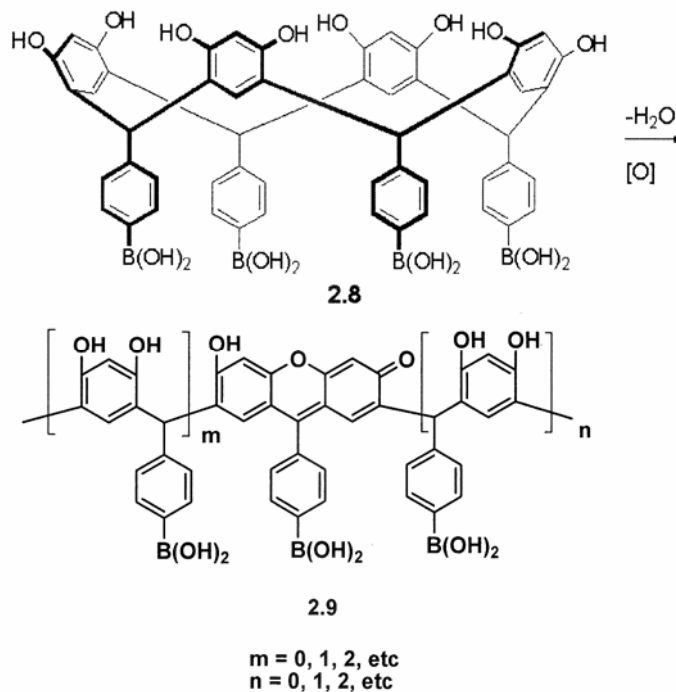
Experimental evidence for the formation of various xanthene dye derivatives from the thermolysis of **2.2b** is also provided by the Strongin group. Table 2.1 shows mass spectrometric data for the presence of higher homologues of **2.5** (entries 1 and 2) and xanthene materials **2.6** (entries 4-6).^{2,9} Consequently, the acyclic xanthene oligomers form during an acid-catalyzed reverse condensation reaction of resorcinarene macrocycles (Figure 2.3).

Table 2.1. MALDI MS of acyclic oxidized and unoxidized products from the thermolysis of **2.2b**.

Entry	Structure	TLC R _F	(<i>m/z</i>) calcd	(<i>m/z</i>) obsd
1	2.5 , R=Me, m=1, n=0	0.29	382.41	381.89
2	2.5 , R=Me, m=3, n=2	0.44	926.36	926.28
3	2.4 ^a	0.44	226.23	225.61
4	2.6 , R=Me, m+n=4	0.26	906.01	906.33
5	2.6 , R=Me, m+n=3	0.84	770.79	770.82
6	2.6 , R=Me, n=1, m=0	0.79	362.51	361.38

Solutions containing millimolar concentrations of compound **2.8** develop micromolar levels of chromophore **2.9** *in situ* have been reported (Scheme 2.1).^{2,2} The colored material **2.9** enabled saccharide detection via UV-Vis or fluorescence spectroscopy. Further spectroscopic studies proved that the formation of anionic sugar-boronate complexes of **2.9** result in the sugar-induced spectral changes as boron becomes a charged sigma bond donating group to the chromophore moiety.^{2,2}

Scheme 2.1. The *in situ* ring opening of resorcinarene boronic acid macrocycle **2.8** affords acyclic oligomers (**2.9**) containing xanthene chromophores.



The selective colorimetric detection of fructose in neutral media at rt was later studied. Under the conditions used, it was concluded that concurrent fructose and glucose signaling may be achieved via dual wavelength monitoring when a large (100-fold) excess of glucose:fructose is present in solution. Additionally, fluorescence emission for glucose and fructose was discovered. In the fluorescence measurements, glucose solution emission was moderately enhanced compared that of to fructose-containing solutions. The emission intensity enhancement was ascribed to structural rigidification of **2.9** via bis-boronate chelation of glucose.^{2,13}

Having already proven (i) the origin of the chromophore **2.9** and (ii) the general signal transduction mechanism promoted by sugar binding, the main goal of the work

described herein is to clearly define the stereo- and regiochemical requirements for attaining selectivity induced by specific saccharides. Towards this end I tested two hypotheses.

The first hypothesis is that the very high degree of fructose selectivity previously reported by our group is due to a synergy between colorless **2.8** and colored **2.9**. I have examined cooperative binding interaction between **2.8**, **2.9** and the sugar in detail. Clearly understanding structure-activity relationships is very important for us to formulate hypotheses about sensing methods in natural media. I demonstrate a potentially practical application via the selective detection of fructose in a commercial honey sample. I also show that the mechanistic findings can be applied towards the selective detection of bioactive disaccharides for which there are currently no comparable assays.

The second hypothesis is that receptor mixtures may be designed for improved detection of specific analytes based on complementary chemosensor absorptions and selectivities for saccharide mutarotational isomeric forms. Progress is described, using ribose and the rare bioactive sugar allose as target analytes. A boronic acid-based sensor selective for ribose and allose functioning with no interference from fructose and other commonly encountered monosaccharides has not been previously described. Detailed information for ribose and its derivatives' selectivity is described in Chapter 3.

2.2 Results and Discussion

Aryl monoboronic acid compounds are well-known to exhibit relatively very high affinity for fructose as compared to other monosaccharides. Recent examples of monoboronic acid-containing chemosensors reveal that relative affinities towards other

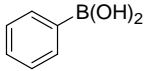
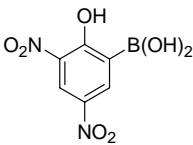
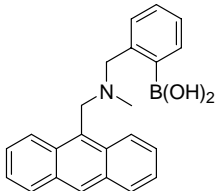
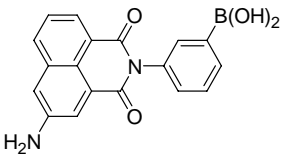
specific saccharides may vary based on receptor structure and conditions.^{2.15} Solutions of resorcinarene boronic acids can exhibit color changes that are highly selective for fructose at room temperature.^{2.22} In the present study, a unique degree of colorimetric selectivity for fructose is attained as compared to several other sugars initially dissolved in neutral buffered media. Many of the analytes investigated include those which are major components in honey (Figure 2.6).^{2.25} The lack of significant colorimetric response to potentially interfering saccharides offers promise towards developing a non-enzymatic fructose assay (*vide infra*).

Colored solutions (60 mM phosphate buffer, pH 7.4, 1:9 H₂O:DMSO) of **2.8** and trace **2.9** display observable color changes (light red to yellow) not only in the presence of D-fructose, but also with D-galactose, D-arabinose and D-altrose (which are not present in honey, Figure 2.7). Under our current conditions involving buffered media, the UV-Vis absorbance changes are monitored at both 355 nm (previous work in aqueous DMSO entailed measurements at 460 nm^{2.2, 2.13}) and 535 nm. No significant color changes are observed in response to D-glucose, D-ribose and D-allose.



Figure 2.6. A selective solution color change is observed for D-fructose when added to colored solutions of **2.8** and **2.9**: (a) D-fructose, (b) D-glucose, (c) D-psicose, (d) D-allose, (e) D-ribose, (f) D-xylose, (g) D-trehalose, (h) melezitose, (i) D-turanose, (j) D-maltose, (k) sucrose, (l) D-raffinose. Sugars in vials labeled a, b and g-l are found in honey.

Table 2.2. Selectivity of arylboronic acid chemosensors to various monosaccharides.

Compound	Selectivity	Conditions	Method	Ref
	D-fructose > D-tagatose > L-arabinose > D-ribose > D-galactose > D-xylose > D-mannose > D-glucose > maltose > lactose > sucrose	phosphate buffer pH 7.4	UV-Vis	2.17
	D-fructose > D-glucose > D-galactose	phosphate buffer pH 7.4.	UV-Vis	2.18
	D-fructose > D-allose > D-galactose > D-glucose	MeOH:H ₂ O medium (1:2)	fluorescence	2.19
	D-galactose > D-glucose > D-fructose	DMSO- phosphate buffer pH 4.0	Fluorescence	2.20

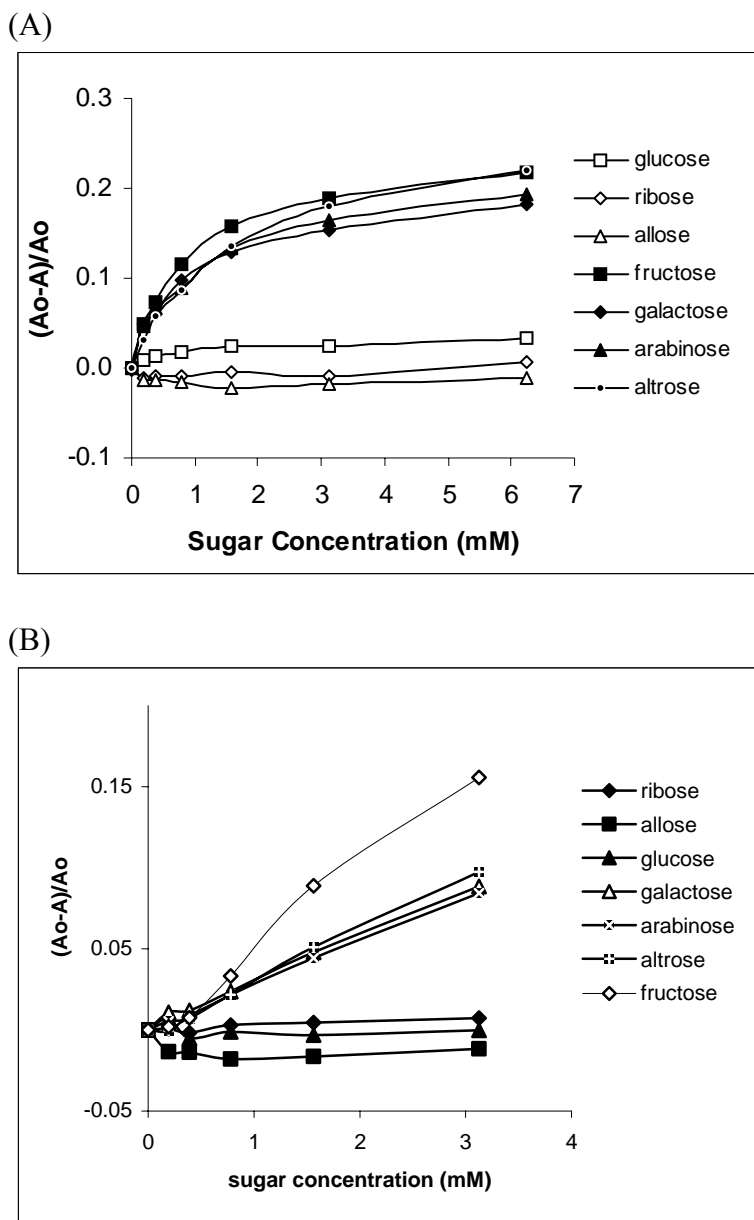


Figure 2.7. Plots of relative absorbance changes vs. concentration of various sugars in solutions comprised of phosphate buffer (0.1 mL, 60 mM, pH = 7.4) added to **2.8** in DMSO (3.4 mM, 0.9 mL) at 355 (A) nm and (B) 535 nm.

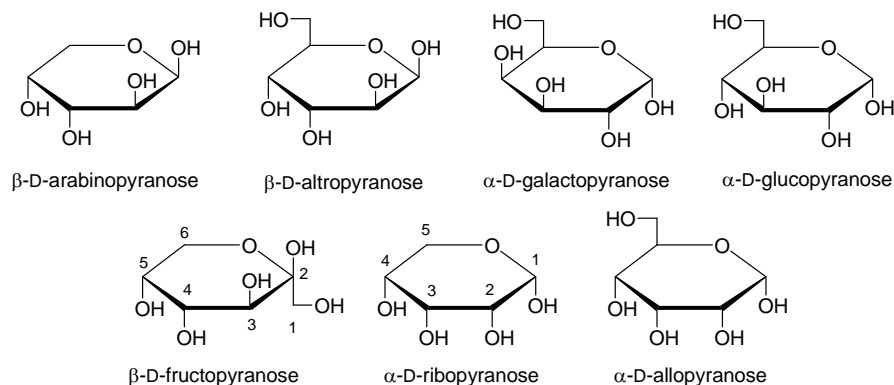
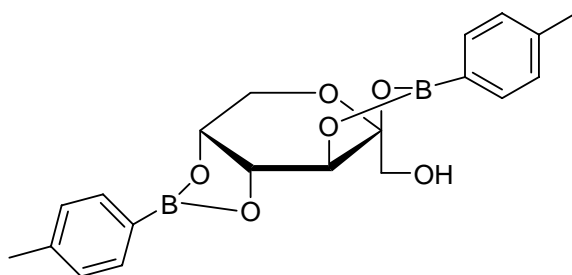


Figure 2.8. Pyranose forms of sugars used in the study shown in Figure 2.7. Only those compounds containing pairs of vicinal *cis*-diols on opposite faces of the pyranose ring (i.e., ribose, altrose, galactose and fructose) afford colorimetric responses.

D-Glucose, D-ribose and D-allose, however, should readily form cyclic boronate esters and thus are expected to induce spectrophotometric changes.^{2.15} For example, the reported stability constants of model arylboronate complexes of ribose and arabinose are 1.38 and 1.40, respectively.^{2.16} The degree of complexation of ribose and arabinose is 65 % and 74 %.^{2.16} Based on these facts alone, one would predict ribose to afford a spectrophotometric response similar to that of arabinose. In fact, all seven monosaccharides shown in Figure 2.8 should promote significant colorimetric signaling, based on their known affinities to model arylboronic acids.^{2.15, 2.16} Moreover, the relative selectivities I observe in Figure 2.7 for the specific sugars studied does not correspond to known related chemosensing agents (for example, compare to Table 2.2).^{2.15, 2.16} The mechanism of signal transduction in colored solutions of **2.8** and **2.9** thus merited further examination.

Analysis of Pyranose Structures. A comparison of the pyranose forms of each of the sugars used in the studies reveals that each saccharide affording a colorimetric response possesses two distinct pairs of vicinal *cis*-diols, each of which resides on

opposite faces of the monosaccharide ring. In contrast, α -ribopyranose and α -allopyranose possess contiguous *cis*-tetrol configurations but do not promote absorbance responses. The α -glucopyranose structure also exhibits a single vicinal *cis*-diol pair for cyclic boronate formation. However, glucose is not readily detectable under our current conditions. Interestingly, our research group previously determined the apparent equilibrium constant ($K_{\text{exp}}(\text{app})$) to be 65.0 in colored DMSO:H₂O solutions of **2.8** and glucose in buffered media at room temperature.^{2,2}



2.10

Table 2.3. Proportions (%)[*] of fructose p-tolyboronic acid complexes and free fructose isomers in (CD₃)₂SO. Equilibrium mixtures at different boronic acid:fructose ratios.^{2,21}

Boronic acid : fructose ratio	1:1	2:1	4:1
β -D-fructose 2,3:4,5-bis(<i>p</i> -tolylboronate) (2.10)	6	33	67
β -D-fructose 2,3 (<i>p</i> -tolylboronate)	46	47	28
α -D-fructose 1,3 (<i>p</i> -tolylboronate)	5	5	2
β -D-fructose 1,2 (<i>p</i> -tolylboronate)	8	5	2
α -D-fructose 1,3 (<i>p</i> -tolylboronate)	4	3	1
β -D-fructopyranose	7	-	-
β -D-fructofuranose	11	2	-
α -D-fructofuranose	5	-	-

[*] relative to total amount of complexes and free fructose.

The observed pattern of structure and signaling might be rationalizable in the context of earlier NMR-based studies by Norrild and Eggert^{2,21} and more recent findings by Nicholls.^{2,16} Norrild reported that the abundance of complex **2.10** in DMSO solutions is a function of the ratio of arylboronic acid moieties:fructose (Table 2.3).^{2,21} Importantly, the analogous *bis*-boronic acid-fructose complex was also assigned (as well as several other complexes, *vide infra*) via ¹³C NMR (peak at C-2 resonating at 105.0 ppm) in our laboratory during prior extensive studies of the interactions between **2.8** and fructose in 1:9 D₂O:(CD₃)₂SO solutions.^{2,2}

In order to afford a visual signal, chromophore **2.9** must be involved in the binding process. An intermolecular ternary *bis*-boronate complex between two molecules of chromophore **2.9** and fructose may form. However, colorless **2.8** is present in very large excess compared to **2.9**.^{2,2} A predominant chromophoric complex responsible for fructose-promoted signal transduction would thus embody a ternary complex **2.11** (Figure 2.9), formed from colorless **2.8**, fructose and chromophore **2.9**.

Recently, Nicholls reported that certain saccharides, such as fructopyranose and galactopyranose, can adopt twist conformations upon boron complexation.^{2,16} This reduces the C-O torsion angles in the O-C-C-O bonds in each of the two pairs of boronic acid-binding vicinal *cis*-hydroxyls (Figure 2.9). In other words, it allows each binding vicinal hydroxyl pair to assume a more eclipsed conformation. This aids in 5-membered ring cyclic boronate ester formation.^{2,16}

Our molecular simulations of **2.11** are in excellent agreement with those findings reported employing other arylboronates.^{2,16} Figure 2.9 shows fructose bound to **2.8** and **2.9**. The AM-1 calculated structure shows β-fructopyranose in a twist conformation.

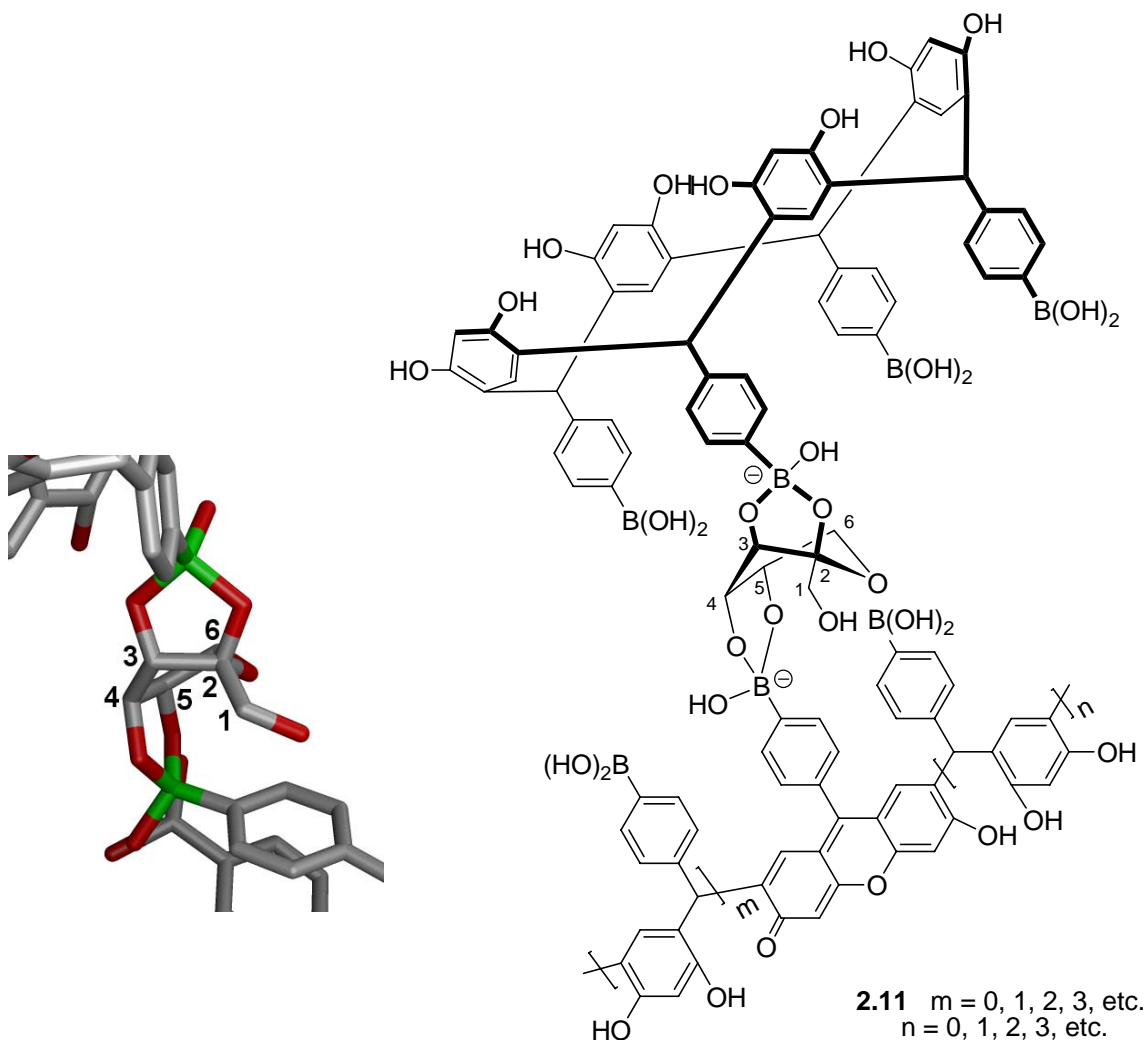


Figure 2.9. Left: Representation of the complete structure of complex **2.11**. Right: Expansion showing the fructopyranose region of the AM-1 simulated structure of one isomeric *bis*-boronate complex **2.11**, showing fructose in a twist conformation.

Formation of a sterically unencumbered, colored ternary bis-boronate complex via the binding of two receptors is favored only in cases where the second *cis*-diol pair of the sugar resides on the opposite face of the pyranose ring. For instance, ternary complex formation involving ribopyranose, containing a contiguous *cis*-tetrol (Figure 2.8), would be too sterically hindered. Thus, on the basis of this analysis, no colorimetric response should be observed for ribose and related monosaccharides such as allose.

Glucopyranose contains only one vicinal *cis*-diol. According to this analysis, it should bind colorless **2.8** but not have an available *cis*-diol for chromophore binding.

Di- and Trisaccharides. Since two pairs of properly spaced vicinal *cis*- diols are needed to promote signal changes, I expected that the analogous oligosaccharide-induced signaling should occur in cases where each terminal sugar residue possesses a vicinal *cis*-diol. For example, lactulose (Figure 2.10) possessing a pair of vicinal *cis*-diols on each residue can be readily detected. However, this analysis does not appear to be valid since lactose, which contains available vicinal *cis*-diols on each residue, does not afford an appreciable signal change under our conditions. Furthermore, maltulose, which possesses a *cis*-diol only on one terminus, also promotes significant signaling (Figures 2.11 and Figure 2.12). Fluorescence spectra give the same trend as produced from UV-Vis. (Figure 2.13). Hence, hypothesis one may not be applicable to all cases.

Analysis of Furanose Structures. Tridentate complexation can involve addition of a fourth ligand to boron deriving from the sugar moiety. It is well-known that the hybridization change from an sp^2 neutral boronate (sugar binds via two hydroxyls) to an sp^3 anionic boronate (sugar binds via three hydroxyls, or two hydroxyls with a water or hydroxide molecule serving as the fourth ligand to boron) results in signal transduction in conjugated systems.^{2.2, 2.15} Cyclic boronate ester formation leads to the enhanced Lewis acidity of boron, due to its constraint in a ring structure, thereby heightening its reactivity and inter- or intramolecular addition of a nucleophile. In the case of **2.9**, boronate anion formation produces a solution color change via σ -bond electron donation which alters the ionization state of the dye.^{2.2}

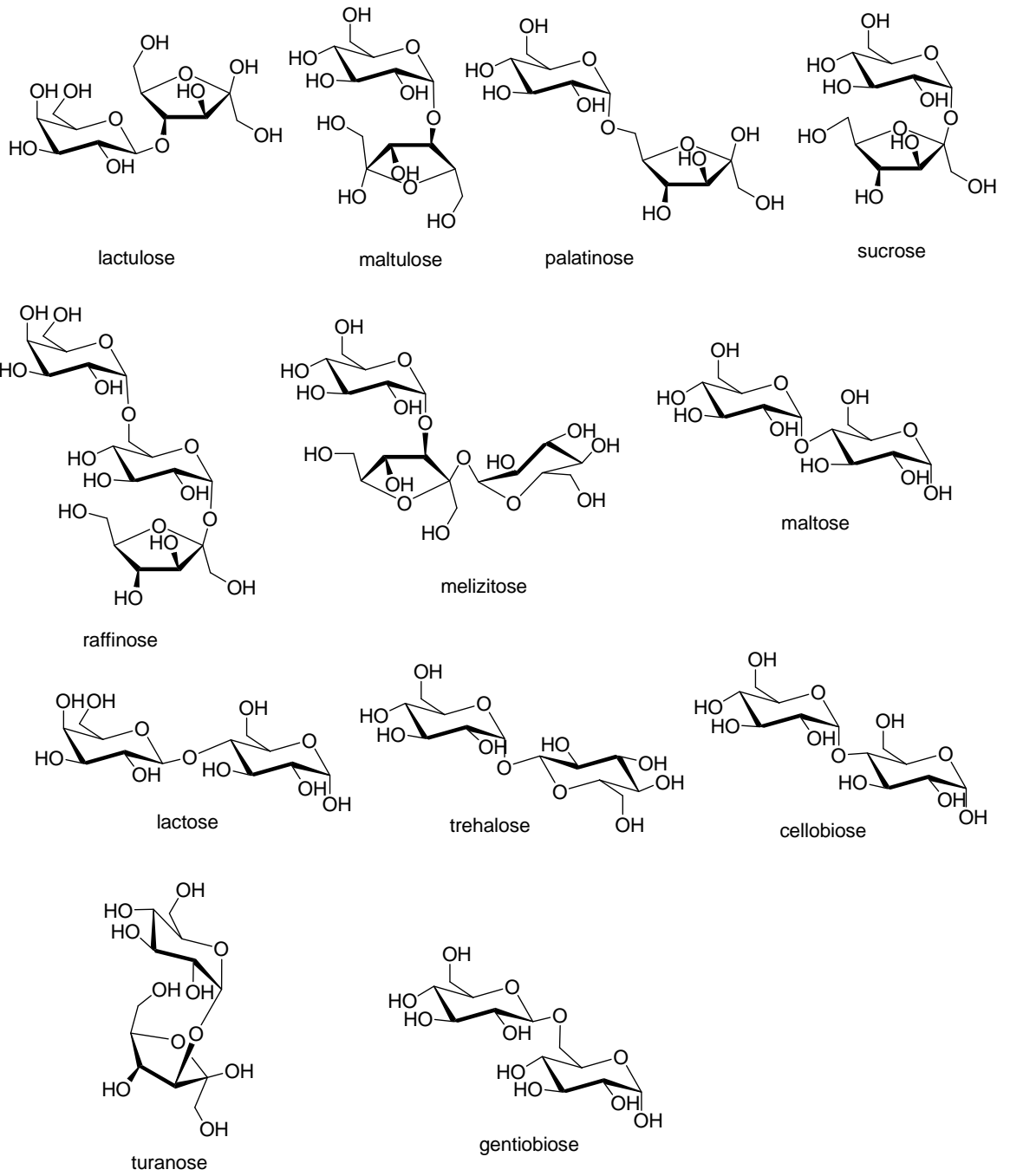


Figure 2.10. Di-and trisaccharides studied.

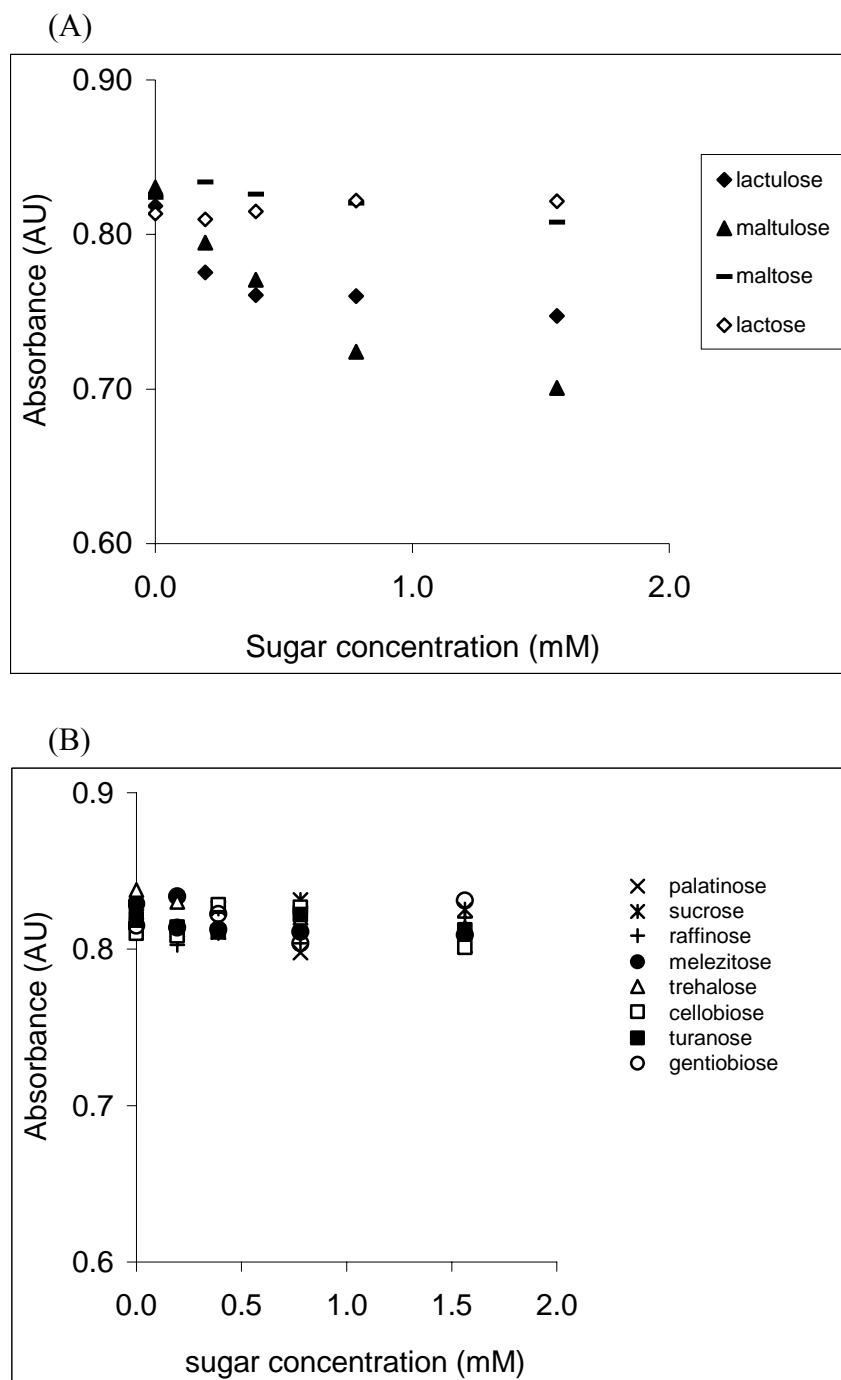


Figure 2.11. (A) Concentration *vs.* absorbance spectral responses at 355 nm of four of the disaccharides shown in Figure 2.10. (B) Concentration *vs.* absorbance spectral responses at 355 nm of eight of the disaccharides shown in Figure 2.10. The largest spectral responses of all of the sugars in Figure 2.10 are observed for lactulose and maltulose solutions. The UV-Vis spectra of the remaining di- and trisaccharides shown in Figure 2.10 exhibit no significant spectral responses at 355 nm or 535 nm (see also Figure E1 of Appendix E).

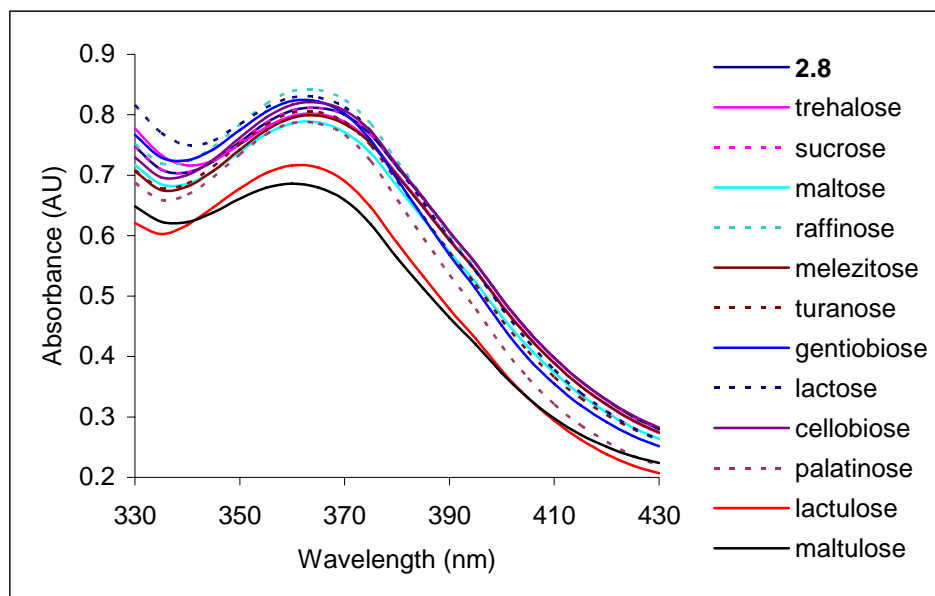


Figure 2.12. UV-Vis spectra responses of a solution of **2.9** ($1 \times 10^{-3} M$) and **2.8** with added di- and trisaccharides ($5 \times 10^{-3} M$), all in 9:1 DMSO:phosphate buffer (0.06 M, pH 7.4) of the disaccharides shown in Figure 2.10.

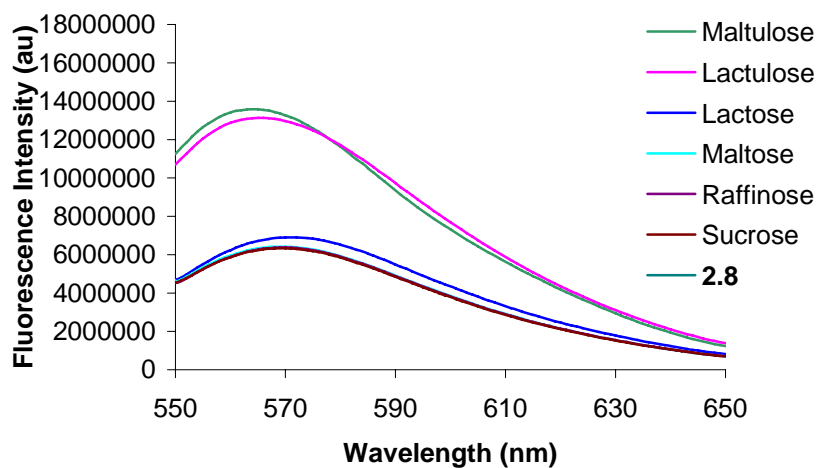


Figure 2.13. Fluorescence emission spectra of a solution of **2.8** ($1 \times 10^{-3} M$) and **2.8** with added di- and trisaccharides ($1.85 \times 10^{-3} M$), all in 9:1 DMSO:phosphate buffer (0.05 M, pH 7.4) excited at 535 nm. This result shows the selectivity for lactulose and maltulose. The other di- and tri saccharides tested afford no detectable signal. Only lactulose and maltulose can adapt the proper terminal residue configurational preference.

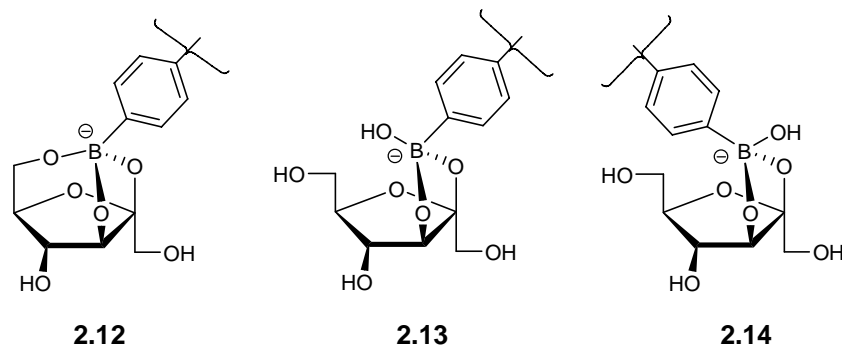


Figure 2.14. Anionic fructofuranose-boronate ester structures.

Previously our research group reported ^{13}C NMR evidence for the occurrence of a distinct intramolecular tridentate fructose complex (**2.12**, Figure 2.14) in $\text{D}_2\text{O}/\text{DMSO}$ solutions.^{2,2} The analogous tridentate structure also occurs in significant proportions compared to other complexes in aqueous alkaline solutions of fructose and model arylboronic acids.^{2,21} The use of the neutral buffer 9:1 $\text{DMSO}:\text{H}_2\text{O}$ solvent system in the current study diminishes the formal intermolecular addition of solution-derived hydroxide to the sugar-boronate complex (resulting, for instance in **2.13** and **2.14**, after subsequent deprotonation), as our research group have clearly demonstrated previously in related systems^{2,22} by limiting the availability and reactivity of the external hydroxide nucleophile.

Thus, in more basic solutions, any sugars possessing at least one vicinal *cis*-diol should more readily produce a signal due to intermolecular hydroxide addition. Selectivity should be diminished due to the increased levels of hydroxide. Glucose, allose and ribose indeed afford significant spectral responses in 9:1 $\text{DMSO}:\text{H}_2\text{O}$ wherein the aqueous portion is adjusted to pH 10 (Figure 2.15, compare to Figure 2.7, A).

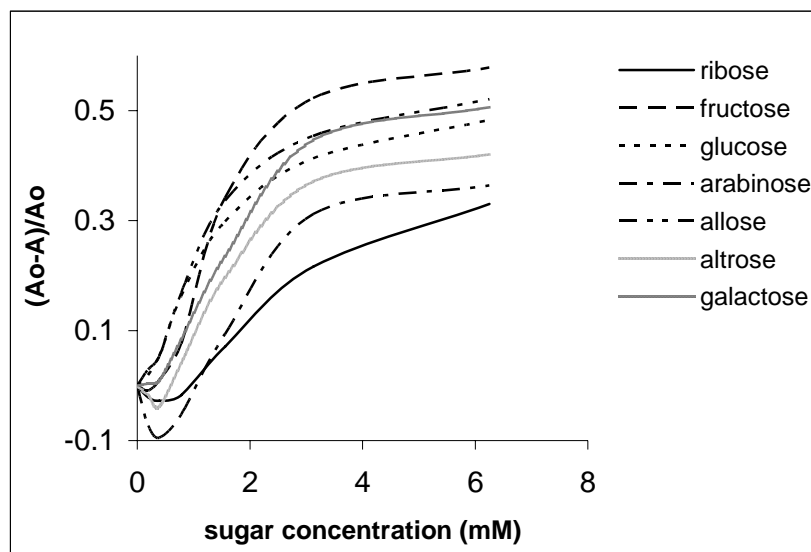


Figure 2.15. Plots of relative absorbance changes at 355 nm vs. the concentration of various sugars in solutions comprised of carbonate buffer (0.1 mL, 40 mM, pH = 10.0) added to **2.8** in DMSO (3.4 mM, 0.9 mL) at 355 nm. Analogous trends in absorbance changes vs. concentration are also observed at 535 nm.

The ability of fructose to form tridentate structures should be favored due to the well-known reactivity of the anomeric (and adjacent) hydroxyl. Additionally, the relatively nucleophilic primary hydroxyl of β -fructofuranose is suitably positioned to also react with boron (Figure 2.14, **2.12**). Importantly, galactose, arabinose and altrose, which also promote spectral responses under neutral conditions (Figure 2.8) possess a furanose structure similar to that of β -fructofuranose, wherein the same three binding OH-groups (anomeric and adjacent as well as the primary hydroxyl) have analogous relative configurations (Figure 2.16). The saccharides that possess other configurations of these three specific hydroxyls in their furanose forms do not afford significant signal changes. To test this hypothesis, I also examined lyxose, mannose and tagatose. Each of these sugars may adopt furanose structures wherein the three binding hydroxyls (on the 1,2 and 5 carbons in the case of aldoses and on the 2,3 and 6 carbons for ketoses) are all on the same face of the furanose ring for cooperative binding to boron. As expected, each of these sugars induced signaling that was selective over psicose, xylose, ribose, glucose and allose (Figure 2.17) which cannot adopt the requisite furanose structures.

I therefore attribute the selective detection of lactulose and maltulose to the configurations of their terminal fructose residues which can embody furanoses with a favorable orientation of their three key hydroxyls. Three hydroxyl groups that can participate in cooperative binding to form an anionic boronate complex must be positioned on the same face of the monosaccharide to induce signaling, according to furanose structure analysis. Lactulose and maltulose are important disaccharides as a prebiotic oligosaccharide in milk^{2,23} and as a marker of digestive disorders in infants,^{2,24} respectively. This finding may help serve as the basis of analyses derived from specific

linkage patterns as well as the precise stereo- and regiochemistry of terminal sugar residues of oligosaccharides.

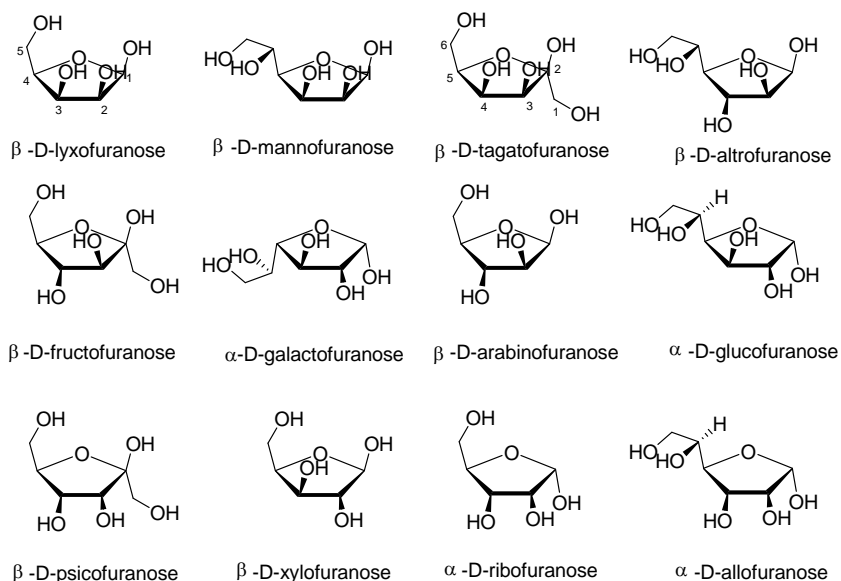


Figure 2.16. Furanose forms of sugars. Only aldoses with hydroxyls on carbons 1,2 and 5, and ketoses with hydroxyls on carbons 2,3 and 6 residing on the same side of the furanose ring exhibit signal transduction (Figure 2.17).

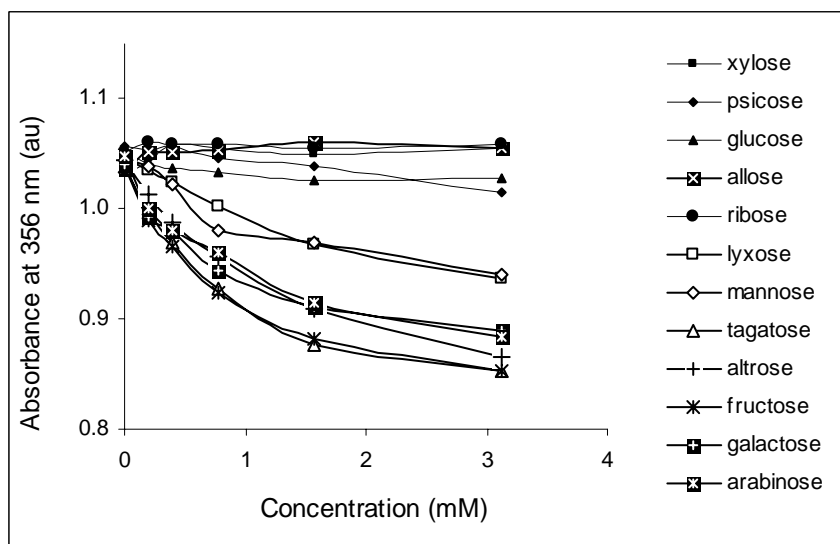


Figure 2.17. Plots of absorbance vs. the concentration of various monosaccharides in phosphate buffer (0.1 mL, 60 mM, pH = 7.4) added to **2.8** in DMSO (3.4 mM, 0.9 mL) at 355 nm.

Thus, based on the experimental evidence shown above, sugars which can form boronic acid-furanose tridentate complexes with specific configurations is the cause of the signal transduction under my experimental conditions.

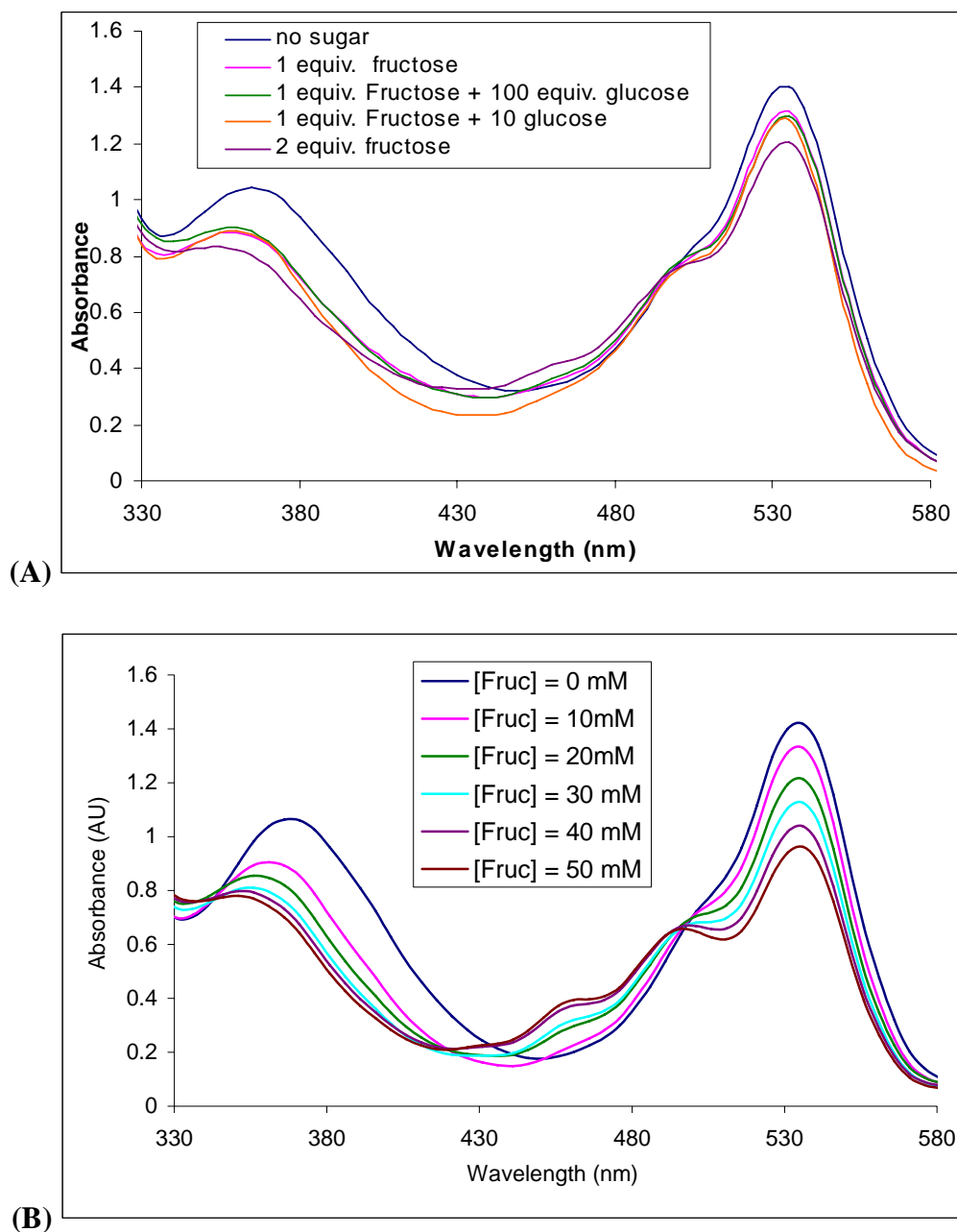


Figure 2.18. (A) UV-Vis spectra of solutions of **2.8** with fructose, glucose or their mixture in 9:1 DMSO:phosphate buffer (60 mM pH 7.4). (B) UV-Vis spectra of solutions of **2.8** with different concentrations of fructose ([Fruc]) in 9:1 DMSO:phosphate buffer (60 mM pH 7.4).

The Detection of Fructose in Honey. There are no sugars in honey at significant levels which can form sterically unencumbered tridentate complexes with **2.8** and **2.9**, other than fructose. D-fructose and D-glucose are the major components in honey, representing 65-95% of the total solids.^{2.25} Figure 2.18 shows clearly that with the application of the above mentioned method, fructose can be detected without obvious interference of 100-fold excesses amount of glucose. There are several important reasons for monitoring fructose levels in food. High fructose intake has been implicated in the pathogenesis of atherosclerosis, elevated triglyceride levels and insulin resistance in humans.^{2.26} Non-enzymatic glycosylation products form more rapidly from fructose than from glucose.^{2.27} The popular use of food additives such as high fructose corn syrup is responsible for an estimated 9% of the daily caloric intake of Americans.^{2.28} The determination of fructose in common foods is thus of interest. A specific significant concern is the fact that fructose has been cited as an adulterant in commercial honey.^{2.29} The determination of fructose in honey has long been of great of interest. However, the reported methods consist of distinctive drawbacks. It is often expensive and time consuming using conventional method such as NMR, HPLC, and carbon isotope ratio analysis to detect fructose in honey. Enzyme sensors are easy to use and highly specific, nonetheless, the unstable enzymes are relatively expensive and need to be protected during manufacturing and specially maintained to prevent decomposition. Except for cost and instability, immune response is another drawback that researchers need to concern. Color assays based on synthetic chromophores to detect sugars usually require harsh conditions like highly toxic/corrosive reagents, high temperature, sometimes require multi steps and have reproducibility or interference limitations (Table 2.4).^{2.30-2.35} The

advantages of using resorcinarene boronic acid include ease of synthesis and maintenance, less expensive, usually conducted in room temperature and under milder conditions, etc.

Table 2.4. Representative color tests based on non-enzymatic assays. Note the harsh conditions required. The assays often suffer from significant interference from competing analytes.

dinitrosalicylic acid assay for reducing sugar ^{2.31}	Interference by CO ₂ and dissolved O ₂ as well as certain metal ion and requires heating at 100 °C.
Nelson-Somogyi method for reducing sugar ^{2.32}	Requires toxic Na ₂ HAsO ₄ as well as H ₂ SO ₄ .
ferric-orcinol assay for pentose ^{2.30}	Includes the use of HCl and requires heating to 100 °C. Interference from hexoses can be significant and standards contain hexoses and pentoses in the expected amounts are needed.
phenol-boric acid-sulfuric acid assay for ketose ^{2.30}	Uses phenol and H ₂ SO ₄ . Different ketoses give different responses. Reproducibility dependent upon the manner of H ₂ SO ₄ addition.
Morgan-Elson assay for hexosamine ^{2.33}	Uses corrosive acids. Prior acetylation of free hexosamines is often required. Heating at 100 °C required.
Carbazole assay for uronic acids ^{2.34}	Interference from neutral carbohydrates, cysteine, other thiols and proteins. Different uronic acids afford different responses. Heating at 100 °C required.
Warren assay for sialic acid ^{2.35}	Necessitates prior periodate oxidation and toxic sodium arsenate, redistilled cyclohexanone and heating at 100 °C. Interference from fructose (reduced absorbance) and fructose.

Although other boronic acid-based compounds and methods may be fructose-selective, and potentially useful in an assay for fructose, very many would suffer from significant interference from glucose.^{2.15} Figure 2.18 shows clearly that with the application of the above mentioned method, fructose can be detected voiding the

interference of excess amount of glucose. Despite the wide variety of boronic acid chemosensors reported, no simple and direct assay for the selective detection of fructose in honey has been previously described.

The spectrophotometric analysis of fructose in honey is performed via a standard addition method. Standard addition is the benchmark quantitative validation assay in complex natural matrices. It permits statistical validation of an assay, via an acceptable % recovery of standards, when certified samples are unavailable.

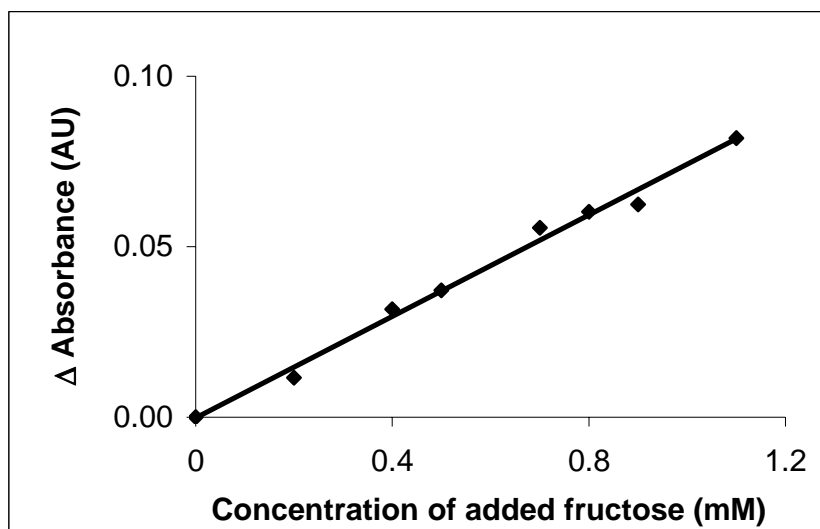


Figure 2.19. The calibration curve validated by the addition of fructose standards to a solution of honey (0.32 mg/mL) and **2.8** (3.4 mM) in a 1:9 mixture of phosphate buffer (0.1 mL, 60 mM, pH = 7.4) and DMSO at 355 nm.

Standard addition of fructose (Figure 2.19) using colored solutions of **2.8** and **2.9** results in a good linear range of 0-12 mM of fructose and a correlation factor of 0.995, at 355 nm. For % recovery determinations, known amounts of fructose are added to the honey samples before treatment. The absorbance difference with respect to the original

sample is correlated with the fructose concentration from the calibration curve. The percent recovery was 101.2 % with a R.S.D. (relative standard deviation) of 4.9 % ($n=8$). At 535 nm, standard addition of fructose using colored solutions of **2.8** and **2.9** results in a good linearity also with correlation factor of 0.998.

2.3 Conclusion

A major goal of this study was to understand the origin of the selective colorimetric signal transduction mechanism in resorcinarene-derived xanthenes and other xanthenes containing boronic acids. The first hypothesis driving this study involved a potential synergy between **2.8** and **2.9** in solution is not the best description explaining selective saccharide detection under my experimental conditions. I presented strong evidence that those sugars which can exhibit hydroxyl configurations analogous to those found in fructofuranose, form a specific tridentate complex with **2.9** with high selectivity. This finding is successfully applied to explaining selectivity in the detection of specific disaccharides via terminal sugar residues. The findings reported herein allow better understanding of spectrophotometric signaling and should permit one to better predict potential interferences in challenging natural matrices.

2.4 Experimental Section

UV-Vis spectra are acquired on a Spectramax Plus 384 UV-Vis spectrophotometer (Molecular Devices Ltd.) using a 1 cm quartz cell at 25 °C. NMR spectra are obtained with a Bruker DPX DPX-300 spectrometer. ^{13}C NMR spectra are acquired using $\text{D}_2\text{O}:\text{DMSO-}d_6$, 1:9. Altrose and allose were purchased from OMICRON Biochemicals, Inc. and Fluka respectively. The remaining chemicals were purchased

from Sigma-Aldrich Ltd. and used without further purification. Compound **2.8**^{2.1} is prepared via methods Dr. Strongin's research group /reported previously.

Solutions of **2.8** containing colored **2.9** are prepared by dissolving **2.8** (3.4 mM) in DMSO and heating until a gentle reflux (3 min) followed by cooling to rt. These solutions are mixed at rt with the corresponding sugars which are previously dissolved in phosphate buffer (pH = 7.4, 60 mM). The final solution proportion in each experiment is 9:1 DMSO:buffer. The mixtures stand at rt for 25 min before recording UV-Vis spectra.

For the standard addition experiments, a stock solution of honey is prepared by mixing 32 mg of commercial honey (generic class A, purchased at a local Albertsons[®] supermarket) in 10 ml of phosphate buffer solution (pH = 7.4, 60 mM). The solution is filtered through Millipore[®] YM-3 centrifugal membranes with the aid of a GRAHAAM-FIELD Centrifuge (3000 rpm). Fructose standards in phosphate buffer (pH = 7.4, 60 mM) are added to the filtrate, followed by the addition of a pre-heated colored DMSO solution of **2.8** (3.4 mM) in order to construct a calibration curve (standard addition method). The proportion of DMSO:buffer is 9:1, final volume 1 mL. For % recovery determinations, known amounts of fructose (1-12 mM) are added to the honey samples before the filtration steps. UV-Vis spectra are recorded for (i) the **2.8** and honey solution (A_0) and (ii) for the solutions of **2.8**, honey with added fructose (A).

Semiempirical molecular modeling analysis is performed using CS MOPAC/ChemOffice 6.0 (CambridgeSoft) and the potential function AM1. Molecular graphics images are produced using the UCSF Chimera package from the Computer Graphics Laboratory, University of California, San Francisco.

2.5 References

- 2.1 Lewis, P. T.; Davis, C. J.; Saraiva, M.; Treleaven, W. D.; McCarley, T. D.; Strongin, R. M. *J. Org. Chem.* **1997**, *62*, 6110.
- 2.2 He, M.; Johnson, R. J.; Escobedo, J. O.; Beck, P. A.; Kim, K. K.; St. Luce, N. N.; Davis, C. J.; Lewis, P. T.; Fronczek, F. R.; Melancon, B. J.; Mrse, A. A.; Treleaven, W. D.; Strongin, R. M. *J. Am. Chem. Soc.* **2002**, *124*, 5000.
- 2.3 Davis, C. J.; Lewis, P. T.; McCarroll, M. E.; Read, M. W.; Cueto, R.; Strongin, R. M. *Org. Lett.* **1999**, *1*, 331.
- 2.4 Sen, R. N.; Sinha, N. N. *J. Am. Chem. Soc.* **1923**, *45*, 2984.
- 2.5 Lewis, P. T.; Davis, C. J.; Cabell, L. A.; He, M.; Read, M. W.; McCarroll, M. E.; Strongin, R. M. *Org. Lett.* **2000**, *2*, 589.
- 2.6 Gupta, S. N.; Linden, S. M.; Wrzyszczyński, A.; Neckers, D. C. *Macromolecules*, **1988**, *21* 51.
- 2.7 Agbaria, K.; Biali, S. E. *J. Org. Chem.* **2001**, *66*, 5842.
- 2.8 Schneider, H.-J.; Schneider, U. *J. Inclusion Phenom.* **1994**, *19*, 67. (b) *Container Molecules and Their Guests*, Cram, D. J.; Cram, J. M., The Royal Society of Chemistry: Cambridge, U.K. 1994. (c) Sherman, J. C. *Tetrahedron* **1995**, *51*, 3395. (d) Timmerman, P.; Verboom, W.; Reinhoudt, D. N. *Tetrahedron* **1996**, *52*, 2663. (e) Jasat, A.; Sherman, J. C. *Chem. Rev.* **1999**, *99*, 931. (f) Rudkevich D. M.; Rebek, J. *Eur. J. Org. Chem.* **1999**, *9*, 1991.
- 2.9 Weinelt, F.; Schneider, H.-J. *J. Org. Chem.* **1991**, *56*, 5527.
- 2.10 Fronczek, F. R.; Johnson, R. J.; Strongin, R. M. *Acta Cryst.* **2001**, *E5*, o447-o448.
- 2.11 Chen, C.-T.; Yan, S.-J. *Tetrahedron Lett.* **1969**, 3855. (b) Head, D. L.; McCarty, C. G. *Tetrahedron Lett.* **1973**, 1405.
- 2.12 Fronczek, F. R.; St. Luce, N. N.; Strongin, R. M. *Acta Cryst.*, **2001**, *C57*, 1423.
- 2.13 Rusin, O.; Alpturk, O.; He, M.; Escobedo, J. O.; Jiang, S.; Dawan, F.; Lian, K.; McCarroll, M. E.; Warner, I. M.; Strongin, R. M. *J. Fluoresc.* **2004**, *14*, 611.
- 2.14 Kim, K. K.; Escobedo, J. O.; St. Luce, N. N.; Rusin, O.; Wong, D.; Strongin, R. M. *Org. Lett.* **2003**, *5*, 5007.
- 2.15 Reviews: (a) James, T. D.; Shinkai, S. *Top. Curr. Chem.* **2002**, *218*, 159. (b) Wang, W.; Gao, X.; Wang, B. *Curr. Org. Chem.* **2002**, *6*, 1285.
- 2.16 Nicholls, M. P.; Paul, P. K. C. *Org. Biomol. Chem.* **2004**, *2*, 1434.

- 2.17 Springsteen, G.; Wang, B. *Tetrahedron* **2002**, 58, 5291.
- 2.18 Ni, W.; Fang, H.; Springsteen, G.; Wang, B.. *J. Org. Chem.* **2004**, 69, 1999.
- 2.19 James, T. D.; Sandanayake Samankumara, K. R. A.; Shinkai, S. *Angew. Chem. Int. Ed. Engl.* **1996**, 35, 1911.
- 2.20 Cao, H.; McGill, T.; Heagy, M. D. *J. Org. Chem.* **2004**, 69, 2959.
- 2.21 Norrild, J. C.; Eggert, H. *J. Am. Chem. Soc.* **1995**, 117, 1470. (b) Norrild, J. C.; Eggert, H. *J. Chem. Soc., Perkin Trans 2* **1996**, 2583.
- 2.22 Yang, Y.; Lewis, P. T.; Escobedo, J. O.; St. Luce, N. N.; Treleaven, W. D.; Cook, R. L.; Strongin, R. M. *Collect. Czech. Chem. Commun.* **2004**, 69, 1282.
- 2.23 Rudolfova J.; Curda, L. *Chemicke Listy* **2005**, 99, 168.
- 2.24 Morales, V.; Olano, A.; Corzo, N. *J. Agric. Food Chem.* **2004**, 52, 6732.
- 2.25 Doner, L. W. *J. Sci. Fd. Agric.* **1977**, 28, 443. (b) Mateo, R.; Bosch-Reig, F. *J. Agric. Food Chem.* **1998**, 46, 393. (c) Joshi, S. R.; Pechhacker, H.; Willam, A.; Von Der Ohe, W. *Apidologie* **2000**, 31, 367. (d) Cotte, J. F.; Casabianca, H.; Chardon, S.; Lheritier, J.; Grenier-Loustalot, M. F. *J. Chromatogr., A* **2003**, 145, 1021. (e) Cordella, C. B. Y.; Militao, J. S. L. T.; Clement, M.; Cabrol-Bass D. *J. Agric. Food Chem.* **2003**, 51, 3234. (f) Terrab, A.; Diez, M. J.; Heredia, F. J. *Int. J. Food Sci. Technol.* **2003**, 38, 395.
- 2.26 MacDonald, I. *Adv. Exp. Med. Biol.* **1975**, 60, 57. (b) Thorburn, A. W.; Storlein, L. H.; Jenkins, A. B.; Khouri, S.; Kreagen, E. W. *Am. J. Clin. Nutr.* **1989**, 49, 1155.
- 2.27 Bunn, H. F.; Higgins, P. J. *Science* **1981**, 213, 222. (b) Burden, A. C. *Lancet* **1984**, 11, 986. (c) Suárez, G.; Rajaram, R.; Oronski, A. L.; Gawinowicz, M. A. *J. Biol. Chem.* **1989**, 264, 3674.
- 2.28 Bantle, J. P.; Raatz, S. K.; Thomas, W.; Georgopoulos, A. *Am. J. Clinical Nutrition* **2000**, 72, 1128.
- 2.29 Irudayaraj, J.; Sivakesava, S. *Trans. ASAE* **2001**, 44, 643.
- 2.30 M. F. Chaplin, "Monosaccharides," in *Carbohydrate Analysis. A Practical Approach* Chaplin, M.F.; Kennedy, J. F., Eds., Oxford University Press, Oxford, **1994**, p2, p4, p5, p8.
- 2.31 P. Bernfeld, *Methods in Enzymology, Vol. 1*. Colowick, S. P. and Kaplan, N. O., Eds. Academic Press, New York, **1955**, p149.

- 2.32 (c) M. Somogyi, *J. Biol. Chem.* **1952**, *195*, 19.
- 2.33 Reisseg, J. L.; Strominger, J. L.; Leloir, L. F. "A Modified Colorimetric Method for the Estimation of *N*-Acetylamino Sugars," *J. Biol. Chem.* **1955**, *217*, 959.
- 2.34 Taylor, K. A.; Buchanan-Smith, J. G. "A Colorimetric Method for the Quantitation of Uronic Acids and a Specific Assay for Galacturonic Acid," *Anal. Biochem.* **1992**, *201*, 190.
- 2.35 Warren, L. "The Thiobarbituric Acid Assay of Sialic Acids," *J. Biol. Chem.* **1959**, *234*, 1971.

CHAPTER 3

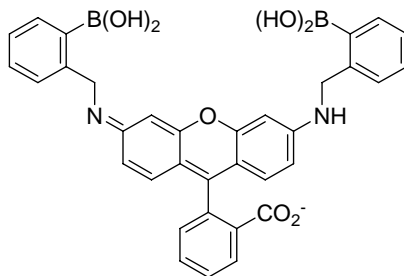
STEREOCHEMICAL AND REGIOCHEMICAL TRENDS IN THE SELECTIVE SPECTROPHOTOMETRIC DETECTION OF SACCHARIDES APPLYING RHODAMINE BORONIC ACID*

3.1 Introduction

Most arylboronic acid indicators for sugars are inherently selective for fructose or, by design, selective for glucose.^{3.1} There is an unmet demand for chemosensors that promote the detection of other saccharides. Monitoring sugar levels is important in industry, biomedical research and health care.

Herein I describe a boronic acid-functionalized rhodamine derivative (**3.1**)^{3.2} which displays an unprecedented degree of colorimetric and fluorimetric selectivity for ribose and ribose derivatives. For instance, adenosine as well as nucleotides and nucleosides can be detected selectively compared to fructose, glucose and other common saccharides. The hypothesis driving this investigation is that the characteristic regio- and stereochemical saccharide mutarotational isomer structures of specific sugars can guide indicator design.^{3.3}

Scheme 3.1. Structure of compound **3.1**.



3.1

*Reprinted in part with permission from *Journal of the American Chemical Society*, 2006, Volume 128, pages 12221-12228; Shan Jiang, Jorge O. Escobedo, Kyu Kwang Kim, Onur Alpturk, George K. Samoei, Sayo O. Fakayode, Isiah M. Warner, Oleksandr Rusin, and Robert M. Strongin; Stereochemical and Regiochemical Trends in the Selective Detection of Saccharides. Copyright 2006 American Chemical Society.

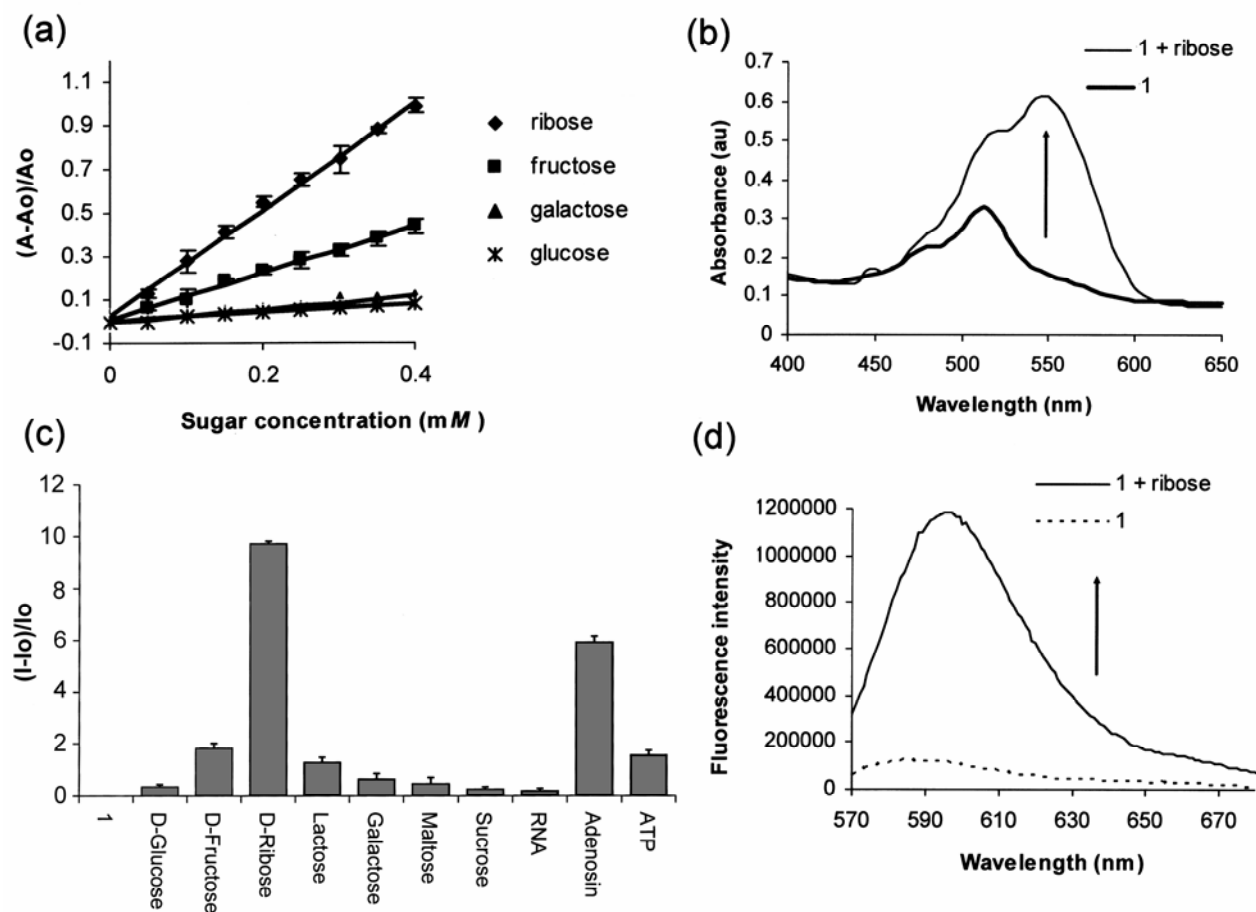
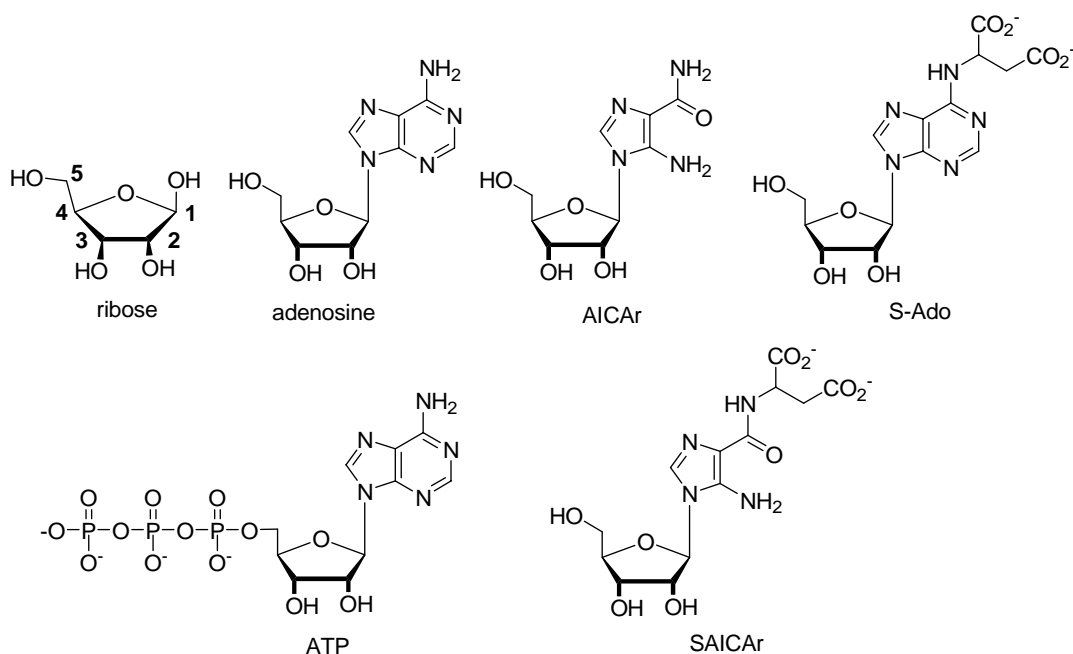


Figure 3.1. (a) Relative absorbance changes vs. concentration of various monosaccharides in phosphate buffer (0.1 mL, 60 mM, pH 7.4) added to **3.1** ($7.2 \times 10^{-5} M$) in DMSO (0.9 mL) and monitored at 560 nm. (b) The UV-Vis spectra of a solution of **3.1** ($7.2 \times 10^{-5} M$) alone and **3.1** with added ribose ($4 \times 10^{-4} M$). (c) Relative fluorescence emission spectra at 597 nm of **3.1** ($4 \times 10^{-9} M$) and saccharides and saccharide-containing molecules ($1.85 \times 10^{-3} M$) in 9:1 DMSO:phosphate buffer (0.05 M, pH 7.4) excited at 565 nm. (d) Fluorescence emission spectra of a solution of **3.1** ($4 \times 10^{-9} M$) and **3.1** with added ribose ($1.85 \times 10^{-3} M$) in 9:1 DMSO:phosphate buffer (0.05 M, pH 7.4) excited at 565 nm.

The Selective Detection of Ribose Compared to Common Monosaccharides.

Ribose has been used as an anti-Hepatitis B virus (HBV) and anti-Epstein Barr virus (EBV) agent.^{3,4} The presence of excessive amounts of ribose has been reported in the cerebrospinal fluid (CSF, 47-146 μM) and urine (5-102 μM) of patients with ribose-5-phosphate isomerase deficiency, a disorder associated with leukoencephalopathy.^{3,5} Examination of the spectral response of compound **3.1** to added ribose as compared to fructose, galactose or glucose (Figures 3.1a and 3.1b) shows that it is ribose-selective. Ribose is detected colorimetrically in this example at levels potentially relevant for diagnosing ribose-5-phosphate isomerase deficiency. The selectivity for ribose is confirmed by fluorescence spectroscopy. The emission of solutions containing **3.1** and ribose as well as ribose-containing compounds is generally larger compared to other common sugars and related biomolecules studied to date (Figure 3.1c).

Scheme 3.2. Structures of ribose and selected ribosides and ribotides.



Detection of Ribosides and Ribotides: Biomarkers of Inborn Errors of Purine Biosynthesis. Recently, a new and devastating inborn error of purine biosynthesis, AICA-ribosiduria, was discovered. The child studied in this first case excreted massive levels of AICAr in her urine (280 mmol/mole creatinine). In addition, succinylaminoimidazolecarboxamide riboside (SAICAr) and succinyladenosine (S-Ado) were present at levels of 45 and 80 mmol/mole creatinine. These two latter succinylpurines are analogs of AICAr. They are also the key urinary biomarkers for the other inborn error of purine biosynthesis, adenosuccinate lyase (ADSL) deficiency. AICAr, S-Ado and SAICAr and congeners are not present in the urine of healthy patients. In ADSL-affected children, extremely high levels, 1-10 mM in urine, 0.1 mM in cerebrospinal fluid (CSF), are present. ADSL results in mental retardation, congenital blindness, epilepsy and dysmorphism.^{3,6}

Based on the results shown in Figure 3.1 showing selectivity for ribose and adenosine, I hypothesized that the detection of inborn errors of purine biosynthesis biomarkers could also be feasible using **3.1**. Commercially available AICAr, used as a surrogate for SAICAr and S-Ado, can be readily detected in solutions containing **3.1** (Figure 3.2). Under identical experimental conditions, ATP is also detectable.

Nucleosides and nucleotides such as ATP and congeners were found at double the normal levels (ca. 1600 mmol/mL erythrocytes) in the blood of the patient with AICA-ribosiduria. Compound **3.1** may thus serve as a basis of future studies for a general chemical test for inborn errors of purine biosynthesis. One of the many challenges remaining involves addressing the remaining interfering signals from fructose.

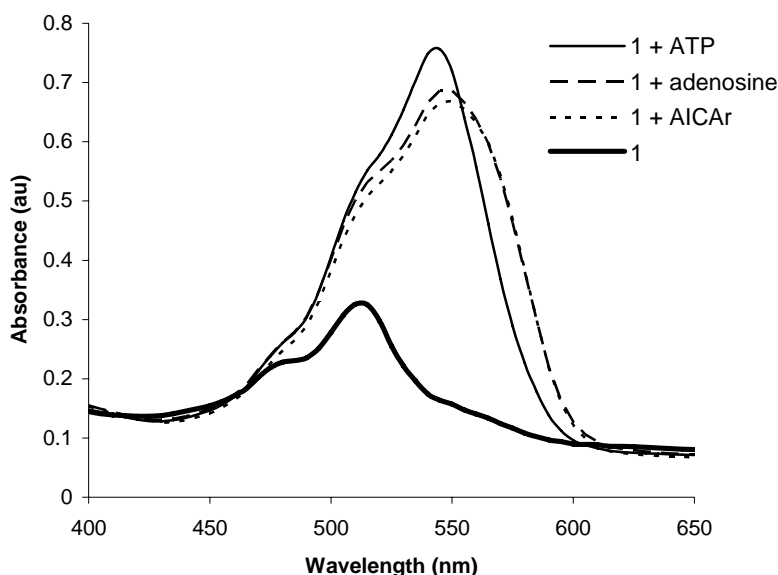


Figure 3.2. UV-Vis spectra of solutions containing **3.1** ($7.2 \times 10^{-5} M$) in 9:1 DMSO:phosphate buffer (0.06 M, pH 7.4) and **3.1** in the presence of $4 \times 10^{-4} M$ solutions of ATP, adenosine and AICAr.

Addressing Fructose Interference. Overcoming the high affinity of arylboronic acids for fructose in order to detect glucose selectively has been addressed by many researchers to date.^{3.1} The main strategy has been to design receptors which can bind a glucose molecule selectively via two boronic acids in a bidentate fashion.^{3.7} Alternatively, in the current study, fructose-induced interference is eliminated by using a combination of receptors exhibiting complementary affinities and spectral properties.

Fructose-selective Materials Used in Conjunction with 3.1 Heighten Selectivity for Ribose-containing Compounds. We have previously reported an extensive study of the mechanism of chromophore formation in resorcinarene solutions.^{3.8a} Solutions containing millimolar concentrations of compound **3.2** developed micromolar levels of chromophore **3.3** *in situ*. The colored material **3.3** enabled saccharide detection via UV-Vis and fluorescence spectroscopy. Extensive spectroscopic

studies proved that the formation of anionic sugar-boronate complexes of **3.3** resulted in the sugar-induced spectral changes, as boron became charged. In chapter 2, I have described resorcinarene boronic acid (**3.2**) and its associated chromophoric species (**3.3**) produced by its oxidation for the selective detection of fructose (Figure 3.3).^{3,8}

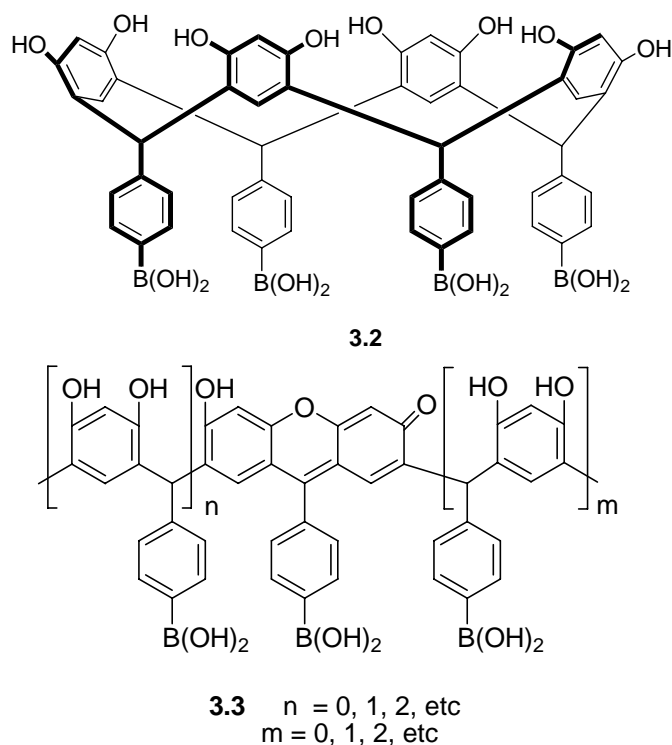


Figure 3.3. Structures of the resorcinarene boronic acid **3.2** and its chromophoric products (**3.3**) formed *in situ*.

I thus hypothesize that fructose-reactive **3.2** (and **3.3**) should bind fructose and remove fructose-derived signals from solutions containing ribose-selective **3.1**. I indeed observe that essentially no response due to fructose (and the two other most common blood monosaccharides, galactose and glucose) occurs (Figure 3.4) upon adding **3.2** to solutions containing **3.1** for ribose detection.

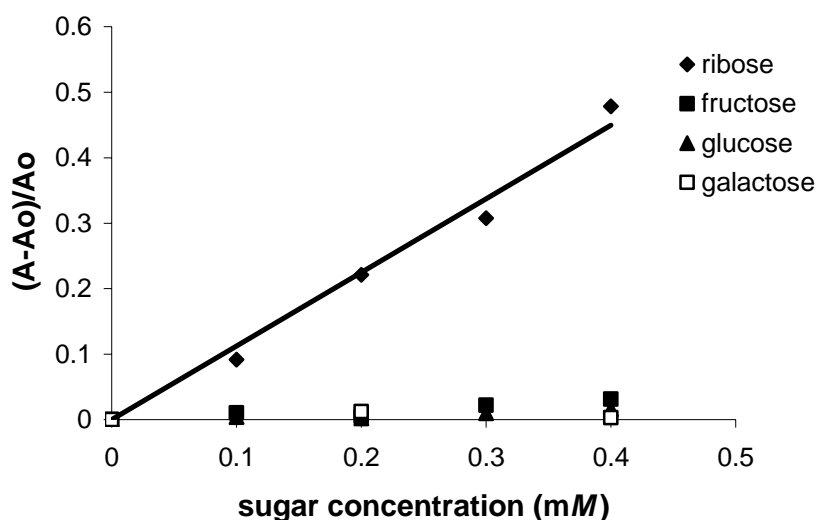


Figure 3.4. Relative absorbance changes vs. concentration of ribose, fructose, galactose and glucose in solutions comprised of phosphate buffer (0.1 mL, 60 mM, pH = 7.4) added to **3.1** (0.07 mM) in DMSO (0.9 mL) and **3.2** (1.9 mM) monitored at 560 nm. A comparison to Figure 3.1a shows that the use of **3.1** combined with **3.2** removes significant fructose interference under these conditions.

3.2 Discussion

The Chemoselective Signaling of 3.1 Is Unique Compared To Other Boronic Acid Dyes. Ribose exhibits 1:1 binding to **3.1** according to the continuous variation method (supporting information). Table 3.1 displays the apparent binding constants (K_{eq}) corresponding to complexes of **3.1** with various monosaccharides. The order of affinities is: ribose > allose > fructose > galactose > altrose > glucose > arabinose. The latter trend does not correlate well with the generic binding affinities involving phenylboronic acid and monosaccharides (Table 3.1). For instance, based on the reported similar binding constants of model arylboronate complexes of ribose and arabinose^{3,9} and the similar degree of complexation of ribose and arabinose (65 % and 74 %, respectively),^{3,3c} one would have predicted ribose to afford a spectrophotometric response similar to that of

arabinose in solutions containing **3.1**. Since boronic acid binding alone cannot account for the colorimetric and fluorimetric selectivity observed using **3.1**, I thus hypothesize that secondary interactions with the rhodamine chromophore are occurring when **3.1** binds to specific sugars.

Table 3.1. Apparent binding constants (K_{eq}) of the complexes of various monosaccharides and compound **3.1** ($7.2 \times 3.10^{-5} M$ in 9:1 DMSO:phosphate buffer 60 mM, pH 7.4). Values are the average of three runs rounded to two significant figures.

Saccharide	$K_{eq} (M^{-1})$	
	Calculated values for 3.1	Literature values for phenylboronic acid ^a
Ribose	2400	24
Allose	1500	-
Fructose	1100	160
Galactose	310	15
Altrose	270	-
Glucose	200	4.6
Arabinose	120	25

^a See reference 3.9.

NMR Studies Show That 3.1 Binds Ribose in the Furanose Form. The ¹H NMR spectrum of a solution of **3.1** and ribose (0.15 M NaOD/D₂O) reveals a preference for binding ribofuranose over ribopyranose (Figure 3.5).^{3,10} Ribofuranose possesses pairs of *cis*-diols for cyclic boronate formation that more eclipsing compared to its pyranose forms.^{3,3} Ribose acetonide formation is preceded to occur at its 2,3-hydroxyls in 90 % yield (Scheme 3.3).^{3,11}

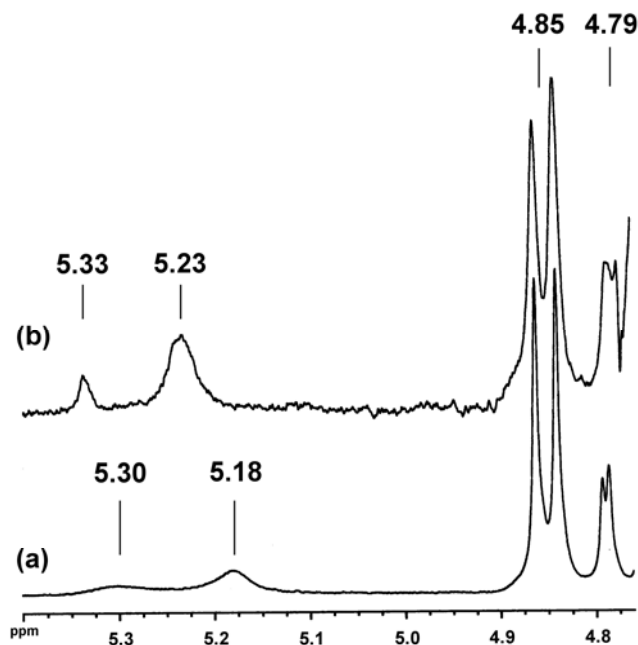
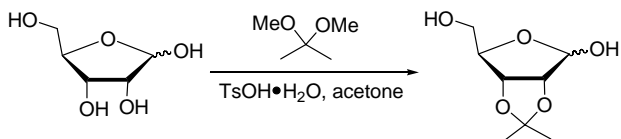


Figure 3.5. Expansion of the ^1H NMR spectra of solutions of (a) D-ribose and (b) a mixture of **3.1** and D-ribose (0.15 M NaOD/D₂O). The resonances shown correspond to the anomeric protons of each of the four cyclic forms. The assignments are: δ (ppm): 5.30 (α -ribofuranose), 5.18 (β -ribofuranose), 4.85 (β -ribopyranose) and 4.79 (α -ribopyranose). Upon the addition of **3.1** only the resonances corresponding to the ribofuranoses exhibit a downfield shift. This is expected as a result of cyclic boronate formation with ribofuranose (reference 3.3c).

Scheme 3.3. Formation of ribose acetone via selective reaction of the 2,3-hydroxyls in 90 % yield (reference 3.11).



Ribose, Allose, Talose, Psicose, Adenosine, Nucleotides and Nucleosides Exhibit Common Furanose Configurations. I include a total of 11 commercially available monosaccharides in our study (Figure 3.6). Psicose, allose, talose and ribose

are the only monosaccharides to afford spectral changes in solutions of **3.1** containing **3.2** (Figure 3.7). D-Psicose is a rare sugar under consideration as a direct substitute for D-fructose.^{3.12} Allose is a rare sugar which exhibits scavenging activity toward reactive oxygen species (ROS) and a potent inhibitory effect on the production of ROS from stimulated neutrophils.^{3.13} Additionally, allose has been used to reduce thrombus formation during post-operative period in combination with other anti-clotting drugs.^{3.14} It has recently been shown to be active against ovarian cancer cell lines.^{3.15} D-Talose has shown inhibitory effects on the growth of leukemia L1210 cells.^{3.16} Tagatose (as well as fructose, *vide supra*) which has a relatively strong binding affinity for phenylboronic acid (comparable to fructose, Table 3.1) affords no detectable signal.

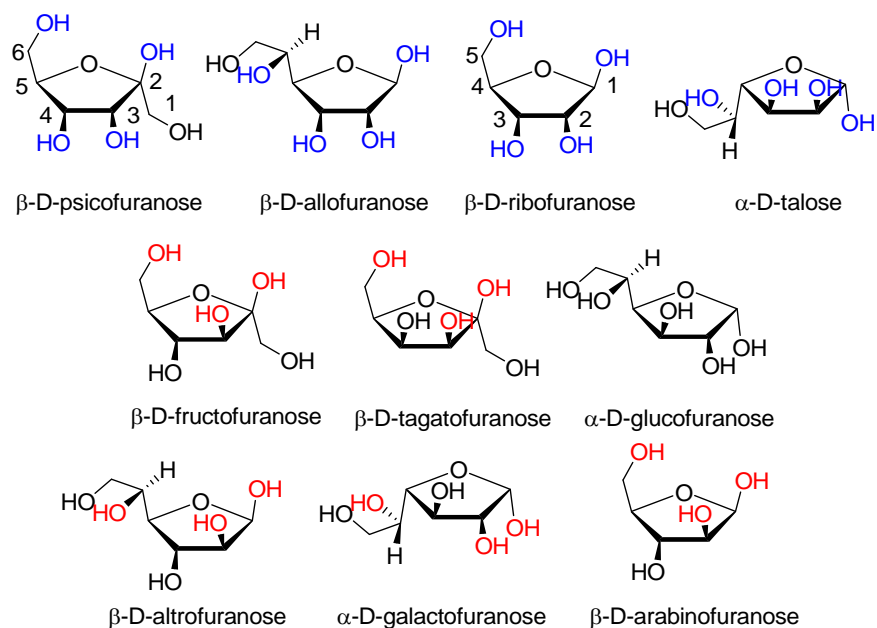


Figure 3.6. Structures of 11 monosaccharides in their furanose forms. Compound **3.1** is selective for sugars with hydroxyls shown in blue. Compound **3.3** is selective for sugars with hydroxyls shown in red.

The rare ketohexose psicose exhibits a furanose form in which the 3,4-*cis* diols are *anti* to the 6-OH. Analogously, the rare aldopentoses allose and talose each possess a 2,3-*cis* diol moiety *anti* to the 1,4- substituents (shown in blue). Importantly, this is also a common feature of ribose, adenosine and the nucleotides and nucleosides.

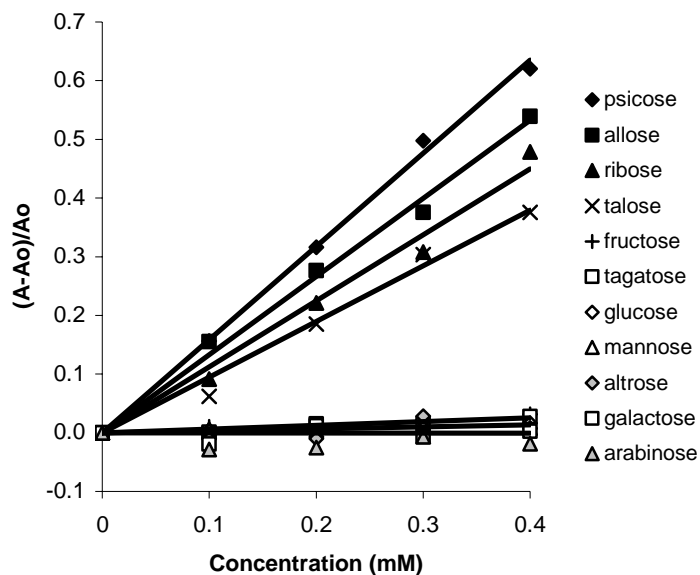


Figure 3.7. Plots of relative absorbance changes vs. concentration of 11 monosaccharides in solutions comprised of phosphate buffer (0.1 mL, 60 mM, pH = 7.4) added to **3.1** (0.07 mM) in DMSO (0.9 mL) and **3.2** (1.9 mM) monitored at 560 nm.

Simulations Show That Ribose and Congeners Can Selectively Undergo Secondary Interactions with the Fluorophore Moiety of 3.1. There is precedence for secondary interactions (e.g., in the case of oligosaccharides) affording enhanced fluorescence or UV-Vis signaling in boronic acid dyes.^{3.6a,3.17} Sugars possessing pentafuranose configurations with alpha 2,3-*cis* diols (for boronate ester formation) and beta 1,4-substituents allow the 1,4-substituents to undergo secondary interactions with

the rhodamine chromophore of **3.1**. Similarly, hexafuranoses exhibiting alpha 3,4-*cis* diols and beta 6-OH substituents should also undergo analogous secondary interactions.

Recently, Anslyn showed that in protic media (H₂O or MeOH), and particularly with relatively weaker nitrogen nucleophiles, a solvent molecule adds to boron and disrupts the B-N dative interaction between arylboronic acids containing proximal amino groups.^{3,18} This results in a zwitterion wherein the nitrogen atom is protonated as the boron atom adopts *sp*³ hybridization and negative charge upon addition of the fourth (solvent) ligand. A hydrogen bond is concomitantly formed between the proton on nitrogen and the solvent (hydroxy or methoxy) molecule attached to boron (Figure 3.8).

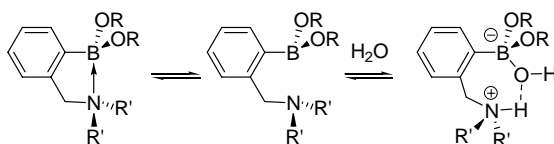


Figure 3.8. The effect of solvation on the B-N bond in *o*-(*N,N*-dialkylaminomethyl)phenylboronic esters (adapted from reference 3.18).

Simulations of the boronate complexes of **3.1** with the furanose forms of ribose, fructose and glucose, performed using structures that would result from solvolysis of boron, reveal how secondary interactions between the sugar moiety and the chromophore may occur selectively in the cases of ribose and its analogs. The simulations how pentafuranoses that can exhibit an alpha 2,3-*cis* diol and beta 1,4 diol configuration may have a tighter interaction with the rhodamine chromophore as compared to boronate complexes of fructose (which exhibits a well-known motif of intramolecular tridentate hydroxyl binding to boron, *vide infra*) and glucose which can bind to boron via the anomeric 1 and 2-*cis* hydroxyls (Figure 3.9 and Figure 3.10).

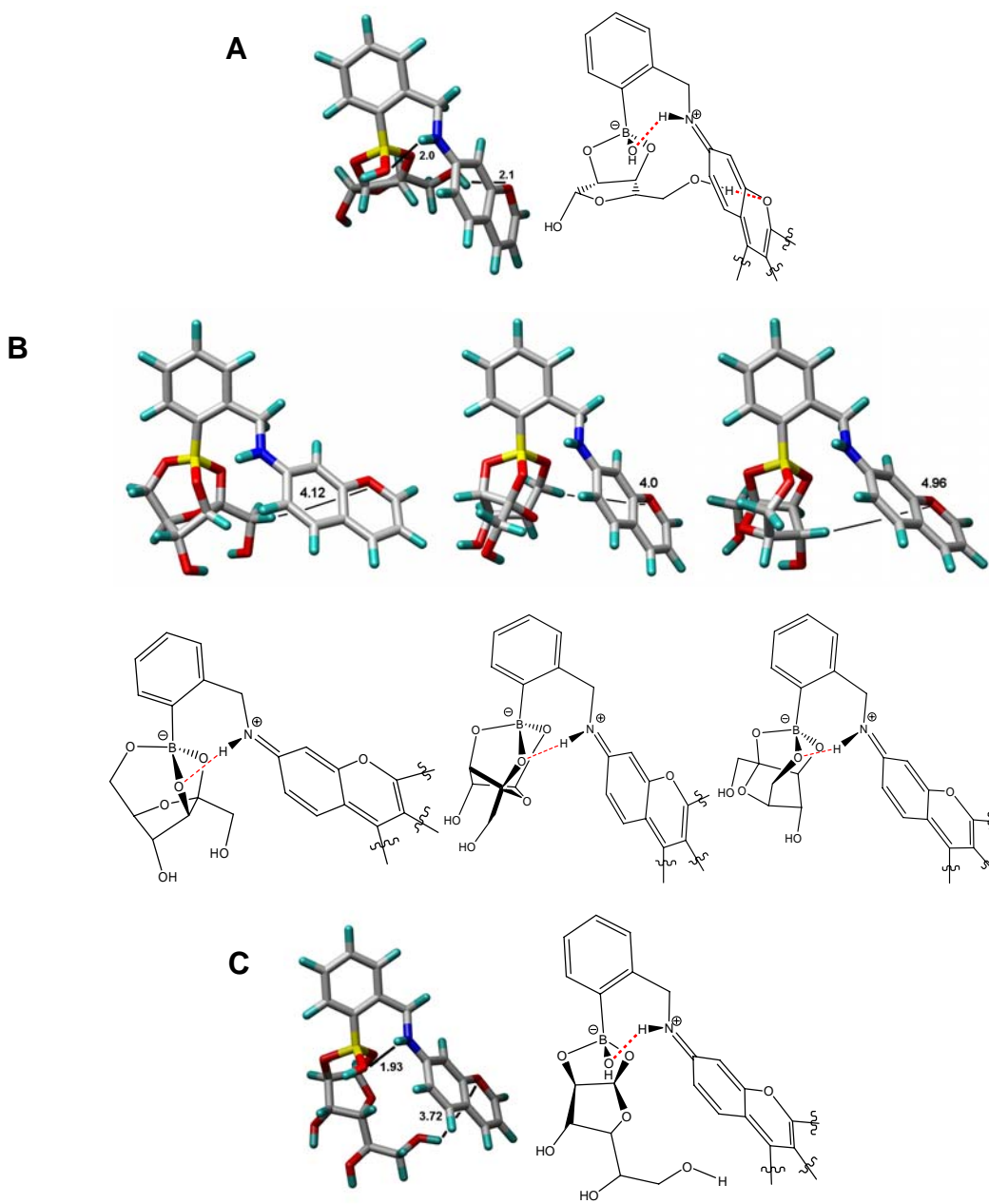


Figure 3.9. Energy-minimized structures of boronates derived from **3.1** and ribofuranose (“endo” isomer, structure A), fructofuranose (3 rotamers, structures B) and glucofuranose (“exo” isomer, structure C, the complementary conformers of the ribo- and glucofuranose boronates are included in Figure E4). A subunit of the the rhodamine chromophore moiety is shown for clarity and used in the simulations in order to simplify the calculations. The above calculated structures show that the ribofuranose complex exhibits the relatively best geometry for promoting direct contacts between the bound sugar moiety and the chromophore moiety of **3.1**. Studies aimed at evaluating the specific interactions between ribose, adenosine, ribosides and ribotides with **3.1** that might involve π - π stacking, σ - π interactions and/or charged hydrogen bonding between the sugar and the rhodamine carboxylate functionality, are ongoing.

The Development of 3.2 and 3.3 As Off-on Colorimetric Indicators for Sugars with Selectivity Complementary to 3.1. Figure 3.10 shows that fluorescence emission enhancement in solutions containing **3.2** and **3.3** (using the neutral buffer sugar solution protocol described above for the studies involving **3.1**, where sugar in buffer is mixed with dye dissolved in DMSO) follows the expected pattern based on the affinity for phenylboronic acid according to Wang's^{3,9} prior studies (Table 3.1) fructose > arabinose > ribose > galactose > glucose. The concentration vs. absorbance changes of these latter as well as other sugars, as monitored by UV-Vis spectroscopy at 535 nm, is shown in Figure 3.11. There is scatter or no useful signal obtained from psicose, ribose, glucose and allose. Signaling due to the addition of tagatose, fructose, altrose, galactose and arabinose is observed. This trend is in contrast to the responses using **3.1** (*vide supra*) which exhibits signal enhancement in the presence of psicose, ribose and allose with no detectable interference from altrose, galactose and arabinose.

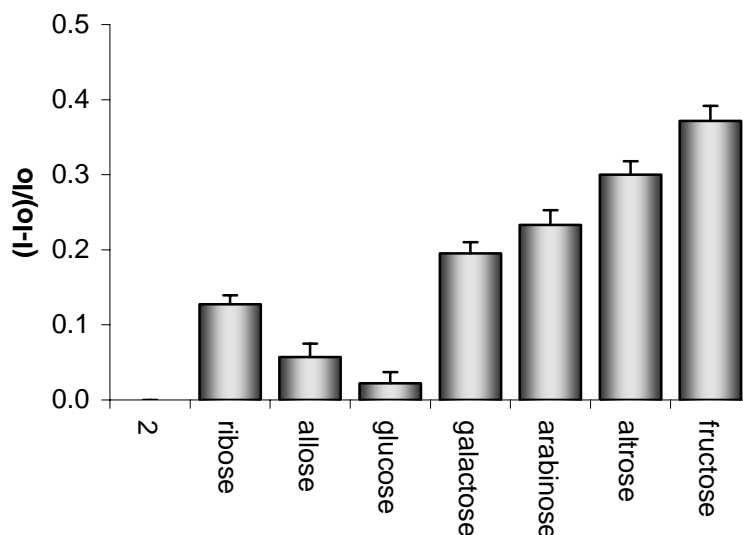


Figure 3.10. Relative fluorescence emission spectra at 574 nm of **3.2** ($5.75 \times 10^{-5} M$) and monosaccharides ($1.85 \times 10^{-3} M$) in 9:1 DMSO:phosphate buffer (0.05 M, pH 7.4) excited at 550 nm.

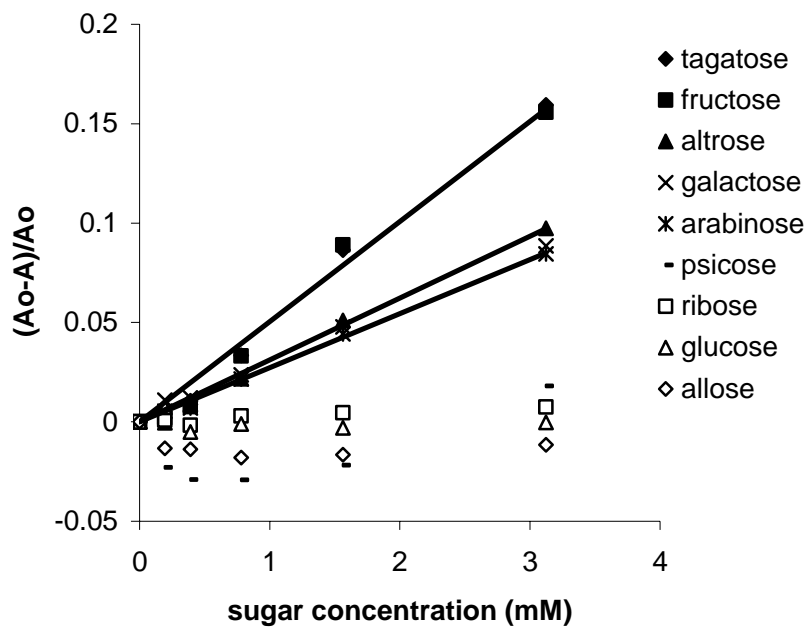


Figure 3.11. Relative absorbance changes vs. the concentration of various monosaccharides in phosphate buffer (0.1 mL, 60 mM, pH = 7.4) added to **3.2** in DMSO (3.4 mM, 0.9 mL) at 535 nm.

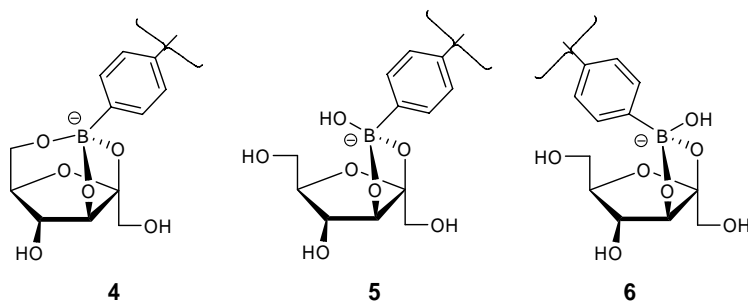


Figure 3.12. Anionic fructofuranose-boronate ester structures.

Previously, our research group^{3.6a} and others^{3.3b} have reported ¹³C NMR evidence for the occurrence of a distinct intramolecular tridentate fructose complex (**3.4**, Figure 3.12) in D₂O/DMSO solutions. The ability of fructose to form tridentate structures can be favored due to the well-known reactivity of the anomeric (and adjacent) hydroxyl.

Additionally, the relatively nucleophilic primary hydroxyl of β -fructofuranose is suitably positioned to also react with boron. Importantly, galactose, arabinose and altrose, which also promote spectral responses under neutral conditions (Figure 3.11) possess a furanose structure similar to that of β -fructofuranose, wherein the same three binding OH-groups (anomeric and adjacent as well as the primary hydroxyl) have analogous relative configurations (Figure 3.6). Each of these sugars may adopt furanose structures wherein the three binding hydroxyls (on the 1,2 and 5 carbons in the case of aldofuranoses and on the 2,3 and 6 carbons for ketofuranoses) are all on the same face of the furanose ring for cooperative binding to boron (Figure 3.6, key hydroxyls are shown in red). The saccharides that possess other configurations of these three specific hydroxyls in their furanose forms do not afford significant signal changes. Thus, each of these sugars induced signaling that is selective over psicose, ribose, glucose and allose (Figure 3.11) which cannot adopt the requisite furanose structures.

3.3 Conclusion

A major goal of this study was to understand the origin of the selective signal transduction mechanism in xanthene-containing boronic acids. Strong evidence is presented to show that sugars which can share the same hydroxyl configurations as ribofuranose promote signaling in solutions of **3.1** with high selectivity. This is the initial example of a boronic acid chemosensor which exhibits distinctive selectivity for ribose, adenosine and derivatives as well as rare sugars such as allose and talose.

In contrast, sugars possessing configurations analogous to those found in fructofuranose can form a specific tridentate complex with **3.3**, resulting in selective colorimetric and fluorimetric signaling. This latter finding is successfully applied to explaining selectivity in the detection of specific disaccharides via their terminal sugar

residue linkage and configurational patterns. When receptors with different optical response properties are used in tandem, interfering signals can be virtually eliminated in a relatively simple manner. The design and study of new xanthene dyes, such as **3.1**, **3.3** and related compounds, is ongoing in our lab.

3.4 Experimental Section

UV-Vis spectra were acquired on a Spectramax Plus 384 UV-Vis spectrophotometer (Molecular Devices Ltd.) using a 1 cm quartz cell at 25 °C. Fluorescence emission spectra were recorded using a spectrofluorimeter SPEX Fluorolog-3 equipped with double excitation and emission monochromators, and 400W Xe lamp and 1 cm quartz cell at 25 °C. Altrose and allose were purchased from OMICRON Biochemicals, Inc. and Fluka respectively. The remaining sugars as well as 4-formylphenylboronic acid and resorcinol were purchased from Sigma-Aldrich Ltd. and used without further purification. Compounds **3.1** and **3.2** were prepared according to procedures reported earlier.^{3,2,3,19}

Solutions of **3.2** are dissolved **3.1** in DMSO, heated at a gentle reflux (3 min) followed by cooling to rt. These solutions were mixed at rt with the corresponding sugars previously dissolved in phosphate buffer (pH = 7.4, 60 mM). For experiments leading to removal of fructose interference, a DMSO solution of **3.1** ($7.2 \times 10^{-5} M$) would be added. The final solution proportions were 9:1 DMSO:buffer. The mixtures stood at rt for 25 min before recording UV-Vis or fluorescence spectra.

Semiempirical molecular modeling analysis was performed in two steps, using MOPAC with the potential function AM1 (Chem3D 7.0, CambridgeSoft) to obtain an optimized geometry and then energy-minimization using MM2 (Chem3D 7.0, CambridgeSoft). Molecular graphics images were produced using the UCSF Chimera

package from the Computer Graphics Laboratory, University of California, San Francisco.

3.5 References

- 3.1. Recent reviews: (a) James T. D.; Shinkai, S. *Top. Curr. Chem.* **2002**, *218*, 159. (b) Wang, W.; Gao, X. M.; Wang, B. H. *Curr. Org. Chem.* **2002**, *6*, 1285. (c) Striegler, S.; *Curr. Org. Chem.* **2003**, *7*, 81. (d) Cao, H. S.; Heagy, M. D. *J. Fluoresc.* **2004**, *14*, 569.
- 3.2. Kim, K. K.; Escobedo, J. O.; Rusin, O.; Strongin, R. M. *Org. Lett.* **2003**, *5*, 5007.
- 3.3. Examples of related prior studies on saccharide conformational preferences and boronic acid complexation: (a) Norrild, J. C.; Eggert, H. *J. Am. Chem. Soc.* **1995**, *117*, 1470. (b) Norrild, J. C.; Eggert, H. *J. Chem. Soc., Perkin Trans 2* **1996**, 2583. (c) Nicholls, M. P.; Paul, P. K. C. *Org. Biomol. Chem.* **2004**, *2*, 1434.
- 3.4. (a) Omran, H.; McCarter, D.; St. Cyr, J.; Luederitz, B.. *Exp. & Clin. Cardiol.* **2004**, *9*, 117. (b) Dodd, S. L.; Johnson, C. A.; Fernholz, K.; St. Cyr, J. A. *Med. Hypotheses* **2004**, *62*, 819. (c) Lortet, S.; Zimmer, H.-G. *Cardiovasc. Res* **1989**, *23*, 702. (d) Takagi, Y.; Nakai, K.; Tsuchiya, T.; Takeuchi, T. *J. Med. Chem.* **1996**, *39*, 1582.
- 3.5. Marie, S.; Heron, B.; Bitoun, P.; Timmerman, T.; Van den Berghe, G.; Vincent, M. F. *Am. J. Hum. Genet.* **2004**, *74*, 1276.
- 3.6. Jaeken, J.; Van den Berghe, G. *Lancet II* **1984**, 1058.
- 3.7. Shiomi, Y.; Saisho, M.; Tsukagoshi, K.; Shinkai, S. *J. Chem. Soc., Perkin Trans I* **1993**, 2111.
- 3.8. (a) He, M.; Johnson, R. J.; Escobedo, J. O.; Beck, P. A.; Kim, K. K.; St. Luce, N. N.; Davis, C. J.; Lewis, P. T.; Fronczek, F. R.; Melancon, B. J.; Mrse, A. A.; Treleaven, W. D.; Strongin, R. M. *J. Am. Chem. Soc.* **2002**, *124*, 5000. (b) Rusin, O.; Alpturk, O.; He, M.; Escobedo, J. O.; Jiang, S.; Dawan, F.; Lian, K.; McCarroll, M. E.; Warner, I. M.; Strongin, R. M. *J. Fluoresc.* **2004**, *14*, 611.
- 3.9. Springsteen, G.; Wang, B. *Tetrahedron* **2002**, *58*, 5291.
- 3.10. The ¹H NMR assignments for D-ribose are based on the ones reported by: Benesi, A. J.; Falzone, C. J.; Banerjee, S.; Farber, G. K. *Carbohydr. Res.* **1994**, *258*, 27.
- 3.11. Cho, J. H.; Bernard, D. L.; Sidwell, R. W.; Kern, E. R.; Chu, C. K. *J. Med. Chem.* **2006**, *49*, 1140.
- 3.12. Matsuo, T.; Suzuki, H.; Hashiguchi, M.; Izumori, K. *J. Nutr. Sci. Vitaminol.* **2002**, *48*, 77.

- 3.13. Murata, A.; Sekiya, K.; Watanabe, Y.; Yamaguchi, F.; Hatano, N.; Izumori, K.; Tokuda, M. *J. Biosci. Bioeng.* **2003**, *96*, 89.
- 3.14. Austin, W. C.; Humoller, F. L. *J. Am. Chem. Soc.* **1934**, *56*, 1152.
- 3.15. Sui L, Dong YY, Watanabe Y, Yamaguchi F, Hatano N, Izumori K, Tokuda M. *Anticancer Res.* **2005**, *25*, 2639.
- 3.16. Lerner, L. M.; Mennitt, G. *Carbohydr. Res.* **1994**, *259*, 191.
- 3.17. Nagai, Y.; Kobayashi, K.; Toi, H.; Aoyama, Y. *Bull. Chem. Soc. Jpn.* **1993**, *66*, 2965.
- 3.18. Zhu, L.; Shabbir, S. H.; Gray, M.; Lynch, V. M.; Sorey, S.; Anslyn, E. V. *J. Am. Chem. Soc.* **2006**, *128*, 1222.
- 3.19. (a) Lewis, P. T.; Davis, C. J.; Saraiva, M.; Treleaven, W. D.; McCarley, T. D.; Strongin, R. M. *J. Org. Chem.* **1997**, *62*, 6110. (b) Davis, C. J.; Lewis, P. T.; McCarroll, M. E.; Read, M. W.; Cueto, R.; Strongin, R. M. *Org. Lett.* **1999**, *1*, 331.

CHAPTER 4

SELECTIVE DETECTION OF CYSTEINE AND HOMOCYSTEINE USING A FLUORESCIN DIALDEHYDE*

4.1 Introduction

This was a collaborative project with other members of my research group. My own specific contributions to this project included:

1. Synthesis of fluorescein dialdehyde. I contributed to the synthesis of fluorescein dialdehyde derivative (4.6). I conducted every step to the final product, which was used in the detection of cysteine and homocysteine by our group.

2. UV-Vis and Fluorescence experiments. I contributed, in conjunction with Dr. Oleksandr Rusin, to the UV-Vis and fluorescence studies of homocysteine in deproteinized human blood plasma.

4.2 Formation of Cysteine and Homocysteine

Cysteine (4.1) and homocysteine (4.2) are among the most important naturally occurring thiols and are of great concern to public health. Homocysteine was first discovered by Butz and du Vigneaud at the University of Illinois via heating methionine in sulfuric acid.^{4.1} Though discovered in 1932, homocysteine was not found to be health related until the early 1960s when children with mental retardation, dislocation of ocular lenses, seizures and skeletal abnormalities were found to have high concentrations in their urine.^{4.2}

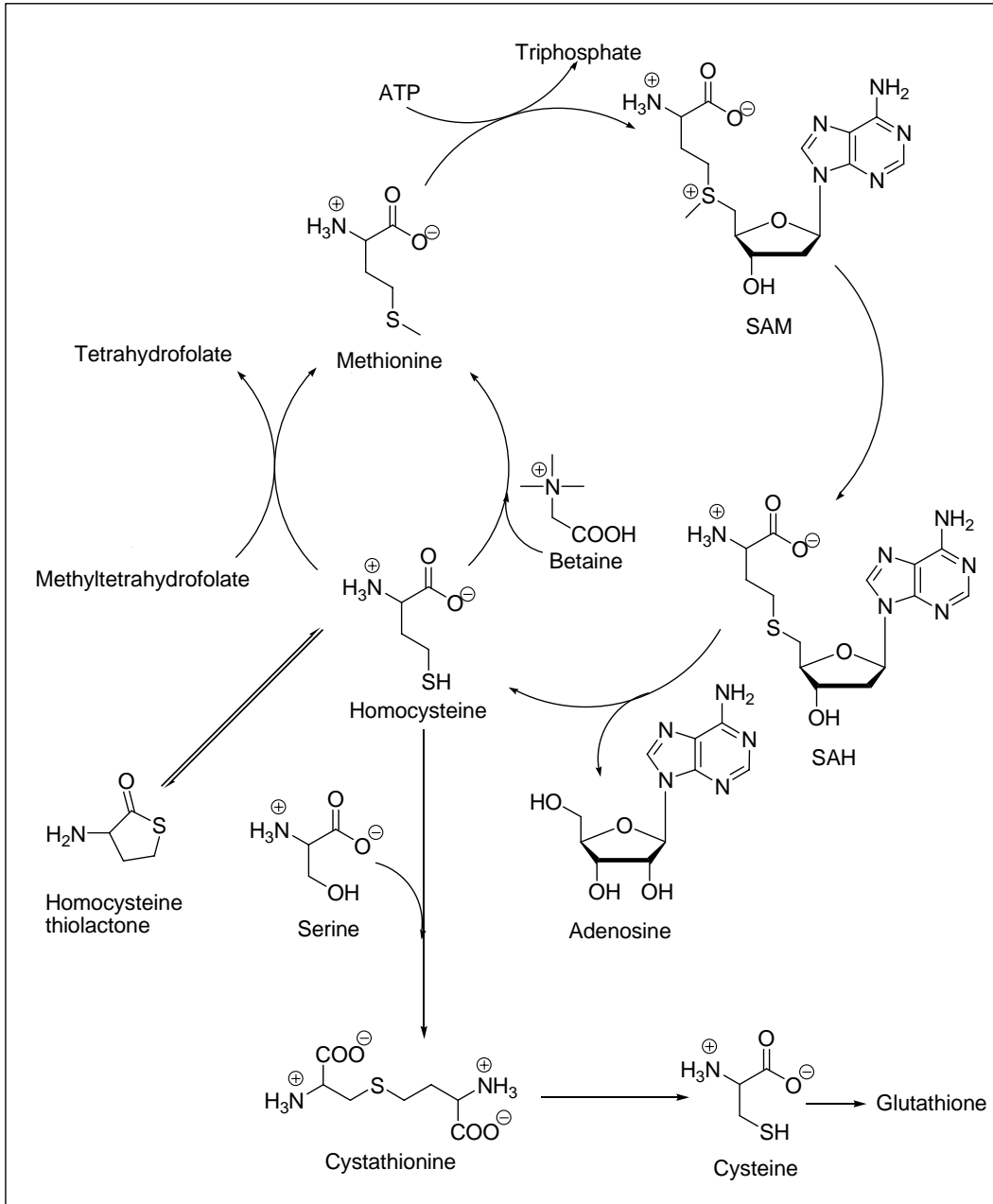
*Reprinted in part with permission from *Journal of the American Chemical Society*, 2003, Volume 126, pages 438-439; Oleksandr Rusin, Nadia N. St. Luce, Rezik A. Agbaria, Jorge O. Escobedo, Shan Jiang, Isiah M. Warner, Fareed B. Dawan, Kun Lian, and Robert M. Strongin; Visual Detection of Cysteine and Homocysteine. Copyright 2006 American Chemical Society.

The discovery of homocystinuria (homocysteine excreted in the urine) initiated an upsurge of interest in homocysteine. The structures of homocysteine and cysteine are very similar.

The poor water solubility of cystine reduces its ease of excretion. It therefore accumulates either in urine, resulting in cystinuria^{4.3} or in various organs of the body, leading to, for example, kidney stones.^{4.4} Low levels of cysteine are also involved in liver damage, slowed growth, muscle and fat loss, hair depigmentation, lethargy, and other metabolic pathways involving homocysteine are shown in Scheme 4.1. Homocysteine, an intermediate metabolite, mainly arises from the demethylation of methionine. In biological systems, L-methionine first reacts with ATP affording S-adenosylmethionine (SAM), a widely used methyl donor for many reactions.^{4.6} In the presence of a methyltransferase, S-adenosylhomocysteine (SAH) is produced via demethylation of SAM.^{4.7} The subsequent hydrolysis of SAH by the enzyme S-adenosylhomocysteine hydrolyase gives rise to homocysteine.^{4.8} The intake of homocysteine from the diet is very small. The homocysteine in the human body mainly originates from the metabolism of methionine. The methionine-derived homocysteine can be consumed in three distinct metabolic pathways, i.e. remethylation back to methionine, conversion to cysteine and formation of an intramolecular thioester.^{4.9, 4.10, 4.11, 4.12} Homocysteine metabolism through transulfuration is the major pathway to afford cysteine, which serves as a source of glutathione, sulfate and sulfite. The proper function of the related proteins plays an important role in adjusting cysteine and homocysteine metabolism. There are also other factors affecting the distributing of cysteine and homocysteine such as transport, intracellular import and export, and cellular uptake and output. Mechanistic

understanding of the distribution and the transportation of the thiols in human body is of importance for understanding of their possible roles in disease.

Scheme 4.1. Metabolism of Homocysteine.



4.3 Homocysteine in Plasma

Homocysteine exists in several forms after being released into plasma.^{4.13-4.15} The disulfide form with another thiol molecule such as proteins (more than 70%), homocysteine or other low-molecular-weight thiols. Hence, only a small fraction of homocysteine is present in plasma as reduced, free form. However, the amount of homocysteine normally refers to the total amount of bonded disulfide and free homocysteine.^{4.15}

4.4 Relevance of Homocysteine to Public Health

When the dynamic equilibrium of homocysteine metabolism is interrupted due to either nutritional deficiency or genetic defects, excess amounts of homocysteine accumulate in blood plasma (hyperhomocysteinemia) or urine (homocystinuria). It is known that elevated homocysteine in plasma is an independent risk factor associated with serious disorders such as Alzheimer's and cardiovascular diseases.^{4.16, 4.17} The former is a disorder in the human brain and the latter includes dysfunctional conditions of the heart and blood vessels which supply oxygen and nutrition to the body. Homocysteine is also related to a number of other diseases such as neural tube defects,^{4.18} pregnancy complications,^{4.19} and renal failure.^{4.20} Therefore, the detection of cysteine and homocysteine are of importance for diagnosing and understanding disease states.

Due to the health risks associated with homocysteine, improved detection methods of biological important thiols have been a focus of numerous research efforts. The current methods, including mass spectrometry, chromatographic separations, immuno- and enzymatic assays, and electrochemical technology have some intrinsic restrictions. The challenges with many current detection methods include harsh

conditions, tedious procedures, long run times,^{4.21} and high operating temperatures.^{4.8, 4.10,}

4.11

4.5 Synthesis of Fluorescein Dialdehyde Derivative 4.6

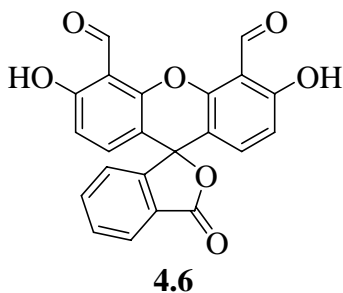
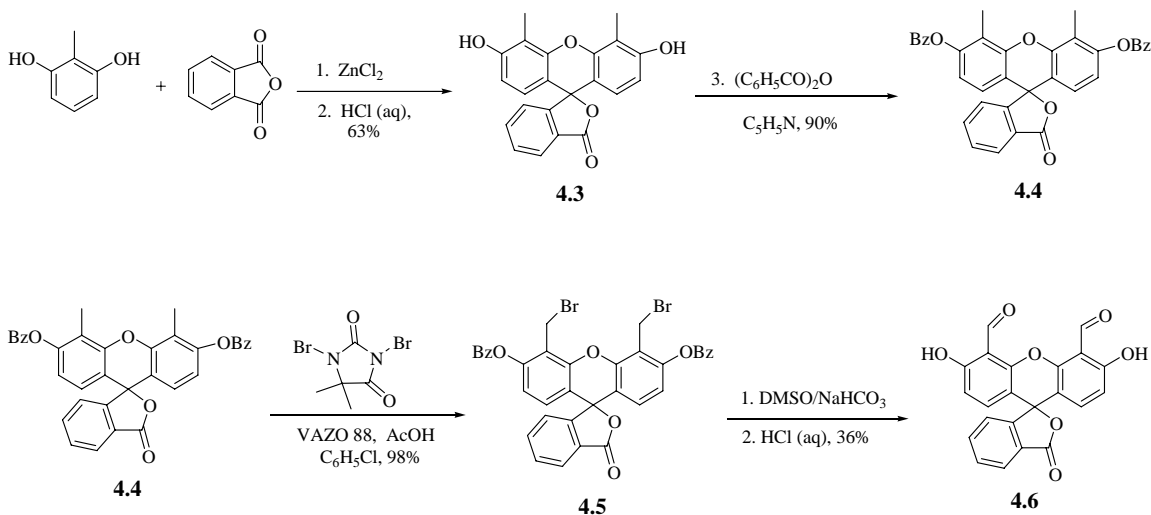


Figure 4.1 Compound **4.6**.

The synthesis of fluorescein dialdehyde derivative **4.6** (Figure 4.1) was reported by Burdette as a reaction intermediate in the synthesis of a fluorescent sensor for Zn^{2+} detection.^{4.22} The reactive aldehyde moieties plus the fluorescein chromophore make compound **4.6** a potential sensor for cysteine and homocysteine detection (*vide infra*). I was able to synthesize **4.6** with several modifications to the literature procedure.

The synthesis begins by condensing 2-methyresorcinol with phthalic anhydride in the presence of ZnCl_2 to afford compound **4.3**. The intermediate **4.3** wasn't previously isolated; however, I obtained it as a red solid by precipitation using aqueous HCl (6M).

Scheme 4.2 Synthesis of compound 4.6.

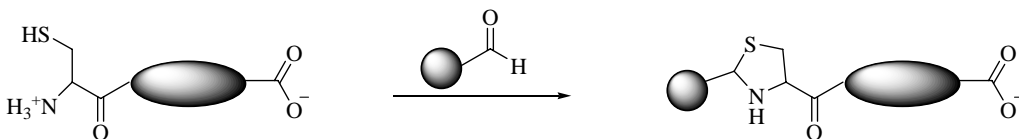


The subsequent protection of compound **4.3** with excess benzoic anhydride followed by bromination with 1,3-dibromo-5,5-dimethylhydantoin in $\text{C}_6\text{H}_5\text{Cl}$ produces fluorescein dibromide **4.5**. Oxidation of compound **4.5** via DMSO (Swern reaction) and work-up with aqueous HCl (2M) gives compound **4.6** (Scheme 4.2).

4.6 Results and Discussion

It is known that the selective reaction of *N*-terminal cysteine with aldehydes to form thiazolidines has been used to label and immobilize proteins and peptides (Scheme 4.3).^{4.23}

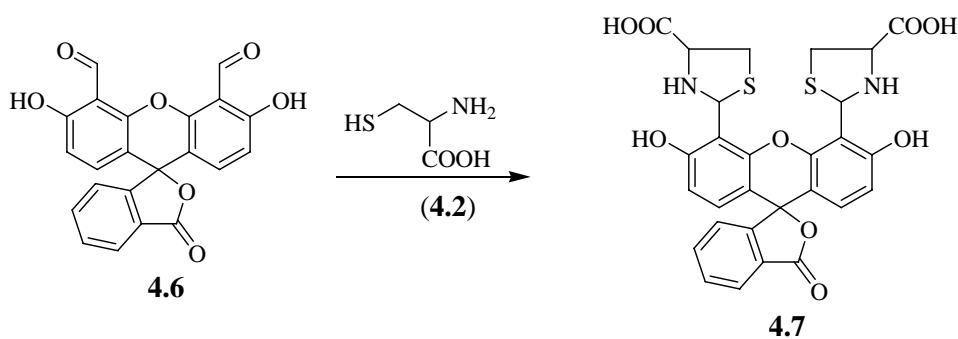
Scheme 4.3 Reaction of cysteine with aldehydes to form thiazolidines.



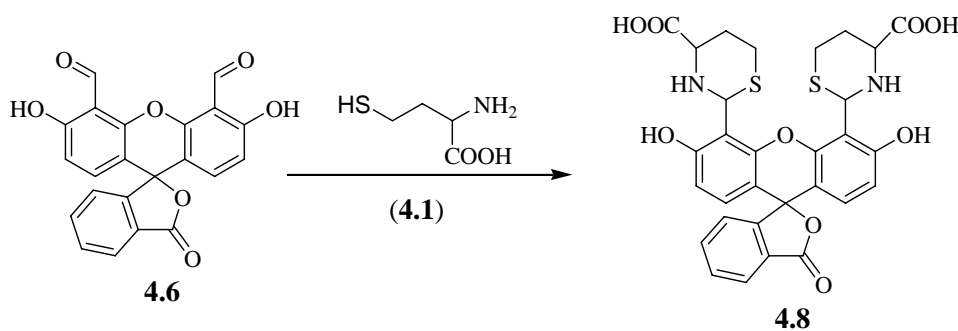
The reaction of the aldehyde moieties of **4.6** with cysteine (Scheme 4.4) and homocysteine (Scheme 4.5) would promote colorimetric and fluorometric responses,

which would be easily monitored. The use of the xanthene dye **4.6** for the efficient detection of cysteine and homocysteine is presented herein. The methodology also shows promise towards the direct and quantitative determination of homocysteine.

Scheme 4.4 Reaction of **4.6** with cysteine **4.1**. Reaction conditions: 0.25 M Na₂CO₃ buffer pH 9.5, followed by precipitation with MeOH.



Scheme 4.5 Reaction of **4.6** with homocysteine **4.2**. Reaction conditions: 0.25 M Na₂CO₃ buffer pH 9.5, followed by precipitation with MeOH.



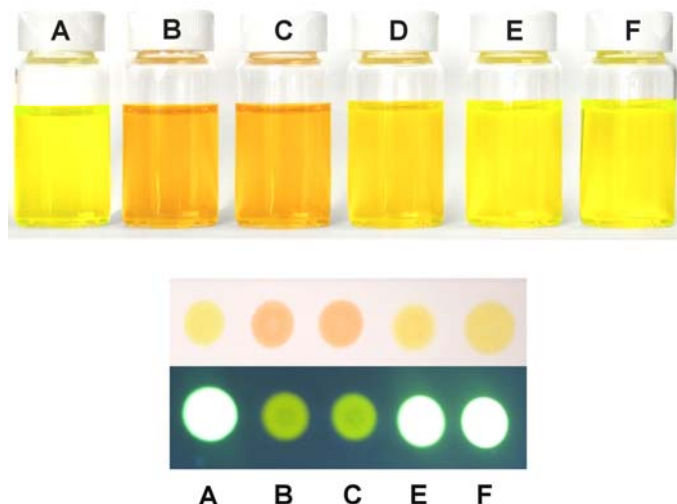


Figure 4.2 Top: color changes of solutions of **4.6** and various analytes. **A** = no analyte, **B** = cysteine, **C** = homocysteine, **D** = bovine serum albumin, **E** = glycine and **F** = *n*-propylamine. Bottom: co-spots of **4.6** ($1.0 \times 10^{-3} M$) with and without various analytes ($1.0 \times 10^{-3} M$) under visible and UV light.

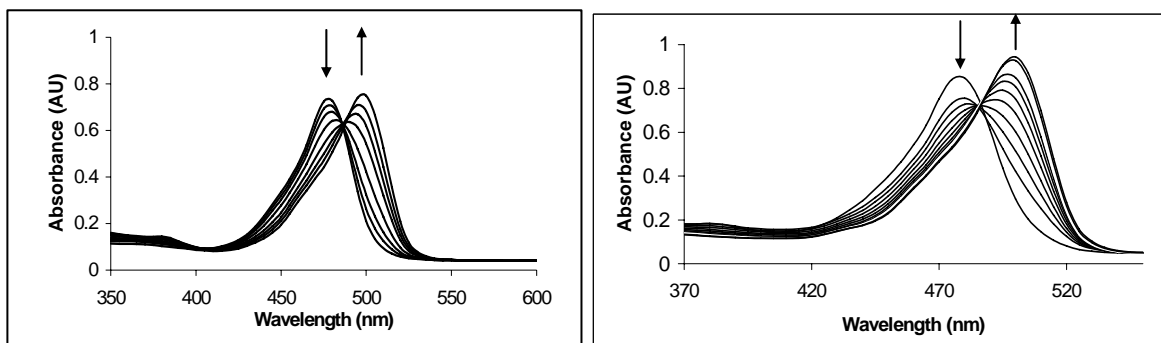


Figure 4.3 Left: Absorption spectra of dialdehyde ($2.5 \times 10^{-6} M$) and cysteine ($4 \times 10^{-6} M - 8 \times 10^{-5} M$) in H_2O , pH 9.5, rt, 5 min. Right: Interaction of the **4.6** ($4 \times 10^{-6} M$) and cysteine (4.9×10^{-5} to $7.4 \times 10^{-4} M$) in deproteinized human blood plasma containing 5.0 mM glutathione at room temperature. Detection limit is $4 \times 10^{-5} M$.

The visual detection of cysteine and homocysteine is shown in Figure 4.2. It illustrates that when cysteine or homocysteine ($1.0 \times 10^{-3} M$) is added to a solution of **4.6** ($1.0 \times 10^{-6} M$), in carbonate buffer at pH 9.5, a solution color change is observed from

bright yellow to brownish-orange. However, no apparent color changes were observed, with the use of a common amine, amino acid, or protein at the same concentrations. Similar effects on a solid support, C₁₈-bonded silica, are also shown in Figure 4.2.

Figure 4.3 illustrates UV-Vis characteristic absorbance changes of cysteine-**4.6** solutions. This solution was readily monitored in the cysteine concentration range of 10^{-5} - 10^{-6} M. A 25 nm red shift is observed from 480 nm to 505 nm with an increase in cysteine concentration.^{4,24} Similar shifts were also displayed in the sample of commercial human blood plasma (previously centrifuged at 3000 g through a cellulose 3000 MW cut-off filter), by adding **4.6** and excess amount of glutathione (1 mM). This resulted in concentration-dependent spectrophotometric changes (Figure 4.3). These results show the potential use of **4.6** for calibration and determination of concentrations of aminothiols in plasma samples in the presence of other biological thiols. Addition of cysteine or homocysteine to solutions of **4.6** results in fluorescence quenching.

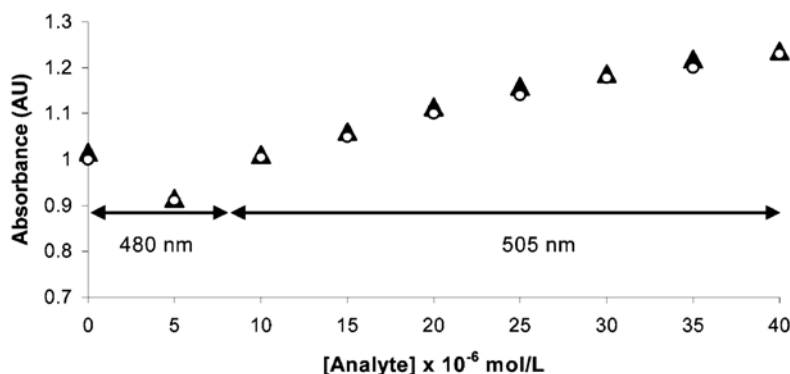


Figure 4.4 Absorbance vs. concentration plots for cysteine (▲) and homocysteine (O) in aqueous solutions of dialdehyde (2.5×10^{-6} M) at pH 9.5.

Solutions of **4.6** containing identical concentrations of **4.1** and **4.2** respectively exhibit similar spectrophotometric changes (Figure 4.4). Absorbance of **4.6** at 480 nm decreases in the presence of 5×10^{-6} M cysteine or homocysteine. For concentrations of

cysteine or homocysteine in the range 10×10^{-6} – 40×10^{-6} the absorbance increases at 505 nm. Poor reactivity of **4.6** with other common thiols (methionine, mercaptoethanol, glutathione), other amino acid (glutamine, serine, glycine, glutamic acid), and amines (D-glucosamine hydrochloride and *n*-propylamine) (8×10^{-4} M, pH 9.5) highlights the selectivity of **4.6** for cysteine and homocysteine. In response to the analytes mentioned above, only about 15% decrease in absorbance at 480 nm is observed. No noticeable wavelength shift is seen (Figure 4.5). Small absorbance decreases without wavelength shifts are also observed in another control experiment using solutions containing **4.6** and bovine serum albumin or urease.

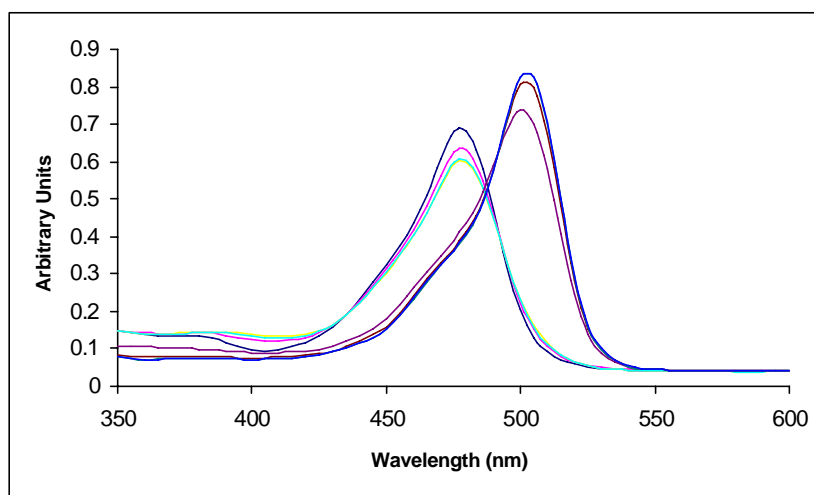


Figure 4.5 Successive addition of serine (to final concentrations of 4×10^{-5} M to 8×10^{-4} M) to an aqueous solution of dialdehyde (2.5×10^{-6} M) at pH 9.5 results only in an absorbance change at 480 nm. Addition of cysteine (to final concentrations of 4×10^{-6} M - 8×10^{-5} M) to the serine-dialdehyde solution produces an absorbance change at 505 nm.

A linear correlation between fluorescence emission intensity and healthy to abnormal homocysteine concentrations in plasma containing **4.1** is shown in Figure 4.6.

This provides a potential method toward calibrating and quantitative determining aminothiols concentrations in human plasma in the presence of other biological thiols.

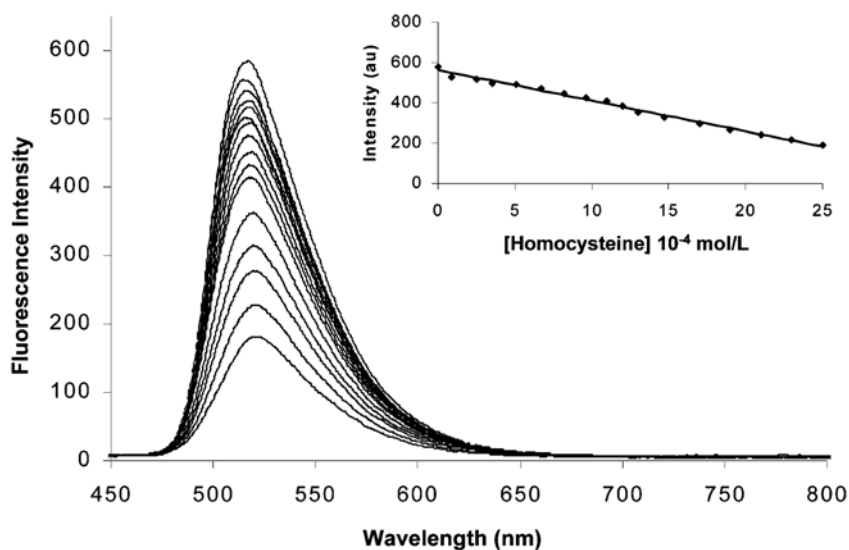


Figure 4.6 Fluorescence emission spectra of **4.6** (5.2×10^{-7} M) and homocysteine (2.9×10^{-6} - 2.5×10^{-3} M) in deproteinized human plasma excited at 460 nm (pH 9.5). (Inset) Fluorescence emission plotted vs [homocysteine].

4.7 Conclusion

We have shown that compound **4.6** can be used to readily detect cysteine and homocysteine in the range of their physiological levels. This is done with negligible interference from amines, amino acids, and certain thiols and proteins. This may allow for the rapid detection of cysteine and homocysteine. We are currently exploring and optimizing new methods for the selective detection of cysteine and homocysteine.

4.8 Experimental Section

Matrix Assisted Laser Desorption Ionization mass spectra were acquired using a Bruker Proflex III MALDI mass spectrometer with either anthracene or dithranol matrices. UV-Visible spectra were recorded at room temperature on a Spectramax Plus (Molecular Devices). Analytical thin-layer chromatography (TLC) was performed using general-purpose silica gel on glass (Scientific Adsorbants). Flash chromatography columns were prepared with silica gel (Scientific Adsorbants, 32-63 μm particle size, 60 \AA). The following compounds were prepared according to literature methods: **4.4**,^{4.22} **4.5**,^{4.22} and **4.6**,^{4.22} All other chemicals were purchased from Sigma or Aldrich and used without further purification. Proton NMR spectra were acquired in either CD_3OD , CH_3OD or $\text{DMSO}-d_6$ on a Bruker DPX-250, DPX-400, or AMX-500 spectrometer. All δ values are reported with $(\text{CH}_3)_4\text{Si}$ at 0.00 ppm or DMSO at 2.45 ppm as references.

4.9 References

- 4.1 Butz LW; du Vigneaud V. "The formation of a homologue of cystine by the decomposition of methionine with sulfuric acid". *J. Biol. Chem.*, **1932**, 99, 135-142.
- 4.2 Carson NAJ; Cusworth DC; Dent CE; Field CMB; Neill DW; Westall RG. "Homocystinuria: A new inborn error of metabolism associated with mental deficiency". *Arch. Dis. Child*, **1963**, 38, 425-436.
- 4.3 Crawhall, J. C.; Watts, R. W. E. *Am. J. Med.* **1968**, 45, 736.
- 4.4 Berlow S. *Adv. Clin. Chem.* **1967**, 9, 165.
- 4.5 Shahrokhian, S. *Anal. Chem.* **2001**, 73, 5972.
- 4.6 Cantoni G. L. "S-adenosylmethionine: A new intermediate form enzymatically from L-methionine and adenosine triphosphate". *J. Biol. Chem.*, **1953**, 204, 403-416.

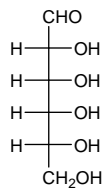
- 4.7 Finkelstein, J. D. "The metabolism of homocysteine: pathways and regulation". *Eur. J. Pediatr.*, **1998**, *157*, Suppl. 2, S40-44.
- 4.8 Cantoni, G. L. "Biological methylation: selected aspects". *Annu. Rev. Biochem.*, **1975**, *44*, 435-451.
- 4.9 Finkelstein, J. D. "Methionine metabolism in mammals". *J. Nutr. Biochem.*, **1990**, *1*, 228-237.
- 4.10 Mudd S. H.; Finkelstein J. D.; Irreverre F.; Laster L. "Transsulfuration in mammals: Microassays and tissue distribution of three enzymes of the pathway". *J. Biol. Chem.*, **1965**, *240*, 4382-4392.
- 4.11 Selhub J. "Homocysteine Metabolism". *Annu. Rev. Nutr.*, **1999**, *19*, 217-246.
- 4.12 Jakubowski, H. "Metabolism of homocysteine thiolactone in human cell cultures". *J. Biol. Chem.*, **1997**, *272*, 1935-1942.
- 4.13 H.; Helland S.; Ueland P. M. "Radioenzymic determination of homocysteine in plasma and urine". *Clin. Chem.*, **1985**, *31*, 624-628.
- 4.14 Araki A.; Sako Y. "Determination of free and total homocysteine in human plasma by high-performance liquid chromatography with fluorescence detection". *J. Chromatogr. Biomed. Sci. App.*, **1987**, *422*, 43-52.
- 4.15 (a) Pasas S. A.; Lacher N. A.; Davies M. I.; Lunte S. M. "Detection of homocysteine by conventional and microchip capillary electrophoresis/electrochemistry". *Electrophoresis*, **2002**, *23*, 759-766. (b) Refsum H.; Helland S.; Ueland P. M. "Radioenzymic determination of homocysteine in plasma and urine". *Clin. Chem.*, **1985**, *31*, 624-628
- 4.16 Refsum H.; Ueland P. M.; Nygard O.; Vollset S. E. "Homocysteine and cardiovascular disease". *Annu. Rev. Med.*, **1998**, *49*, 31-62.
- 4.17 Seshadri S.; Beiser A.; Selhub J.; Jacques P. F.; Rosenberg I. H.; D'Agostino R. B.; Wilson P. W. F. Wolf P. A. "Plasma homocysteine as a risk factor for dementia and Alzheimer's disease". *N. Engl. J. Med.*, **2002**, *346*, 476-483.
- 4.18 Smithells R. W.; Sheppard S.; Schorah C. J.; Seller M. J.; Nevin N. C.; Harris R.; Read A. P.; Fielding D. W. "Possible prevention of neural-tube defects by periconceptional vitamin supplementation". *Lancet.*, **1980**, *i*, 339-340.
- 4.19 Eskes T. K. A.B.; Steegers E. A. P.; Merkus H. M. W. M. "Hyperhomocysteinemia in obstetrics and gynecology: A unifying concept". *Neth. J. Med.*, **1998**, *52*, S16-17.

- 4.20 Wheeler D. C. "Cardiovascular disease in patients with chronic renal failure". *Lancet.*, **1996**, 348.1673-1674.
- 4.21 Ubbink, J. B.; Delport, R.; Riezler, R.; Hayward-Vermaak, W. J. *Clin. Chem.* **1999**, 45, 670.
- 4.22 Burdette, S. C.; Walkup, G. K.; Spingler, B.; Tsien, R. Y.; Lippard, S. J. *J. Am. Chem. Soc.* **2001**, 123, 7831.
- 4.23 Tolbert, T. J.; Wong, C.-H. *Angew. Chem. Int. Ed.* **2002**, 41, 2171 and references cited therein. Reactions of carbonyls with cysteine and homocysteine: (b) Fourneau, J. P.; Efimovsky, O.; Gaignault, J. C.; Jacquier, R.; LeRidant, C. *C. R. Acad. Sci. Ser. C* **1971**, 272, 1982. c) Cooper, A. J. L.; Meinster, A. *J. Biol. Chem.* **1982**, 257, 816.
- 4.24 We obtained analogous absorption spectra under identical conditions but at pH 6.5; however, we observe minor amounts of precipitate.

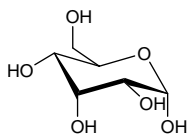
APPENDIX A. STRUCTURES OF TWELVE HEXOSES AND FOUR PENTOSES

1. Hexoses

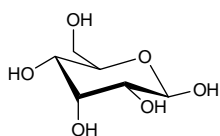
1. D-Allose



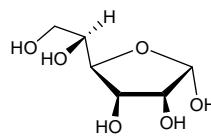
D-alloaldose



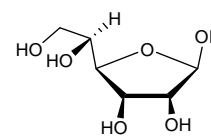
α -D-allopyranose



β -D-allopyranose

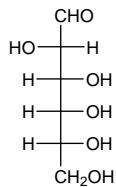


α -D-allofuranose

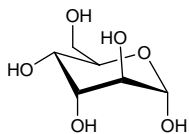


β -D-allofuranose

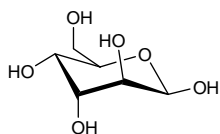
2. D-altrose



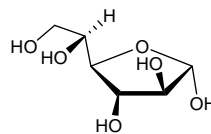
D-altroaldose



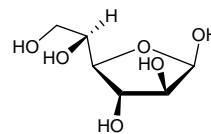
α -D-altropyranose



β -D-altropyranose

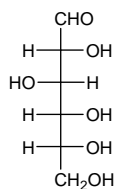


α -D-altrofuranose

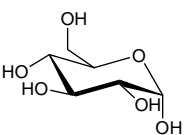


β -D-altrofuranose

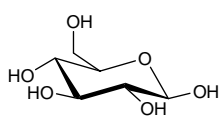
3. D-Glucose



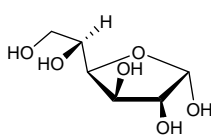
D-glucoaldose



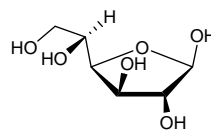
α -D-glucopyranose



β -D-glucopyranose

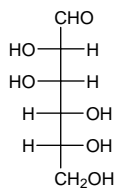


α -D-glucofuranose

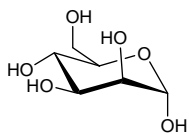


β -D-glucofuranose

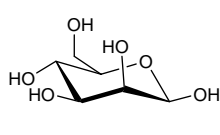
4. D-Mannose



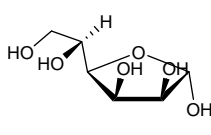
D-mannoaldose



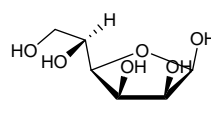
α -D-mannopyranose



β -D-mannopyranose

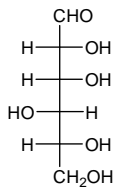


α -D-mannofuranose

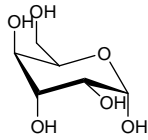


β -D-mannofuranose

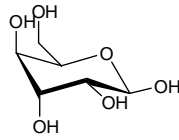
5. D-Gulose



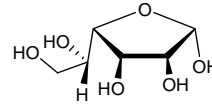
D-guloaldose



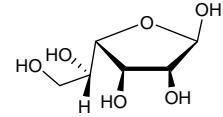
α -D-gulopyranose



β -D-gulopyranose

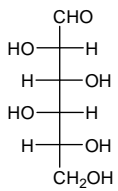


α -D-gulofuranose

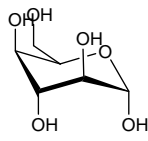


β -D-gulofuranose

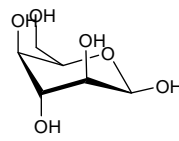
6. D-Idose



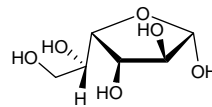
D-idoaldose



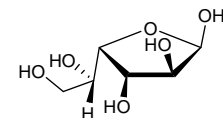
α -D-idopyranose



β -D-idopyranose

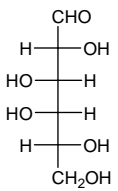


α -D-idofuranose

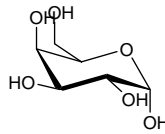


β -D-idofuranose

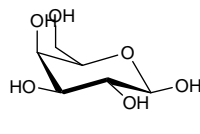
7. D-Galactose



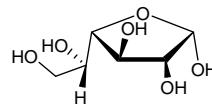
D-galactoaldose



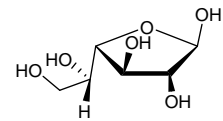
α -D-galactopyranose



β -D-galactopyranose

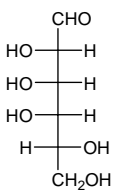


α -D-galactofuranose

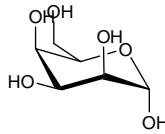


β -D-galactofuranose

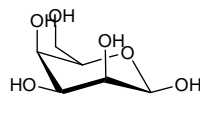
8. D-Talose



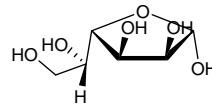
D-taloaldose



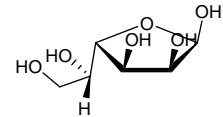
α -D-talopyranose



β -D-talopyranose

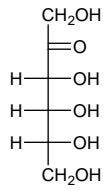


α -D-talofuranose

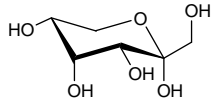


β -D-talofuranose

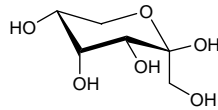
9. D-Psicose



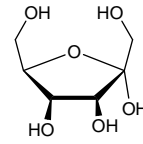
D-psicoketose



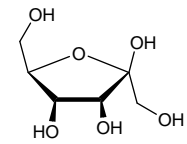
α -D-psicopyranose



β -D-psicopyranose

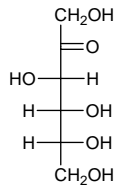


α -D-psicofuranose

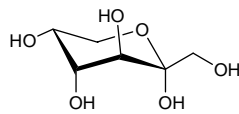


β -D-psicofuranose

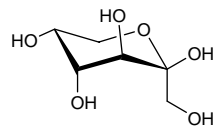
10. D-Fructose



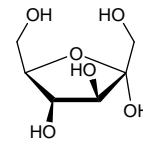
D-fructoketose



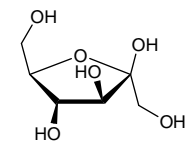
α -D-fructopyranose



β -D-fructopyranose

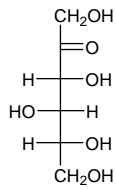


α -D-fructofuranose

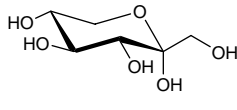


β -D-fructofuranose

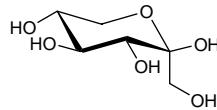
11. D-Sorbose



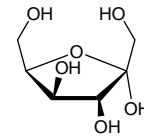
D-sorboketose



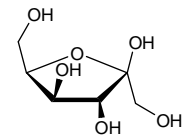
α -D-sorbopyranose



β -D-sorbopyranose

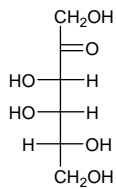


α -D-sorbofuranose

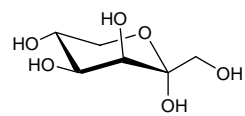


β -D-sorbofuranose

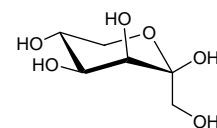
12. D-Tagatose



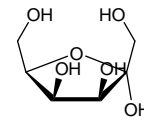
D-tagatoketose



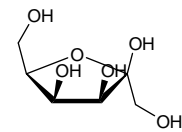
α -D-tagatopyranose



β -D-tagatopyranose



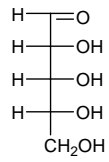
α -D-tagatofuranose



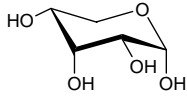
β -D-tagatofuranose

2. Pentoses

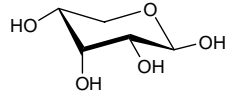
1. D-Ribose



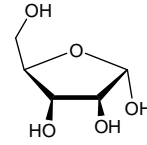
D-riboketose



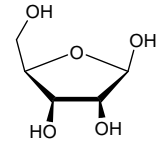
α -D-ribopyranose



β -D-ribopyranose

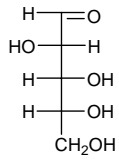


α -D-ribofuranose

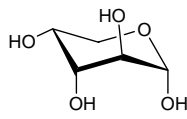


β -D-ribofuranose

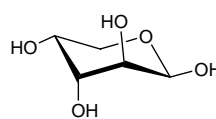
2. D-Arabinose



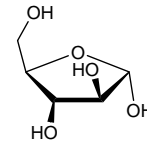
D-arabinoketose



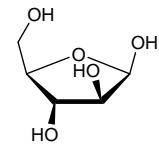
α -D-arabinopyranose



β -D-arabinopyranose

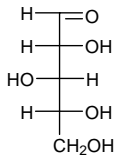


α -D-arabinofuranose

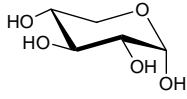


β -D-arabinofuranose

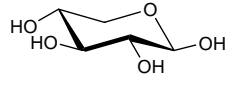
3. D-Xylose



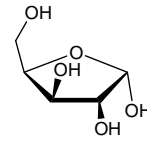
D-xyloketose



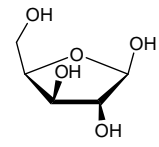
α -D-xylopyranose



β -D-xylopyranose

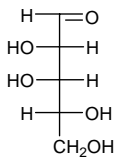


α -D-xylofuranose

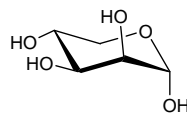


β -D-xylofuranose

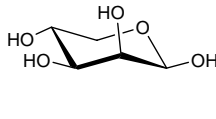
4. D-Lyxose



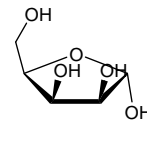
D-lyxoketose



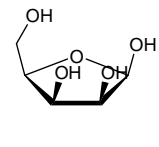
α -D-lyxopyranose



β -D-lyxopyranose



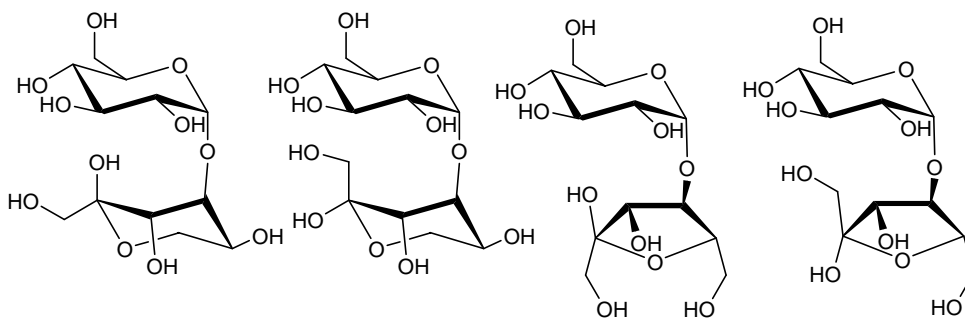
α -D-lyxofuranose



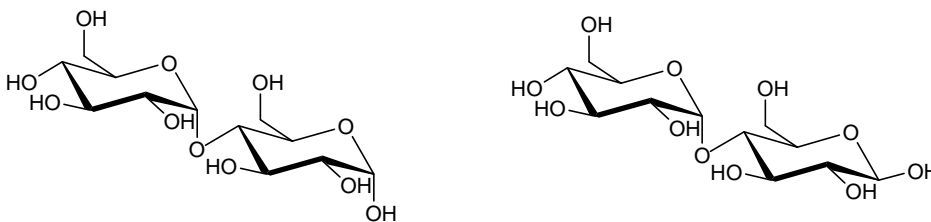
β -D-lyxofuranose

APPENDIX B. STRUCTURES OF FIFTEEN SELECTED DISACCHARIDES

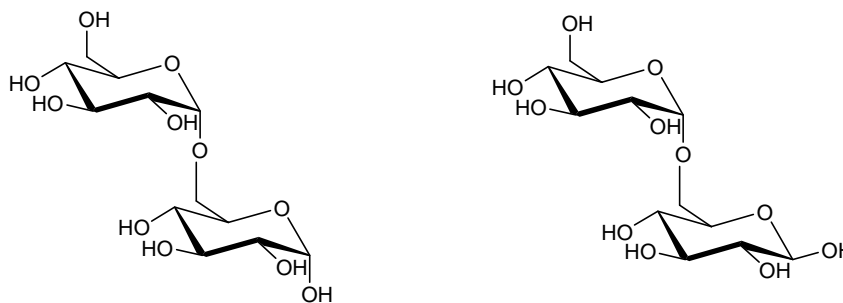
1. Maltulose, or α -D-glucopyranosyl-(1 \rightarrow 4)-D-fructose



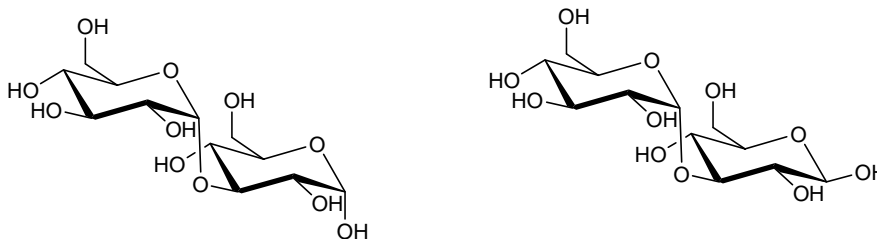
2. Maltose O- α -D-glucopyranosyl-(1 \rightarrow 4)-D-glucopyranose



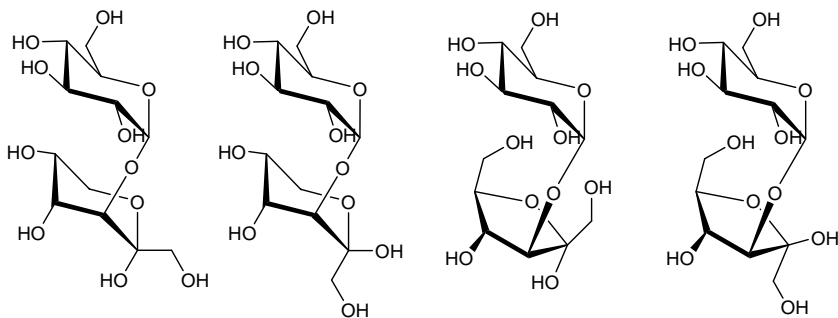
3. Isomaltose or O- α -D-glucopyranosyl-(1 \rightarrow 6)-D-glucopyranose



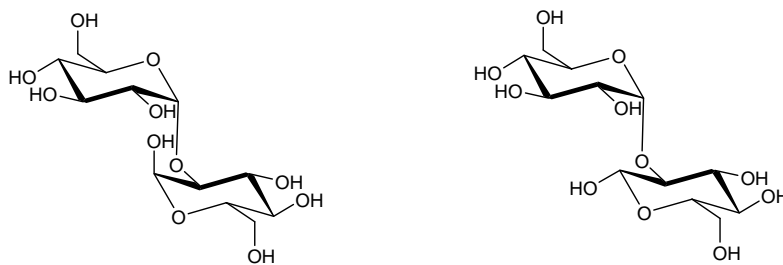
4. Nigerose or O- α -D-glucopyranosyl-(1 \rightarrow 3)-D-glucopyranose



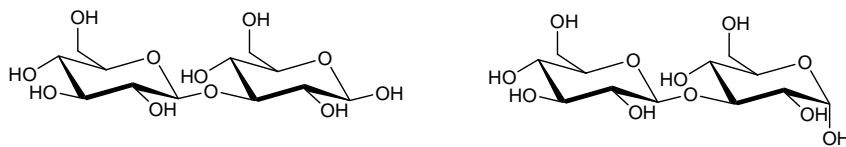
5. Turanose, or O- α -D-glucopyranosyl-(1 \rightarrow 3)-D-fructose



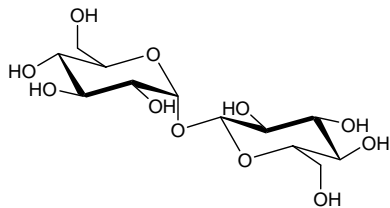
6. Kojibiose or O- α -D-glucopyranosyl-(1 \rightarrow 2)-D-glucopyranose



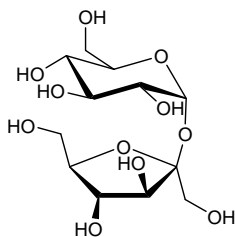
7. Laminaribiose or O- β -D-glucopyranosyl-(1 \rightarrow 3)-D-glucopyranose



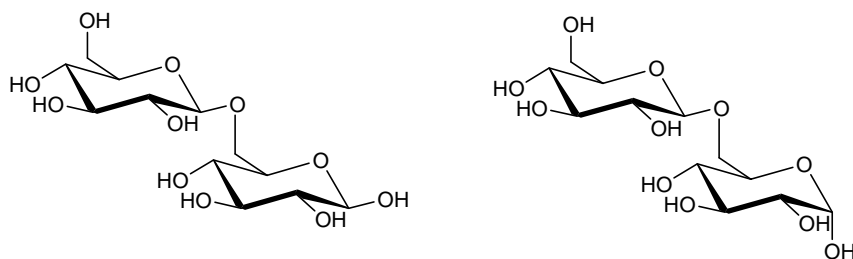
8. α, β -Trehalose or α -D-glucopyranosyl- β -D-glucopyranoside



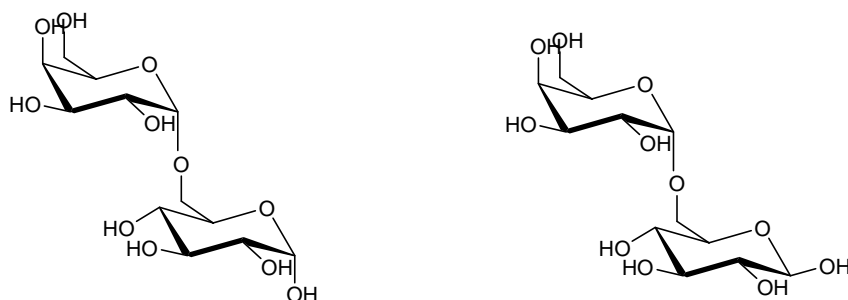
9. sucrose, or α -D-glucopyranosyl- β -D-fructofuranoside



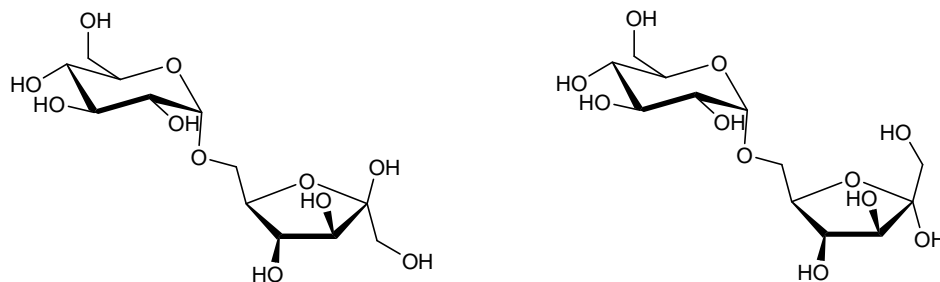
10. Gentiobiose O- β -D-glucopyranosyl-(1 \rightarrow 6)-D-glucopyranose



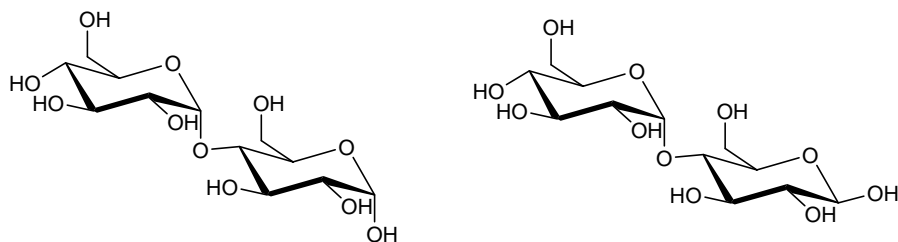
11. Melibiose or O- α -D-galactopyranosyl-(1 \rightarrow 6)-D-glucopyranose



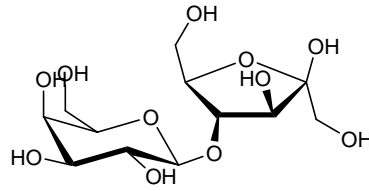
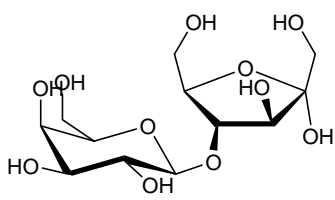
12. Palatinose or O- α -D-glucopyranose- (1 \rightarrow 6)-D- fructofuranose



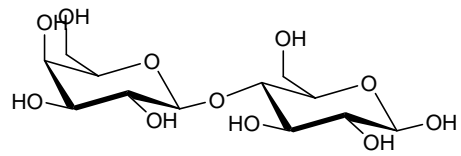
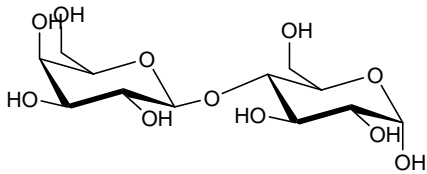
13. Cellobiose or O- β -D-glucopyranosyl-(1 \rightarrow 4)-D-glucopyranose



14. lactulose 4-O- β -D-Galactopyranosyl-D-fructofuranose

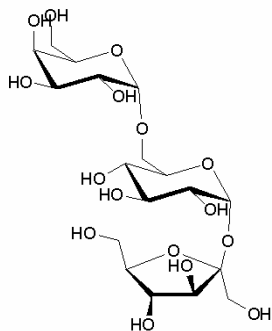


15. Lactose β -D-Gal-(1 \rightarrow 4)- β -D-Glc

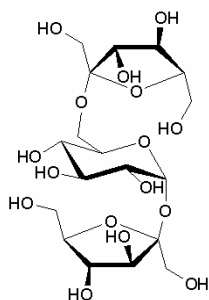


APPENDIX C. STRUCTURES OF TWELVE SELECTED TRISACCHARIDES

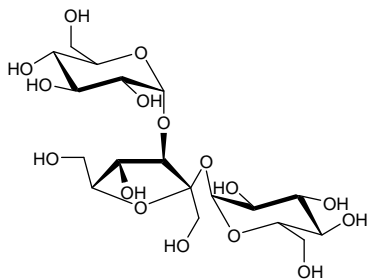
1. Raffinose or O- α -D-galactopyranosyl-(1 \rightarrow 6)-O- α -D-glucopyranosyl- β -D-fructofuranoside



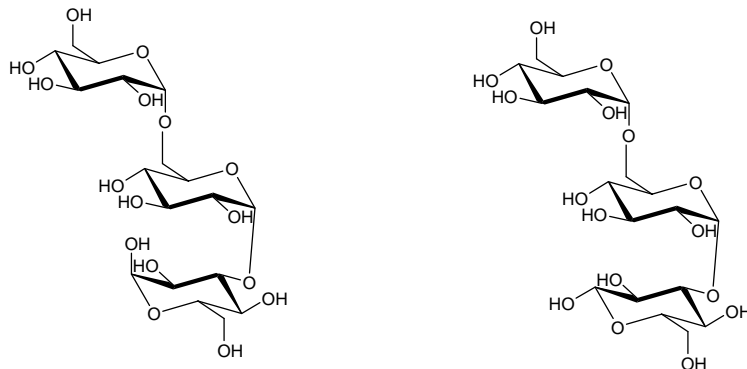
2. Neokestose or O- β -D-fructofuranosyl-(2 \rightarrow 6)-O- α -D-glucopyranosyl- β -D-fructofuranoside



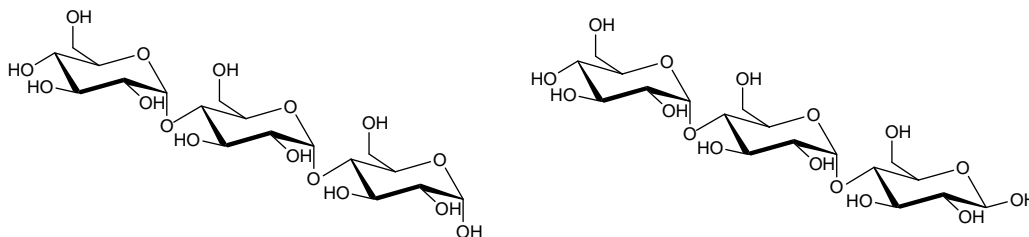
3. Melizitose or O- α -D-glucopyranosyl-(1 \rightarrow 3)-O- β -D-fructofuranosyl-(2 \rightarrow 1)- α -D-glucopyranoside



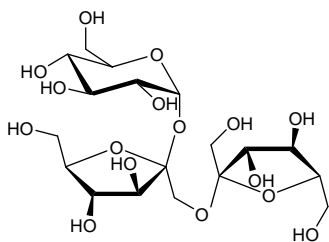
4. 3- α -Isomaltosylglucose or O- α -D-glucopyranosyl-(1 \rightarrow 6)-O- α -D-glucopyranosyl-(1 \rightarrow 3)-D-glucopyranose



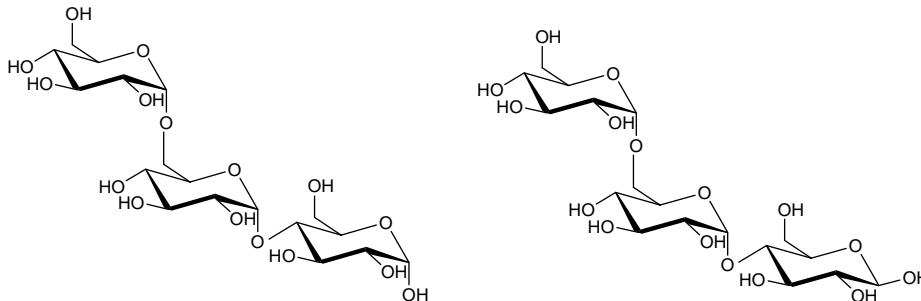
5. Maltotriose or O- α -D-glucopyranosyl-(1 \rightarrow 4)-O- α -D-glucopyranosyl-(1 \rightarrow 4)-D-glucopyranose



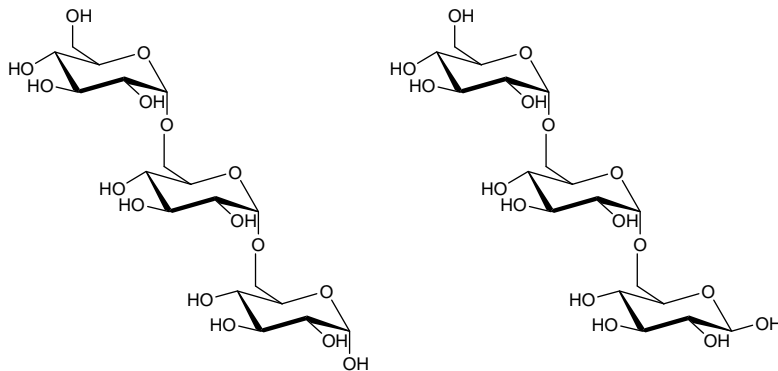
6. 1-Ketose or O- α -D-glucopyranosyl-(1 \rightarrow 2)-O- β -D-fructofuranosyl-(1 \rightarrow 2)- β -D-fructofuranoside



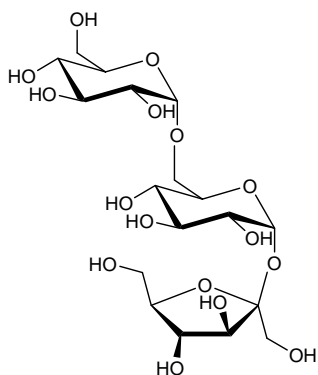
7. Panose or O- α -D-glucopyranosyl-(1 \rightarrow 6)-O- α -D-glucopyranosyl-(1 \rightarrow 4)-D-glucopyranose



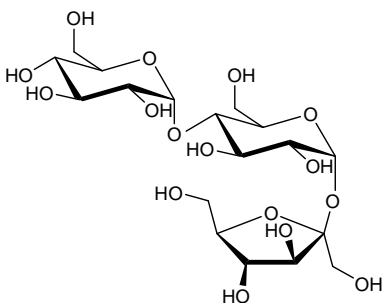
8. Isomaltotriose or O- α -D-glucopyranosyl-(1 \rightarrow 6)-O- α -D-glucopyranosyl-(1 \rightarrow 6)-D-glucopyranose



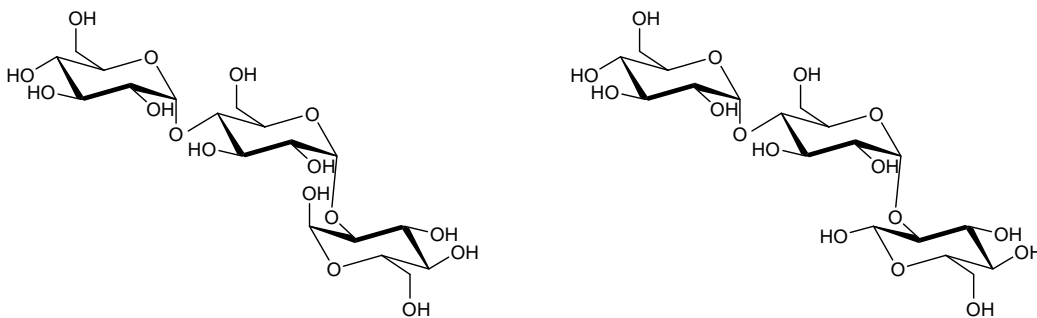
9. Theanderose or O- α -D-glucopyranosyl-(1 \rightarrow 6)-O- α -D-glucopyranosyl- β -D-fructofuranoside



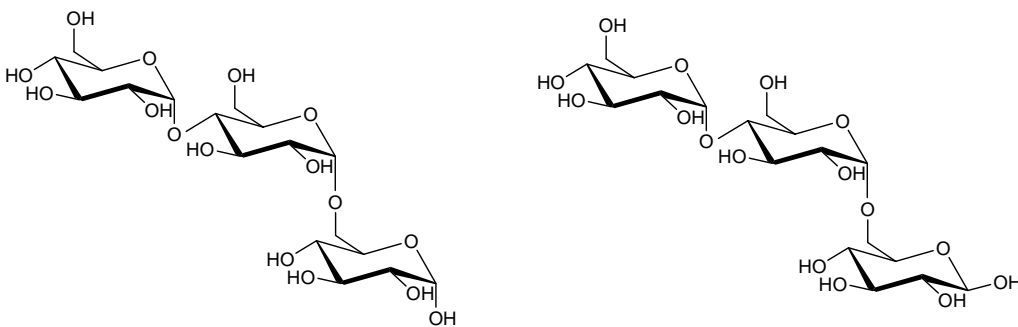
10. Erllose or O α -D-glucopyranosyl-(1 \rightarrow 4)-O α -D-glucopyranosyl β -D-fructofuranoside



11. Centose or O α -D-glucopyranosyl-(1 \rightarrow 4)-O α -D-glucopyranosyl-(1 \rightarrow 2)-D-glucopyranose

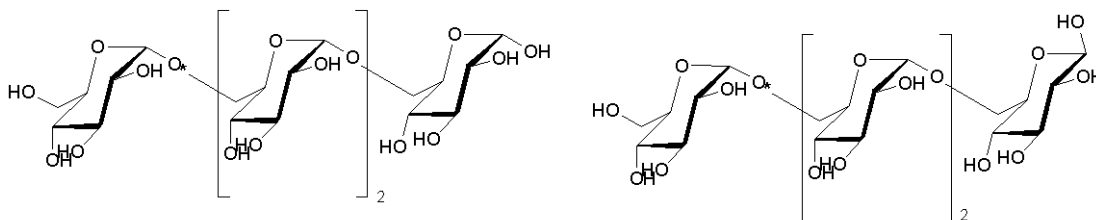


12. Isopanose or O- α -D-glucopyranosyl-(1 \rightarrow 4)-O- α -D-glucopyranosyl-(1 \rightarrow 6)-D-glucopyranose

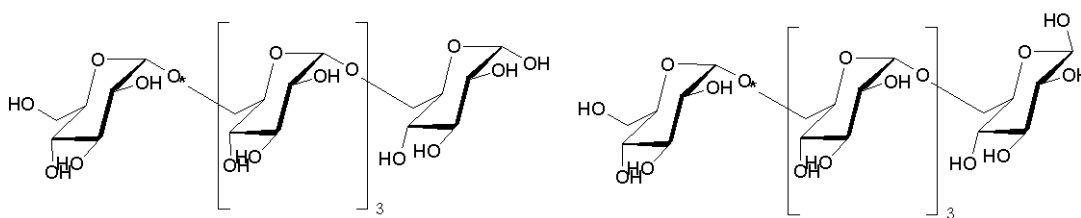


APPENDIX D. STRUCTURES OF THREE SELECTED OLIGOSACCHARIDES

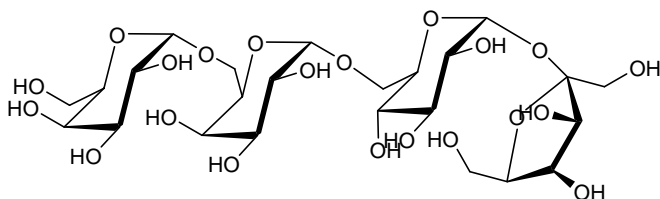
1. Isomaltotetraose or α -D-glucopyranosyl-(1 \rightarrow 6)-[α -D-glucopyranosyl-(1 \rightarrow 6)]₂-D-glucopyranose



2. Isomaltopentaose or α -D-glucopyranosyl-(1 \rightarrow 6)-[α -D-glucopyranosyl-(1 \rightarrow 6)]₃-D-glucopyranose



3. Stachyose or α -D-Gal-(1 \rightarrow 6)- α -D-Gal-(1 \rightarrow 6)- α -D-Glc-(1 \rightarrow 2)- β -D-Fru



APPENDIX E. COLORIMERIC DETECTION OF BIOLOGICAL MOLECULES

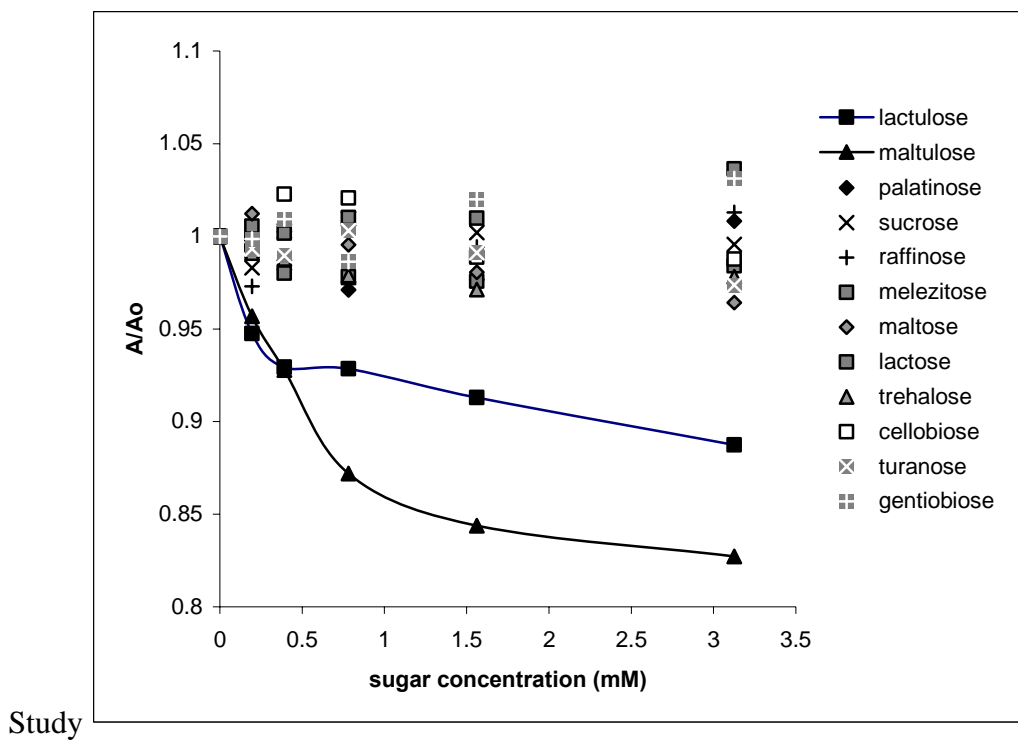


Figure E1. Relative absorbance spectral responses at 535 nm vs concentration of di- and trisaccharides. Selectivity for lactulose and maltulose is exhibited at this wavelength, to a lesser extent than at 355 nm (see Figure 2.11).

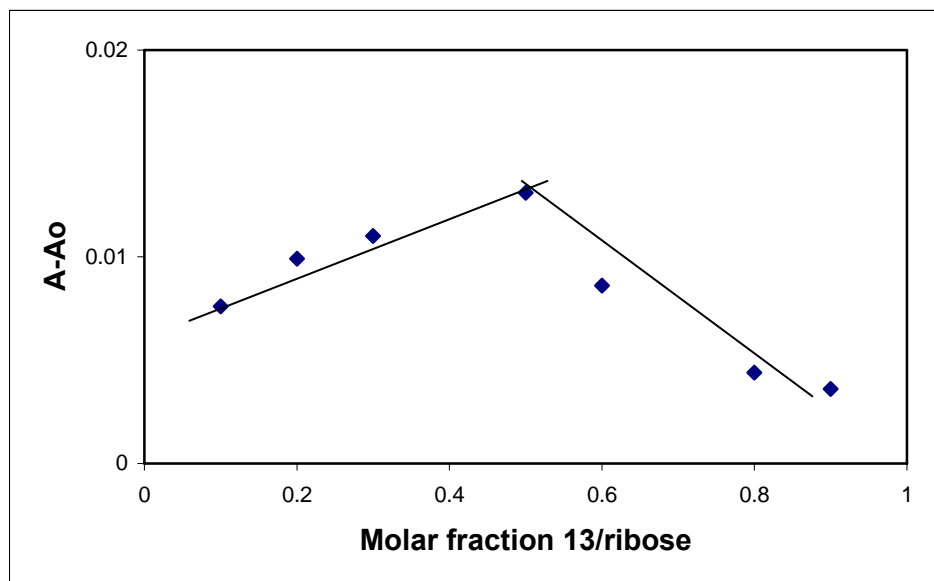


Figure E2. Job's plot of compound **8** and D-ribose in 9:1 DMSO:phosphate buffer (60 mM pH 7.4) showing a 1:1 stoichiometry. A-A₀ is the difference in absorbance intensity of the solution in the presence of D-ribose and the blank (solution containing only **8**) at 510 nm.

Table E1: Percentage recovery of fructose added into Honey measured at 355 mM.

No.	Recovery % at 355mM	Recovery % at 535mM
1	104.4	150.5
2	103.5	143.7
3	103.5	154.9
4	104.0	148.9
5	101.2	143.7
6	100.8	148.9
7	102.6	142.9
8	89.4	145.7
Average	101.2	147.4

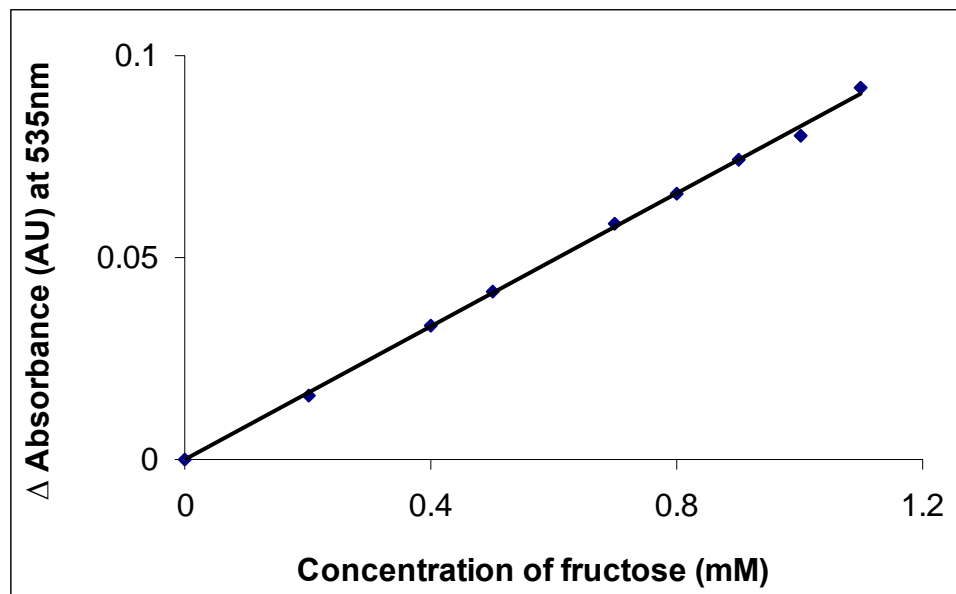


Figure E3. The calibration curve validated by the addition of fructose standards to a solution of honey (0.32 mg/mL) and **1** (3.4 mM) in a 1:9 mixture of phosphate buffer (0.1 mL, 60 mM, pH = 7.4) and DMSO at 535 nm.

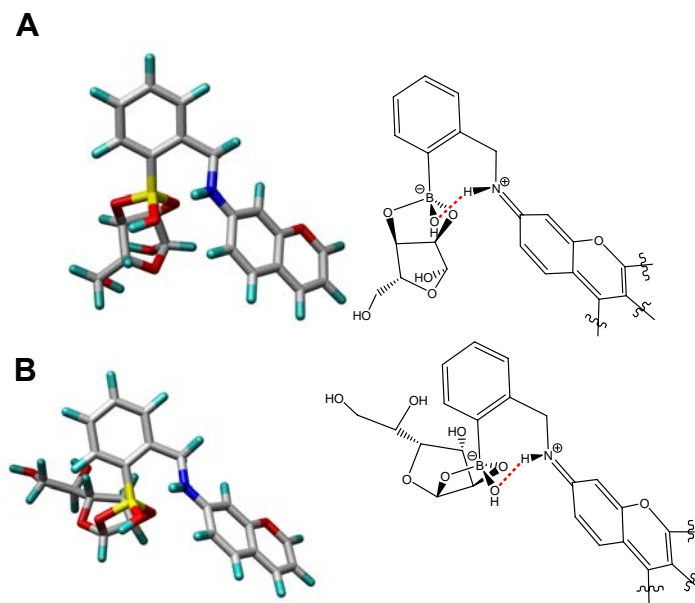


Figure E4. Energy-minimized structures of the complementary conformers derived from **3.1** and ribofuranose (“exo” isomer, structure A), and glucofuranose (“endo” isomer, structure B). A subunit of the the rhodamine chromophore moiety is shown for clarity and used in the simulations in order to simplify the calculations.

References.

1. Breitmaier, E.; Hollstein, U. *Org. Magn. Reson.* **1976**, *8*, 573.

APPENDIX F. LETTERS OF PERMISSION

Page 1 of 1

Karen Buehler

From: Shan Jiang [sjiang1@lsu.edu]
Sent: Thursday, September 21, 2006 11:52 AM
To: copyright@acs.org
Subject: permission

To Whom It May Concern:

I am a graduate student in the Department of Chemistry in Louisiana State University. I am writing to obtain the permission for the use of my contributions to two articles published in the "Journal of the American Chemical Society". I am the first author on one article and fifth author of the other and would like to include my contributions to the articles in my doctoral dissertation. The articles are:

"Stereochemical and Regiochemical Trends in the Selective Spectrophotometric Detection of Saccharides", J. Am. Chem. Soc. 2006, 128, 12221-12228.

"Visual Detection of Cysteine and Homocysteine" J. Am. Chem. Soc. 2004, 126, 438-439.

Thank you very much for your consideration of this request.

Sincerely,

Shan Jiang
Department of Chemistry
Chopping Hall Rm 232
Louisiana State University
Baton Rouge, LA 70803-1804
Tel: 225-578-2706
Fax: 225-578-3458
E-mail: sjiang1@lsu.edu



American Chemical Society

Publications Division
Copyright Office

1155 Sixteenth Street, NW
Washington, DC 20036
Phone: (1) 202-872-4368 or -4367
Fax: (1) 202-776-8112 E-mail: copyright@acs.org

VIA FAX: 225-578-3458 DATE: September 21, 2006

TO: Shan Jiang, Department of Chemistry, Louisiana State University
Chopping Hall, Rm. 232, Baton Rouge, LA 70803-1804

FROM: C. Arleen Courtney, Copyright Associate *C. Arleen Courtney*

Thank you for your request for permission to include **your** paper(s) or portions of text from **your** paper(s) in your thesis. Permission is now automatically granted; please pay special attention to the implications paragraph below. The Copyright Subcommittee of the Joint Board/Council Committees on Publications approved the following:

Copyright permission for published and submitted material from theses and dissertations

ACS extends blanket permission to students to include in their theses and dissertations their own articles, or portions thereof, that have been published in ACS journals or submitted to ACS journals for publication, provided that the ACS copyright credit line is noted on the appropriate page(s).

Publishing implications of electronic publication of theses and dissertation material

Students and their mentors should be aware that posting of theses and dissertation material on the Web prior to submission of material from that thesis or dissertation to an ACS journal may affect publication in that journal. Whether Web posting is considered prior publication may be evaluated on a case-by-case basis by the journal's editor. If an ACS journal editor considers Web posting to be "prior publication", the paper will not be accepted for publication in that journal. If you intend to submit your unpublished paper to ACS for publication, check with the appropriate editor prior to posting your manuscript electronically.

If your paper has not yet been published by ACS, we have no objection to your including the text or portions of the text in your thesis/dissertation in **print and microfilm formats**; please note, however, that electronic distribution or Web posting of the unpublished paper as part of your thesis in electronic formats might jeopardize publication of your paper by ACS. Please print the following credit line on the first page of your article: "Reproduced (or 'Reproduced in part') with permission from [JOURNAL NAME], in press (or 'submitted for publication'). Unpublished work copyright [CURRENT YEAR] American Chemical Society." Include appropriate information.

If your paper has already been published by ACS and you want to include the text or portions of the text in your thesis/dissertation in **print or microfilm formats**, please print the ACS copyright credit line on the first page of your article: "Reproduced (or 'Reproduced in part') with permission from [FULL REFERENCE CITATION.] Copyright [YEAR] American Chemical Society." Include appropriate information.

Submission to a Dissertation Distributor: If you plan to submit your thesis to UMI or to another dissertation distributor, you should not include the unpublished ACS paper in your thesis if the thesis will be disseminated electronically, until ACS has published your paper. After publication of the paper by ACS, you may release the entire thesis (**not the individual ACS article by itself**) for electronic dissemination through the distributor; ACS's copyright credit line should be printed on the first page of the ACS paper.

Use on an Intranet: The inclusion of your ACS unpublished or published manuscript is permitted in your thesis in print and microfilm formats. If ACS has published your paper you may include the manuscript in your thesis on an intranet that is not publicly available. Your ACS article cannot be posted electronically on a publicly available medium (i.e. one that is not password protected), such as but not limited to, electronic archives, Internet, library server, etc. The only material from your paper that can be posted on a public electronic medium is the article abstract, figures, and tables, and you may link to the article's DOI or post the article's author-directed URL link provided by ACS. This paragraph does not pertain to the dissertation distributor paragraph above.

06/07/06

VITA

Shan Jiang was born in Beijing, People's Republic of China on September 18, 1974. He graduated with a Bachelor of Engineering degree in chemical engineering from Beijing Institute of Clothing Technology in Beijing, China. At Beijing Institute of Clothing Technology (BICT), he was the recipient of many honors including Outstanding Student and Excellent Student leader of BICT. He received BICT Top Scholarship four years in a row from 1994 to 1997.

In the fall of 2000, after he worked in Beijing RDB Biodegradable Chemicals and Products Co. for three years, Shan entered the graduate program in the Department of Chemistry at New Mexico Highlands University (NMHU) in Las Vegas, New Mexico. In 2002, he graduated and received a Master of Science degree in chemistry.

About one month after Shan graduated from NMHU, Shan got the opportunity to be enrolled in the doctoral program at Louisiana State University in Baton Rouge, Louisiana. While at LSU, he has been involved in many projects, including synthesis and studies on new materials and mechanisms for the visual detection of biological molecules, under the supervision of Dr. Robert Strongin, giving support to his research group and other groups in the Chemistry Department. Shan Jiang is a member of the American Chemical Society and currently a candidate for the degree of Doctor of Philosophy in organic chemistry, which will be awarded at the May 2007 Commencement.